

Investigations on groundwater dewatering by using
vertical circulation wells: Numerical simulation
method development and field validation

Dissertation

zur Erlangung des mathematisch-naturwissenschaftlichen Doktorgrades

"Doctor rerum naturalium"

der Georg-August-Universität Göttingen

im Promotionsprogramm Geowissenschaften / Geographie

der Georg-August University School of Science (GAUSS)

vorgelegt von

Yulan Schaffer-Jin

aus Yanji, Jilin (China)

Göttingen 2014

Betreuungsausschuss:

Prof. Dr. Martin Sauter

Abteilung Angewandte Geologie, Georg-August-Universität Göttingen

PD Dr. Ekkehard Holzbecher

Abteilung Angewandte Geologie, Georg-August-Universität Göttingen

Mitglieder der Prüfungskommission:

Referent: Prof. Dr. Martin Sauter,

Abteilung Angewandte Geologie, Georg-August-Universität Göttingen

Korreferent: PD Dr. Ekkehard Holzbecher

Abteilung Angewandte Geologie, Georg-August-Universität Göttingen

weitere Mitglieder der Prüfungskommission:

Prof. Dr. Ruud Schotting

Department of Earth Sciences, Utrecht University

Prof. Dr. Sebastian Bauer

Institut für Geowissenschaften, Universität Kiel

Prof. Dr. Thomas Ptak-Fix

Abteilung Angewandte Geologie, Georg-August-Universität Göttingen

PD Dr. Tobias Licha

Abteilung Angewandte Geologie, Georg-August-Universität Göttingen

Dr. Thomas Vienken

Department Monitoring- und Erkundungstechnologien, UFZ Leipzig

Tag der mündlichen Prüfung: 27. Oktober 2014

Short Summary

Construction dewatering is a common engineering problem encountered at construction and mining sites. Successful site dewatering requires proper design and implementation of groundwater lowering techniques depending on excavation dimensions, soil types, and local environmental regulations. Among the dewatering techniques, different types of pumping wells are usually the applied methods of choice. The conventional pumping wells require groundwater abstraction from aquifers and, consequently, the discharge. Environmental problems as a result of massive groundwater abstraction and foreseeable disposal costs are the known consequences. In contrast, the implementation of vertical circulation wells (VCWs) is an innovative approach, which enables dewatering without any net discharge. A VCW consists of an abstraction and an injection screen in the upper and lower part of a single borehole, respectively.

The successful application of this new dewatering technique requires a sufficient knowledge of the influencing factors on the induced groundwater flow patterns and the water table drawdown. Since the groundwater flow near a VCW is very complex, traditional methods neglecting the vertical flow are not sufficient anymore. Therefore, the systematic investigation of the groundwater flow near a VCW and consequently the achieved drawdown is the main focus of the thesis. The investigation includes the development of a comprehensive simulation method, the identification and evaluation of relevant hydrogeological parameters, and eventually the performance of dewatering tests at a field test site.

A novel simulation approach, coupling the arbitrary Lagrangian-Eulerian (ALE) algorithm and the groundwater flow equation, is presented. The obtained results are compared and verified with several analytical solutions. The developed numerical model is suitable for simulating groundwater flow near VCWs, since it is not restricted in considering the vertical flow component. As a result, especially in

unconfined aquifers, the position of the groundwater table can be precisely estimated.

After calibrating the model with observations from several field tests, it is applied to assess the sensitivity of relevant parameters on the groundwater flow and the drawdown. The obtained results show that the drawdown is proportional to the flow rate, inversely proportional to the hydraulic conductivity, and almost independent from the aquifer anisotropy in the direct vicinity of a VCW. Further, the position of the abstraction screen has a stronger effect on drawdown than the position of the injection screen. The circulation field and thus the extension of the influenced area depend on the screen separation length, but mainly on the anisotropy.

To investigate the effects of aquifer layering properties on groundwater flow, the layer structures were characterized in detail with various field methods including several direct-push tests, pumping-, injection-, and circulation flow tests as well as grain-size analysis in the lab. The employed field methods in combination with numerical simulations provide an appropriate base, to further investigate the role of the aquifer layer structure on the drawdown.

The gained insight from this study provides an important contribution and gives practical implications for the future design and operation of VCW for groundwater lowering in unconfined aquifers. Eventually, the thesis highlights the potential of this new dewatering technique as an alternative to conventional dewatering methods.

Kurzfassung

Die künstliche Grundwasserabsenkung stellt eine wichtige Maßnahme für die Entwässerung von Baugruben und bergbaulich genutzten Flächen dar. Eine erfolgreiche und zielgerichtete Absenkung des Grundwasserspiegels setzt ein zweckmäßiges Design und die richtige Auswahl der genutzten Absenkungstechniken voraus. Dabei sind insbesondere die Dimension des abzusenkenden Bereichs, die Untergrundbeschaffenheit sowie zu erfüllende umweltschutzrechtliche Regelungen zu berücksichtigen. Zur Grundwasserabsenkung kommen üblicherweise verschiedene Ausführungen und Anordnungen von Pumpbrunnen zum Einsatz. Konventionelle Pumpbrunnen, welche für Absenkungsmaßnahmen eingesetzt werden, entnehmen Grundwasser aus dem Aquifer. Durch das fortwährende Abpumpen von in der Regel erheblichen Wassermengen können jedoch Umweltprobleme entstehen, und es ist mit zusätzlichen Entsorgungskosten für die Ableitung des geförderten Wassers zu rechnen. Im Gegensatz hierzu stellen vertikale Zirkulationsbrunnen (VCW) einen innovativen Ansatz dar, der eine lokale Grundwasserabsenkung ohne Nettowasserentnahme aus dem Aquifer erlaubt. Ein VCW kann als ein Einbohrlochsystem aufgefasst werden, bei dem im oberen Bereich eines Brunnens Wasser entnommen und dieses in einem separaten, weiter unten installierten Brunnenbereich wieder injiziert wird.

Die erfolgreiche Anwendung dieser neuen Grundwasserabsenkungstechnik erfordert die genaue Kenntnis der Faktoren, welche für die Grundwasserströmungsverhältnisse relevant sind und somit die Absenkung bestimmen. Traditionelle Berechnungsansätze vernachlässigen oft vertikale Grundwasserbewegungen und sind deshalb für die Beschreibung der komplexen Strömungsverhältnisse in unmittelbarer Nähe eines VCW nicht geeignet. Aus diesem Grund steht die systematische Untersuchung der Grundwasserströmung unter Berücksichtigung vertikaler Strömungskomponenten im Hauptfokus dieser Arbeit.

Die Untersuchungen beschäftigen sich in erster Linie mit der Entwicklung einer geeigneten Simulationsmethode, mit der Evaluierung des Einflusses relevanter hydrogeologischer Parameter sowie mit der Durchführung und Auswertung von Pumpversuchen an einem Feldstandort.

Die hier vorgestellte neue Simulationsmethode koppelt den sogenannten Arbitrary-Lagrangian-Eulerian-(ALE)-Algorithmus mit der Grundwasserströmungsgleichung. Die Simulationsergebnisse werden mit mehreren analytischen Lösungen verglichen und verifiziert. Das entwickelte numerische Modell berücksichtigt auch Vertikalströmungen und eignet sich somit zur Simulation der Grundwasserströmung in der Nähe von VCW. Folglich kann nun die Lage des Grundwasserspiegels, vor allem für ungespannte Grundwasserleiter, präzise berechnet werden.

Nach erfolgter Kalibrierung des numerischen Modells anhand von Felddaten wurde eine Sensitivitätsanalyse relevanter Parameter im Hinblick auf die erzielte Absenkung und deren Auswirkungen auf die Grundwasserströmungssituation durchgeführt. Die dabei erhaltenen Ergebnisse zeigen, dass die Grundwasserabsenkung proportional zur Pumprate, indirekt proportional zur hydraulischen Leitfähigkeit und fast unabhängig von der Anisotropie des Grundwasserleiters um den VCW ist. Des Weiteren zeigte sich, dass die Lage des oberen Entnahmepunktes einen größeren Einfluss auf die Absenkung als die Lage des darunter liegenden Injektionspunktes hat. Die Größe des von der Grundwasserzirkulation beeinflussten Bereiches hängt dagegen neben dem Abstand dieser beiden Punkte hauptsächlich auch von der Anisotropie des Aquifermaterials ab.

Um den Einfluss der Hydrostratigraphie auf die Grundwasserströmung zu untersuchen, wurden die Eigenschaften der einzelnen Schichten genau charakterisiert. Hierfür wurden Direct-Push-, Pump-, Injektions- sowie Zirkulationsversuche an einem Feldstandort durchgeführt. Zudem wurden Bohrkerne entnommen und mithilfe von Siebanalysen vertikale Korngrößenverteilungsprofile im Labor bestimmt. Die eingesetzten experimentellen Methoden stellen in Kombination mit numerischen Simulationsrechnungen eine gute Basis dar, um die Rolle der Schichtstruktur im Aquifer besser beurteilen zu können.

Die Untersuchungen leisten somit einen wichtigen Beitrag für das zukünftige Design und den Betrieb von VCW für Grundwasserabsenkungszwecke in ungespannten Grundwasserleitern. Zudem zeigt die hier vorliegende Arbeit das große Potential dieser neuen Grundwasserabsenkungstechnik als vielversprechende Alternative zu konventionellen Absenkungsverfahren auf.

Acknowledgments

Without the financial support of German Federal Environmental Foundation (Deutsche Bundesstiftung Umwelt), this research would have been impossible. I gratefully acknowledge the German Federal Environmental Foundation and the financed DSI project (AZ28299-23).

In the following I would like to express my sincere gratitude to those people, who supported me in multifarious ways during the time of my Ph.D.

First and foremost I record my sincerest gratitude to Prof. Dr. Martin Sauter for the excellent research opportunity, the administrative supports and the freedom to develop scientific ideas. I would like to express my profound thanks to Prof. Dr. Martin Sauter and PD. Dr. Ekkehard Holzbecher for their valuable supervisions, advices and unflinching encouragements from the very early stage of the research to the end. Further, I would like to extend my gratitude to the members of the committee, Prof. Dr. Ruud Schotting, Prof. Dr. Sebastian Bauer, Dr. Thomas Ptak, PD. Dr. Tobias Licha and Dr. Thomas Vienken for their undertaking of the thesis and perceptive feedback.

I would like to thank my colleagues and friends in the department of Applied Geology, where I spent the last few years for my Master study and the PhD research. Among many, I gratefully acknowledge Prof. Dr. Thomas Ptak, PD. Dr. Chicgoua Noubactep, Dr. Mario Schaffer, and Dr. Friedrich Maier for the constructive discussions and the proofreading they offered at any time. Special thanks go to Beka Peters-Kewitz and my friends and office mates Dr. Karsten Nödler, Dr. Martin Nottebohm, and Dr. Sebastian Schmidt.

I was extraordinarily fortunate in having Hölscher Wasserbau GmbH as external research partner. The successful field experiments conducted by them are highly appreciated. I specially dedicate my thanks to Dr. Stefan Ebneth for his support and suggestions as well as his encouraging words. Thank you for providing me the

opportunities to discuss the work not only with the field experts, but also with other researchers in Germany and the Netherlands.

It is my pleasure to pay tribute to Helmholtz Centre for Environmental Research, especially Dr. Thomas Vienken, for providing high resolution aquifer profile with the direct-push tests.

Words fail me to express my love to my parents and my husband. Without their encouragement and unconditional love, I would not have been able to finish my PhD.

Table of Contents

	Page
1 Introduction.....	1
1.1 Background and Motivation	1
1.1.1 Overview of existing dewatering methods	2
1.1.2 Evaluation of groundwater flow to a pumped borehole.....	5
1.1.2.1 Evaluation of dewatering wells using analytical models	6
1.1.2.2 Evaluation of dewatering wells using numerical models.....	7
1.2 Scope, Objectives and further Outline of the Thesis	8
1.3 References	10
2 Borehole Pump and Inject: an Environmentally Sound New Method for Groundwater Lowering.....	13
2.1 Introduction.....	15
2.2 Borehole Pump and Inject	15
2.3 Field Experiments	17
2.4 Modeling.....	19
2.4.1 Differential equation	20
2.4.2 Meshing and discretization.....	21
2.4.3 Model region and boundary conditions.....	21
2.4.4 Input values.....	23
2.5 Results and Discussion.....	24
2.5.1 Aquifer response on pumping test.....	24
2.5.2 Aquifer Response on pump-inject (DSI) Test.....	26
2.5.3 Aquifer parameter evaluation	27
2.5.4 Modelling result of DSI test	28
2.6 Conclusions.....	29
2.7 References	30

3	A Novel Modeling Approach Using Arbitrary Lagrangian-Eulerian (ALE) Method for the Flow Simulation in Unconfined Aquifers.....	32
3.1	Introduction.....	35
3.2	Governing Equations	37
3.3	The Novel Numerical Approach	38
3.3.1	Model domain and groundwater flow equation	38
3.3.2	Tracing free-surface deformation with the ALE method.....	38
3.4	Simulation Experiments	40
3.4.1	Case 1: Steady-state unconfined flow.....	40
3.4.1.1	Analytical approach	40
3.4.1.2	Numerical approach using the ALE method	41
3.4.1.3	Comparison with analytical solutions.....	42
3.4.2	Case 2: Steady-state radial flow towards a well.....	43
3.4.2.1	Analytical approaches	43
3.4.2.2	Numerical model set up	44
3.4.2.3	Simulation result and its comparison with analytical solution	46
3.5	Application Cases	47
3.5.1	The effect of anisotropy on drawdown	47
3.5.2	Pumping and injection from a single borehole.....	49
3.6	Summary and Conclusions	50
3.7	References	51
4	Dual-screened Vertical Circulation Wells for Groundwater Lowering in Unconfined Aquifers	54
4.1	Introduction.....	56
4.2	Site Description and Measurements	58
4.3	The Mathematical Model	59
4.3.1	Unconfined groundwater flow	59
4.3.2	The arbitrary Lagrangian-Eulerian method	60
4.3.3	Streamline simulation.....	61
4.3.4	Model calibration and validation	62
4.4	Sensitivity Analysis	63

4.4.1	Reference case	64
4.4.2	Sensitivity to well design and operation	64
4.4.2.1	Effect of flow rate	64
4.4.2.2	Effect of screen positions	65
4.4.3	Sensitivity of drawdown to change in aquifer characteristics.....	67
4.4.3.1	Effect of change in hydraulic conductivity on drawdown	67
4.4.3.2	Effect of aquifer anisotropy.....	67
4.5	Conclusions.....	69
4.6	References	70
5	Performance of vertical circulation wells for dewatering in layered unconfined aquifers.....	73
5.1	Introduction.....	75
5.2	Site Description	77
5.3	Methodology	79
5.3.1	Field methods for aquifer layer characterization	79
5.3.1.1	Empirical identification of the injection layers	79
5.3.1.2	Aquifer characterization with direct-push technology	79
5.3.1.3	Hydraulic conductivity determination from grain size analysis....	80
5.3.1.4	Pumping test.....	80
5.3.1.5	Injection test	81
5.3.1.6	Vertical circulation flow test	81
5.3.2	Numerical simulation method	82
5.3.3	Numerical model set-up	82
5.4	Results and Discussion.....	84
5.4.1	The characteristics of the aquifer layers	84
5.4.2	Modeling results	86
5.4.3	Sensitivity to the hydraulic conductivity of aquifer layers	89
5.5	Conclusions.....	91
5.6	References	92
6	General Conclusions and Perspectives	95
6.1	Evaluation of Flow and Hydraulic Head Fields for VCWs.....	95
6.2	Further Investigations on VCW installation at Construction Sites and Furture Challenges.....	96

Appendix S1: Site description and measurements	XII
Appendix S2: The Mathematical Model	XII
S2.1 Reference case model.....	XII
S2.2 Model verification, calibration and validation	XIV
S2.2.1 Analytical solution	XIV
S2.2.2 Comparison of simulation results with analytical solution	XV
S2.2.3 Model validation.....	XVI
Appendix S3: Sensitivity Analysis	XVII
S3.1 Effect of screen positions.....	XVII
S3.2 Effect of hydraulic conductivity on drawdown.....	XVIII
Publication List.....	XIX

List of Figures

	Page
Fig. 1.1 Overview on construction dewatering methods.....	2
Fig. 1.2 Comparison of dewatering wells: schematic diagram of groundwater flow and drawdown driven by a discharging well (conventional well on the left) and a non- discharging well (VCW on the right) in an unconfined aquifer.....	3
Fig. 2.1 Sketch of the borehole pump and inject concept.....	16
Fig. 2.2 Overview of Plötzin test site	18
Fig. 2.3 Typical 3D finite element mesh for a single well problem.....	20
Fig. 2.4 Sketch of deformed model region and boundaries in a 2D model.	22
Fig. 2.5 Hydraulic head changes in dependence of distance from the well and well screen position (shallow, middle, deep), observed in a classical pumping test.	25
Fig. 2.6 Hydraulic head changes in dependence of distance from the well and well screen position (shallow, middle, deep), observed in a pump-inject DSI test.....	26
Fig. 2.7 Differences in hydraulic head of model results and pumping test observations in a histogram.	27
Fig. 2.8 Example of model output for vertical cross section around a single well: potential contours (filled) and velocity field in deformed geometry.	28
Fig. 2.9 3D visualization of model output	29
Fig. 3.1 Definition sketch of unconfined groundwater flow for 2D vertical-cross-section geometry.	41

Fig. 3.2 Hydraulic head and flow velocity field along the aquifer. The scale of arrow lines in the figure also implies the flow velocity, which increases with a decrease in hydraulic head. The solid rectangle frame, which stays constant through-out simulation, represents the initial geometry. The deformed geometry is highlighted with the color coded area (red for higher and blue for lower hydraulic heads)..... 42

Fig. 3.3 Comparison of the simulated hydraulic heads with corresponding analytical results..... 43

Fig. 3.4 Definition sketch for 2D vertical-cross-section geometry with labeled boundaries..... 44

Fig. 3.5 Deformed mesh in upper inner part of model region. 46

Fig. 3.6 Steady-state hydraulic head and head difference compared to the analytical solution, versus radial distance (r) from pumping well at aquifer top, middle and bottom ($z/D = 0, -0.5, -1$) when groundwater is pumped from a fully penetrating well on the left hand side..... 47

Fig. 3.7 Hydraulic head distribution with radial distance (r) from pumping well at aquifer top for different anisotropy ratios..... 48

Fig. 3.8 Sketch of the single borehole pumping and injection concept..... 49

Fig. 3.9 2D vertical cross section model output. Shown are the hydraulic head (color plot), the mesh deformation and the velocity field (arrow plot) within the aquifer..... 50

Fig. 4.1 Comparison of the dewatering concept between a VCW and a conventional well. Left: schematic illustration of groundwater flow and drawdown of a VCW. Right: schematic illustration of groundwater flow, discharge, and drawdown of a conventional dewatering well.....57

Fig. 4.2 Model calibration results obtained from comparison of numerical model results corresponding field observations for selected time steps. 63

Fig. 4.3 Effect of the VCW operation flow rate, Q , on the hydraulic head at steady-state. Solid blue line indicates the reference case. The linear

relationship between Q and drawdown is shown for a radial distance of r = 5 m.....	65
Fig. 4.4 Effect of the separation length of the screen intervals, ΔL , on steady-state groundwater flow near the VCW. The location of the abstraction interval is identical. (ref) reference case $\Delta L = 8$ m; (a) $\Delta L = 4$ m; (b) $\Delta L = 12$ m. The diagram depicts the effect of changes in ΔL on hydraulic head. The logarithmic relationship between ΔL and drawdown is shown for a radial distance of r = 5 m.....	66
Fig. 4.5 Effect of anisotropy of the aquifer material, $\alpha = K_z/K_r$, on steady-state groundwater flow near the VCW. The reference case $\alpha = 1$ is depicted in the upper left and groundwater flow for $\alpha = 0.2$ are presented in the upper right figure. The diagram depicts the effect of α on hydraulic head distribution. The non-linear relationship between α and the radial distance of the 80% streamline is also shown.	68
Fig. 5.1 Schematic illustration of groundwater flow patterns and drawdown near a VCW in a layered unconfined aquifer.....	76
Fig. 5.2 (a) Location of Plötzin study site. (b and c) Map of the test site showing the position of the VCW and piezometers. (b) Plan view. (c) Cross-section: core sampling depths and the direct-push slug test intervals (left), depths of abstraction and injection screens and piezometers (right).....	78
Fig. 5.3 Results of direct-push methods and the respective aquifer layers defined in numerical model. EC and HPT profile is shown on the left side. Cross-section view of the model layers (L1-L6), thickness, and calibrated parameters are defined in the middle. VCW screen setting at the test site is illustrated, where the abstraction screen interval is depicted in blue and the injection screen interval is shown in light brown. DPIL and DPST results are shown on the right side. The model layer set-ups for calibrating the pumping test and injection tests are identical. Detailed screen settings are described above.	83

Fig. 5.4 Modeled 2D vertical cross-section of the groundwater flow field near the well. Left: pumping test; middle: injection test; right: circulation test with a VCW. Hydraulic head distributions (color plot), positions of groundwater table (deformed mesh line), equipotential contours (black solid lines with label), and the groundwater flow field (arrow plot) are also presented..... 87

Fig. 5.5 Model calibration results for the conducted pumping tests obtained from the comparison of numerical model results with corresponding field observations for selected time steps. Locations and depths of the piezometers are shown in Figure 5.2 (b and c). 88

Fig. 5.6 Model calibration results for the conducted injection tests obtained from the comparison of numerical model results with corresponding field observations for selected time steps. Locations and depths of the piezometers are shown in Figure 5.2 (b and c). 88

Fig. 5.7 Model calibration results for the conducted circulation flow tests obtained from the comparison of numerical model results with corresponding field observations for selected time steps. Locations and depths of the piezometers are shown in Figure 5.2 (b and c)..... 89

Fig. 5.8 Effect of the hydraulic conductivity of the abstraction layer on steady-state groundwater flow near the VCW. Left: higher hydraulic conductivity case with $K_{abstraction} = 5.79 \times 10^{-3}$; middle: the reference case $K_{abstraction} = 5.79 \times 10^{-4}$; right: lower hydraulic conductivity case with $K_{abstraction} = 5.79 \times 10^{-5}$. Detailed description of the test case can be found in the caption of Figure 5.4..... 90

Fig. 5.9 Effect of the hydraulic conductivity of the injection layer on steady-state groundwater flow near the VCW. Left: higher hydraulic conductivity case with $K_{injection} = 3.87 \times 10^{-2}$; middle: the reference case $K_{injection} = 3.87 \times 10^{-3}$; right: lower hydraulic conductivity case with $K_{injection} = 3.87 \times 10^{-4}$. Detailed description of case can be found in the caption of Figure 5.4. 91

-
- Fig. S1 : Schematic site plan view of the vertical cross section of the test field showing the locations of piezometers and DSI-well screens.....XII
- Fig. S2: Modeled 2D vertical cross-section groundwater flow field near a VCW. Left: hydraulic head distribution (color plot), and position of groundwater table (deformed mesh line), equipotential contours (black solid lines with label), velocity field (arrow plot), 20%, 40%, 60%, 80% flow streamlines (red solid lines); right: hydraulic head (or groundwater level position) change with increasing radial distance from the well.XIV
- Fig. S3: Steady-state hydraulic head at free surface ($z = 0$) and head difference compared to the analytical solution, versus radial distance r from the VCW on the left hand side.XV
- Fig. S4: Steady-state hydraulic head at the depth of abstraction screen centre ($z = -5\text{m}$) and head difference compared to the analytical solution, versus radial distance r from the VCW on the left hand side.....XVI
- Fig. S5: Comparison between the numerical model results and the field observations for the validation experiment. Locations and depths of the piezometers are shown in Figure S1.XVI
- Fig. S6: Effect of the separation length between abstraction and injection screen, ΔL , on steady-state groundwater flow near the VCW. The location of the injection interval is identical. (ref) reference case $\Delta L = 8\text{ m}$; (a) $\Delta L = 4\text{ m}$; (b) $\Delta L = 11\text{ m}$. The detailed figure descriptions for each case can be found in the caption of Figure S3. The scatter plot depicts the effect of ΔL on the hydraulic head.XVII
- Fig. S7: Effect of the change in hydraulic conductivity, K , on the hydraulic head. Homogenous and isotropic aquifer materials ($K = K_r = K_z$) are assumed. The inverse proportional relationship between K and drawdown is shown for a radial distance of $r = 5\text{ m}$XVIII

List of Tables

	Page
Table 1.1 List of analytical solutions applied for different well types.	6
Table 2.1 Input values for reference set up.	24
Table 5.1 Comparison of the obtained hydraulic conductivities with different methods.	84
Table S1: Parameters used for groundwater flow field simulation around a VCW for reference case.	XIII

Chapter 1

1 Introduction

1.1 Background and Motivation

Groundwater, representing 90% of the readily available freshwater resources, plays a vital role in the hydrologic cycle (Freeze and Cherry, 1979; USGS, 2014). Naturally, groundwater is recharged mainly through the infiltration of precipitation water and stored in aquifers. Moreover, it interacts closely with the surface water bodies by re- or discharging into streams, lakes, wetlands, rivers, and the sea. Human efforts to control the groundwater predate recorded history (Powers et al., 2007). These efforts include artificial recharge (infiltration) to augment groundwater resources and groundwater abstraction with the following purposes: (1) supplying water for drinking, irrigation, and industrial use; (2) lowering the groundwater level from a site for land amelioration, i.e., converting the fetid marshes into arable land, and for the underground construction projects such as mining and the building of urban structures, which is known as construction dewatering.

Construction dewatering is defined as the removal of groundwater or the depression of the water table by means of abstraction at construction sites to a level below that of the intended excavation (Harris, 1995; Cashman and Preene, 2003; Powers et al., 2007). Construction projects often entail the excavation below the water table for providing a dry working environment, and consequently require site dewatering in advance. Indeed, the presence of groundwater has a considerable effect on the design of the structure, the construction procedure, and the overall cost of an underground construction project (Wang et al., 2002; Cashman and Preene, 2003;

Powers et al., 2007). The required dewatering can be permanent, for instance, in stabilizing slopes and shallow excavations, or can be temporary (Glossop, 1950).

The development of modern dewatering technology has been started from 18th century with the steam engines developed by James Watt, which were used in mine dewatering (Powers et al., 2007). Since then, a large number of techniques have been established depending on the dewatering scale, site hydrogeological conditions, affordability as well as the relevant regulations. The commonly applied dewatering methods are briefly reviewed in the following section. Nevertheless, the proper design and performance of dewatering systems is still a challenge in the subject of subsurface engineering.

1.1.1 Overview of existing dewatering methods

In order to control the groundwater inflow into an excavation, a number of dewatering methods have been developed. Figure 1.1 provides an overview on the manifold existing dewatering techniques. The currently available dewatering methods can be classified into three general types based on their drainage process, which are pumping with wells, open drainage, and cutting off or exclusion (Puller, 2003; Powers et al., 2007).

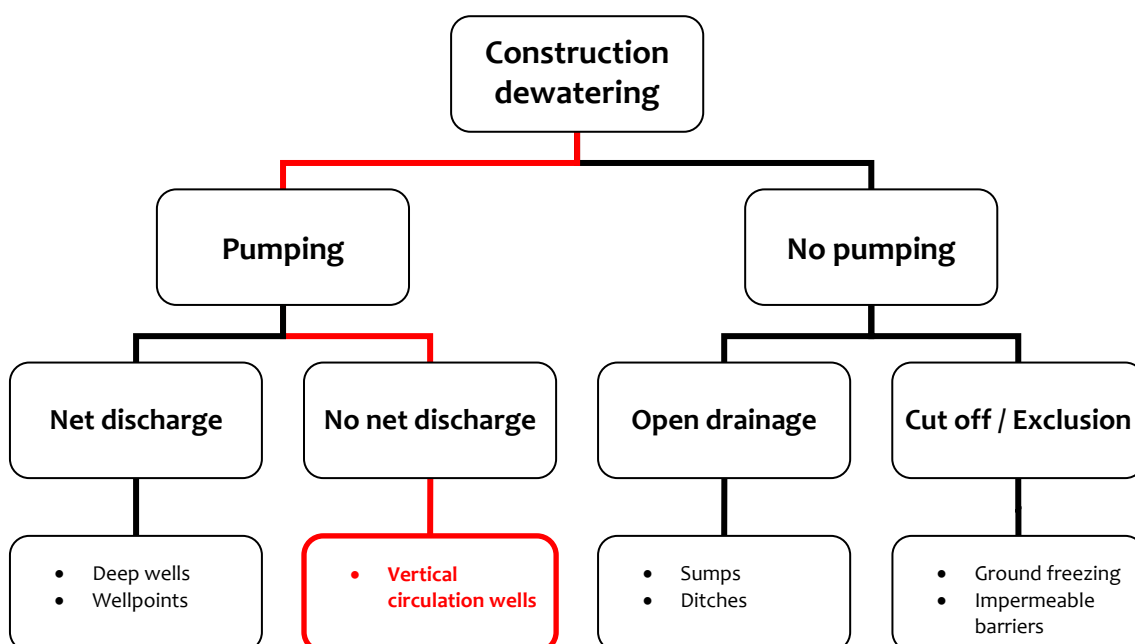


Fig. 1.1 Overview on construction dewatering methods.

If the construction site is undesirable to pump underground, open drainage and/or cut off could be used. *Open drainage* is the process of removing water that has entered an excavation by collecting the water in ditches and sumps and discharging it away. It is one of the cheapest methods and provides localized and very shallow dewatering. The method is suitable to apply in tight, fine grained soils that are of low to moderate hydraulic conductivity (Powers et al., 2007). *Cutting off* or *exclusion* of water is the process of stopping the water entering the excavation area by using impermeable barriers or freezing the ground (Rupprecht, 1979; Grube Jr, 1992; Harris, 1995; Powers et al., 2007). However, these techniques usually require high quality control and also very costly.

More often, it is advisable to lower the water table at construction sites by using different types of the *pumping wells*. In the present thesis, the pumping wells are further classified in two types depending on the water discharge. The theoretical sketch of discharging and non-discharging dewatering wells is compared in Figure 1.2.

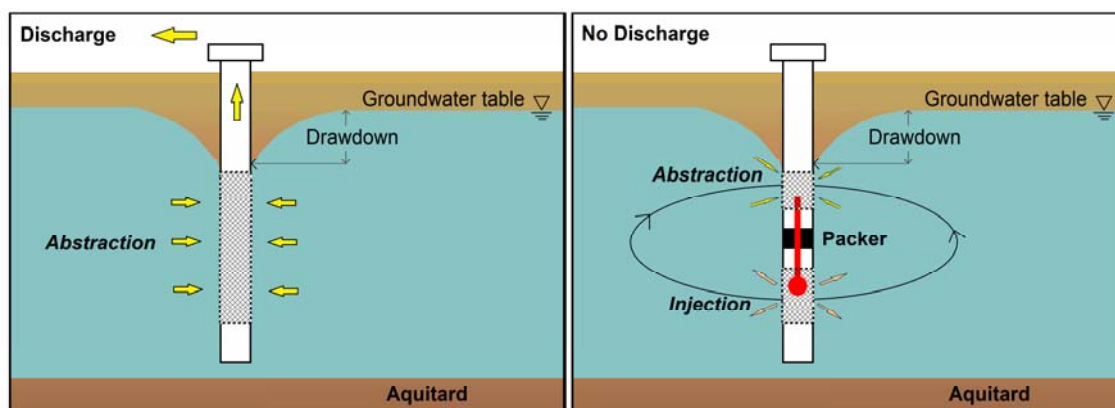


Fig. 1.2 Comparison of dewatering wells: schematic diagram of groundwater flow and drawdown driven by a discharging well (conventional well on the left) and a non-discharging well (VCW on the right) in an unconfined aquifer.

The discharging wells lower the groundwater level by withdrawing the groundwater from an aquifer with abstraction wells, such as wellpoints, deep wells, and horizontal wells etc., and discharging it either into surface water bodies nearby or into other aquifers away from the construction sites (Cashman and Preene, 2003; Powers et al., 2007). Suitable wells can be selected according to the dewatering

scale, and the local aquifer and water conditions. For instance, using wellpoint systems may achieve efficient dewatering in shallow aquifers up to 5-6 m with reasonable costs (Powers et al., 2007; Ye et al., 2012). However, it is not recommended to apply beyond this depth due to the suction lift limitation. Deep wells may overcome this limitation in dewatering depth, since submersible pumps are used rather than suction pumps. In this thesis, these discharging wells resulting groundwater abstraction are referred as *conventional dewatering wells* (or conventional dewatering methods).

The non-discharging wells are a new dewatering system employed for groundwater lowering, which were also introduced as *DSI-wells* in Holzbecher et al. (2011) and Jin et al. (2011 and 2012). This system may synchronously abstract the groundwater through the upper screened section of a dual-screened well and inject it back in the aquifer through the lower screened section. It is, in fact, a *vertical circulation well* (VCW), which results in groundwater circulation in “up-flow” direction.

The conventional dewatering wells are well established systems leading to efficient groundwater dewatering at construction sites. However, no matter which well system is applied, a large amount of groundwater has to be withdrawn from the aquifers. Environmental and geotechnical problems, i.e., soil consolidation and ground surface settlement, contaminant migration, and salt water intrusion etc., are the known consequences of these dewatering methods (Foster et al., 1998; Preene, 2000; Powers et al., 2007; Roy and Robinson, 2009). Moreover, beside the regular dewatering costs, additional costs may be induced to meet the environmental regulations, particularly, if the pumped water is of low quality.

In contrast to the conventional dewatering wells, by applying non-discharging VCWs, the groundwater level can be lowered without any net water discharge, and consequently, the above mentioned adverse environmental effects of conventional dewatering wells may be reduced. However, the groundwater lowering scale is sometimes smaller compared to the conventional dewatering wells due to the water reinjection in the same aquifer.

Moreover, the huge potential of this alternative procedure can only be exploited after a systematic investigation of parameters influencing the system performance.

In the present work, therefore, the focus is given on the optimization of VCW system, following the highlighted red line in Figure 1. The terms VCWs and DSI-wells are randomly interchangeably used through the thesis.

1.1.2 Evaluation of groundwater flow to a pumped borehole

Profound knowledge on the groundwater flow around a well is a prerequisite to predict the drawdown and to gain important implications for the successful operation of different types of the dewatering wells. Here, drawdown refers to the change in hydraulic head due to the pumping in a well (Rushton, 2003). It is usually measured relative to the static (without pumping) condition.

The fundamental governing equation describing flow in porous media is derived from the Darcy's Law and the principle of continuity. For a transient groundwater flow in a heterogeneous and anisotropic aquifer, the governing partial differential equation is given as (Bear, 1972; Freeze and Cherry, 1979):

$$\nabla \cdot \mathbf{K} \nabla h = S \frac{\partial h}{\partial t} - q \quad (1.1)$$

where \mathbf{K} is the tensor of hydraulic conductivity, q is the source and/or sink term, S and h are the specific storage and the hydraulic head formulated, respectively, as:

$$S = \rho g (\alpha + \varphi \beta) \quad (1.2)$$

$$h = p / \rho g + z \quad (1.3)$$

where α and β are compressibility of the porous medium and the fluid, φ is the porosity, p is pressure head, ρ is the density of the fluid, g is the standard acceleration due to gravity, and z is elevation of the fluid at a reference level.

Equation (1.1) can be solved mathematically using either analytical solutions or numerical methods. In many practical situations of groundwater dewatering, these well hydraulic problems involving radial symmetry are often analyzed with analytical models. The analytical solutions are simpler to solve and, therefore, easier to apply compared to the numerical solutions. This is caused by their basic assumptions, such as homogenous and isotropic aquifers having an infinite areal extent.

1.1.2.1 Evaluation of dewatering wells using analytical models

In Table 1.1, some of the frequently applied analytical methods for both discharging and non-discharging wells including their applications are listed. Depending on the borehole penetration types, the discharging well is further classified into the fully and partially penetrated wells. The steady-state radial flow to a fully penetrated well was firstly derived by Dupuit (1863) and Thiem (1906). Subsequently, the wide range of assumed aquifer conditions, i.e., confined, leaking, and unconfined aquifers, lead to a substantial number of analytical solutions for steady-state and the transient flow to a well. Solutions for many different aquifer conditions and well types can be found in Kruseman and Ridder (1990), Rushton (2003), Todd and Mays (2005).

Table 1.1 List of analytical solutions applied for different well types.

Application	Discharging well (fully screened)	Discharging well (partially screened)	Non Discharging well (dual-screened VCW)
Confined aquifer, Steady-state	Dupuit (1863), Thiem (1906)	Huisman Method (in Anonymous 1964)	Kabala (1993), Zlotnik and Ledder (1996)
Confined aquifer, Transient	Theis (1935), Cooper-Jacob (1946)	Hantush (1961a; 1961b)	Zlotnik and Ledder (1996)
Leaky aquifer, Steady-state	De Glee (1930; 1951)	Huisman Method (in Anonymous 1964)	
Leaky aquifer, Transient	Hantush (1956; 1960), Walton (1962), Neuman-Witherspoon (1972)	Weeks (1969)	
Unconfined aquifer, Steady-state	Dupuit (1863), Thiem (1906)		Zlotnik and Ledder (1996)
Unconfined aquifer Transient	Neuman (1972)	Streltsova (1974), Neuman (1974; 1975)	

Compared to the discharging well, there are only a few analytical solutions available to analyze the flow to a non-discharging circulation well. To the author's

knowledge, the groundwater flow induced by a VCW was only considered by Kabala (1993) and Zlotnick and Ledder (1996) by extending the solutions of Hantush (1961b) and Neuman (1972). However, these analytical solutions are limited to simple geometries and idealized cases, i.e., equally and symmetrically distributed screens (Halihan and Zlotnik, 2000). For more complicated aquifer conditions and geometry the application of analytical models is limited. Nevertheless, analytical solutions are often useful, since they may furnish information on the function dependence of one property on the others (Yeh, 1999).

1.1.2.2 Evaluation of dewatering wells using numerical models

Alternatively, for cases where the analytical solutions are inadequate, numerical approximations may be applied by using discrete variables that are defined in grid blocks and/or nodes. Numerical approximations have the advantage that they are sophisticated and applicable for more general situations. The most frequently applied numerical techniques in groundwater flow simulation would be the finite-difference method (FDM), i.e., used in MODFLOW code, and the finite-element method (FEM), i.e., employed in FEFLOW code (Anderson and Woessner, 1992; Yeh, 1999). FDM (Forsythe and Wasow, 1960) is based on the approximation of the derivatives, whereas FEM (Pinder and Gray, 1977) approximates the solution of the function directly. The FDM is relatively simple to implement and the solutions are mass-conservative compared to FEM. FEM is more attractive due to its flexibility in handling complicate geometries and boundaries due to the triangular meshes (Anderson and Woessner, 1992). Beside FDM and FEM a variety of other numerical methods exist such as the integrated finite difference method (IFDM) (Narasimhan and Witherspoon, 1976), the finite volume method (FVM) (Jameson et al., 1981), the boundary integral equation method (BIEM) (Liggett and Liu, 1983), the boundary element method (BEM) (Brebbia et al., 1984), and the analytic element method (AEM) (Strack, 1987) etc.

As introduced above, the focus of the presented work is given on the non-discharging dewatering system using the VCWs. Groundwater flow induced by a VCW is complex and not uniform. Further, significant vertical flow is expected

during the well operation. In addition, heterogeneous aquifer conditions and irregular shape of the well screen design (i.e., different length and diameters for abstraction and injection screens respectively) are often encountered in the field of dewatering. Here, analytical solutions are not sophisticated enough to be applied. Consequently, a flexible numerical model was developed to simulate the groundwater flow and to evaluate the drawdown. The commercial software package COMSOL Multiphysics (2014) using finite-element code was selected in the work.

1.2 Scope, Objectives and further Outline of the Thesis

In this work, the focus is on unconfined aquifers due to their special upper boundary, which is bounded by a perched water table. The pumping of a VCW in an unconfined aquifer causes dewatering of the aquifer and changes the water table position. The *groundwater table* in an unconfined aquifer is usually considered as a *free-surface* where the water pressure equals the atmospheric pressure. In the developed model, the problem domain considers only the saturated parts of an aquifer assuming that there is no groundwater flow occurring above this free-surface. Under this assumption, the pressure component of the hydraulic head in Equation (1.3), $p/\rho g$, turns to zero, and, therefore, the hydraulic head eventually is equal with the elevation component.

The primary objective of this work is to develop a comprehensive model to capture the groundwater flow, especially the precise position of the groundwater table, induced by a VCW in unconfined aquifers. Furthermore, it aims to investigate the influence of relevant well operation and aquifer parameters on the flow and in particular on the drawdown for a better application of the dewatering technology in practice. Eventually, the developed model is used for supporting the evaluation of field tests. A more detailed outline is illustrated in the following.

Chapter 2 introduces the principle of using VCWs for construction dewatering referred as *borehole pump and inject*. This technology was proposed as an environmentally sound dewatering method due to its ability to achieve the water

table drawdown without net abstraction of groundwater from aquifers. The chapter describes the technical setup of the borehole and illustrates the constructed test sites for the field experiments testing the new dewatering method. Site hydrogeology was characterized and the results from the first dewatering test at the test site are presented.

Chapter 3 describes a novel numerical simulation approach, which couples the arbitrary Lagrangian-Eulerian (ALE) algorithm and groundwater flow equation to trace the position of groundwater table (considered as a free-surface) in unconfined aquifers. The problem of interest is the saturated part of an aquifer whereby the free-surface is considered as a moving boundary. The free-surface is handled by imposing an additional hydraulic condition in the Eulerian system to allow the computational mesh to move with the moving boundaries. The developed model is flexible of capturing free-surface in any spatial dimension. Moreover, complex and non-uniform groundwater flow, i.e., vertical flow, is considered in the simulation. The developed simulation approach is verified by comparing the simulation results with the known analytical solutions for selected cases.

Chapter 4 deals with the identification of relevant factors and parameters of VCW operation for dewatering based on field observations and comprehensive numerical simulations. The simulation approach described in Chapter 3 is applied for the evaluation of field tests and for further parameter sensitivity analysis. The influences of well design and operation modes (i.e., flow rates, screen positions) and aquifer characteristics (i.e., hydraulic conductivity, aquifer anisotropy) on drawdown is specially investigated.

In **Chapter 5**, aquifer layers and their characteristics are investigated at a test site by applying different field methods. The practical experiences show that the injection screen of a VCW has to be placed in a sufficiently transmissive layer of an aquifer to guarantee the effectiveness of groundwater injection. Consequently, detailed information on the structure of aquifer layers is required. To accomplish this, various field experiments including direct-push methods, slug test, pumping test, injection test as well as circulation flow test, were performed to characterize the layers of aquifer at the test site. Furthermore, the influence of the hydrogeological

parameters of the aquifer layers on groundwater flow near a VCW is studied through numerical simulations by taking the test site aquifer as a reference.

Chapter 6 summarizes the conclusions respecting the focus of the thesis and gives an outlook for future research.

The **Appendix** lists the journal articles, conference contributions, and miscellaneous publications authored or co-authored by me and related to the presented work.

This thesis is a cumulative dissertation including published journal articles. Hence, the cited literature is listed separately at the end of each chapter.

1.3 References

- Anderson, M.P., Woessner, W.W., 1992. Applied Groundwater Modeling: Simulation of Flow and Advective Transport . Academic Press, USA.
- Anonymous, 1964. Steady flow of groundwater towards wells. Committee for Hydrological Research. T.N.O., Proceedings and Information No. 10. Cited in Kruseman and de Ridder, 1990.
- Bear, J., 1972. Dynamics of Fluids in Porous Media. Dover Publications Inc, New York.
- Brebbia, C.A., Telles, J.C.F., Wrobel, L.C., 1984. Boundary Element Techniques. Springer-Verlag, New York.
- Cashman, P.M., Preene, M., 2003. Groundwater Lowering in Construction: A Practical Guide, Second ed., CRC Press, USA.
- COMSOL Multiphysics, 2014. Version 4.3b, www.comsol.com, [Accessed August 28, 2014].
- Cooper, H.H., Jacob, C E., 1946. A generalized graphical method for evaluating formation constants and summarizing well-field history. Transactions, American Geophysical Union 27, 526-534.
- De Glee, G.I., 1930. Over Groundwaterstromingen bij wateronttrekking door middel van putten. Thesis. J. Waltman, Delft, The Netherlands.
- De Glee, G.J., 1951. Berekeningsmethoden voor de winning van grondwater. Drinkwatervoorziening, 3e Vacantiecursus, 38-80.
- Dupuit, J., 1863. Études théoriques et pratiques sur le mouvement des eaux dans les canaux découverts et à travers les terrains perméables: avec des considérations relatives au régime des grandes eaux, au débouché à leur donner, et à la marche des alluvions dans les rivières à fond mobile, 2nd edn., Dunod, Paris.
- Foster, S.S., Lawrence, A., Morris, B., 1998. Groundwater in Urban Development: Assessing Management Needs and Formulating Policy Strategies. World Bank Publications, Washington, USA.
- Forsythe, G.E., Wasow, W.R., 1960. Finite-Difference Methods for Partial Differential Equations. Wiley. New York.

- Freeze, R.A., Cherry, J.A., 1979. Groundwater. Prentice Hall, USA.
- Glossop, R., 1950. Classification of Geotechnical Processes. *Géotechnique* 2(1), 3-12.
- Grube Jr, W.E., 1992. Slurry trench cut-off walls for environmental pollution control. Slurry walls: Design, construction, and quality control. ASTM STP 1129, 69-77.
- Halihan, T., Zlotnik, V.A., 2000. Asymmetric dipole-flow test in a fractured carbonate aquifer. *Ground Water* 40(5), 491-499.
- Hantush, M.S., 1956. Analysis of data from pumping tests in leaky aquifers. *Transactions, American Geophysical Union* 37, 702-714.
- Hantush, M.S., 1960. Modification of the theory of leaky aquifers. *Journal of Geophysical Research* 65(11), 3713-3725.
- Hantush, M.S., 1961a. Drawdown around a partially penetrating well, *Journal of the Hydraulics Division Proceedings of American Society of Civil Engineers* 87(HY4), 83-98.
- Hantush, M.S., 1961b. Aquifer tests on partially penetrating wells, *Journal of the Hydraulics Division Proceedings of American Society of Civil Engineers* 87(HY5), 171-195.
- Harris, J.S., 1995. Ground freezing in practice. Thomas Telford.
- Holzbecher, E., Jin, Y., Ebneith, S., 2011. Borehole pump & inject: an environmentally sound new method for groundwater lowering. *International Journal of Environmental Protection* 1(4), 53-58.
- Jameson, A., Schmidt, W., Turkel, E., 1981. Numerical solutions of the Euler equations by finite volume methods using Runge-Kutta time-stepping schemes. AIAA paper, 1259.
- Jin, Y., Holzbecher, E., Oberdorfer, P., 2011. Simulation of a novel groundwater lowering technique using arbitrary Lagrangian-Eulerian method. In: COMSOL Conference, Stuttgart, Germany.
- Jin, Y., Holzbecher, E., Sauter, M., Ebneith, S., 2012. Groundwater Sustainability through a Novel Dewatering Technology. In AGU Fall Meeting Abstracts Vol. 1, p. 1385.
- Kabala, Z.J., 1993. The dipole-flow test: a new single-borehole tests for aquifer characterization. *Water Resource Research* 29(1), 99-107.
- Kruseman, G.P., Ridder, N.A. (1990). Analysis and evaluation of pumping test data. International Institute for Land Reclamation and Improvement (ILRI) publication 47, Wageningen, The Netherlands.
- Liggett, J.A., Liu, P.L.F., 1983. The boundary integral equation method for porous media flow. *Applied Ocean Research* 5(2), 117.
- Narasimhan, T.N., Witherspoon, P.A., 1976. An integrated finite difference method for analyzing fluid flow in porous media. *Water Resources Research* 12(1), 57-64.
- Neuman, S.P., 1972. Theory of flow in unconfined aquifers considering delayed response of the water table. *Water Resources Research* 8(4), 1031-1045.
- Neuman, S.P., 1974. Effect of partial penetration on flow in unconfined aquifers considering delayed gravity response. *Water Resources Research* 10(2), 303-312.
- Neuman, S.P. 1975. Analysis of pumping test data from anisotropic unconfined aquifers considering delayed gravity response. *Water Resources Research* 11(2), 329-342.

- Neuman, S.P., Witherspoon, P.A., 1972. Field determination of the hydraulic properties of leaky multiple aquifer systems. *Water Resources Research* 8(5), 1284-1298.
- Pinder, G.F., Gray, W.G., 1977. *Finite Element Simulation in Surface and Subsurface Hydrology*. New York: Academic Press.
- Powers, J.P., Corwin, A.B., Schmall, P.C., Kaeck, W.E., Herridge, C.J., 2007. *Construction Dewatering and Groundwater Control-New Methods and Applications*. Third ed., John Wiley and Sons, USA.
- Preene, M., 2000. Assessment of settlements caused by groundwater control. *Proceedings of the ICE-Geotechnical Engineering*, 143(4), 177-190.
- Puller, M., 2003. *Deep Excavations: A Practical Manual*. Second ed., Thomas Telford, USA.
- Roy, D., Robinson, K.E., 2009. Surface settlements at a soft soil site due to bedrock dewatering. *Engineering Geology* 107(3-4), 109-117.
- Rupprecht, E., 1979. Application of the ground-freezing method to penetrate a sequence of water-bearing and dry formations—three construction cases. *Engineering Geology* 13(1), 541-546.
- Rushton, K.R., 2003. Front Matter, in *Groundwater Hydrology: Conceptual and Computational Models*, John Wiley & Sons, Ltd, Chichester, UK. doi: 10.1002/0470871660.fmatter.
- Strack, O.D., 1987. The analytic element method for regional groundwater modeling. In *Proceedings of the national water well association. Conference on solving groundwater problems with models*. Denver, CO (10-12).
- Streltsova, T.D., 1974. Drawdown in compressible unconfined aquifer. *Journal of the Hydraulics Division* 100(11), 1601-1616.
- Theis, C.V., 1935. The relation between the lowering of the piezometric surface and the rate and duration of discharge of a well using ground water storage. *Transactions of the American Geophysical Union* 2, 519-524.
- Thiem, G., 1906. *Hydrologische Methoden*, JM Gebhardt, Leipzig.
- Todd, D. K., Mays, L. W., 2005. *Groundwater Hydrology*. Third ed., Wiley, New Jersey.
- USGS, U.S. Geological Survey (2014). *The water cycle: groundwater storage*, <http://ga.water.usgs.gov/edu/watercycle/gwstorage.html> [Accessed August 28, 2014].
- Walton, W.C., 1962. *Selected Analytical Methods for Well and Aquifer Evaluation*. Illinois State Water Survey, Bull 49.
- Wang, S.Q., Wee, Y.P., Ofori, G., 2002. DSSDSS: a decision support system for dewatering systems selection. *Building and Environment* 37(6), 625-645.
- Weeks, E.P., 1969. Determining the Ratio of Horizontal to Vertical Permeability by Aquifer-Test Analysis. *Water Resources Research* 5(1), 196-214.
- Yeh, G.T., 1999. *Computational Subsurface Hydrology-Fluid Flows*. Kluwer Academic Publishers, USA.
- Ye, J., Liang, Y.M., Bian, J.H., 2012. Case study on composite method of well point dewatering and plastic drainage plate. *Journal of Waterway and Harbor* 33(4), 358-362.
- Zlotnik, V., Ledder, G., 1996. Theory of dipole flow in uniform anisotropic aquifers. *Water Resources Research* 32(4), 1119-1128.

Chapter 2

2 Borehole Pump and Inject: an Environmentally Sound New Method for Groundwater Lowering

Ekkehard Holzbecher¹, Yulan Jin^{1*}, Stefan Ebneht²

Citation:

Holzbecher, E., Jin, Y., Ebneht, S., 2011. Borehole Pump & Inject: an Environmentally Sound New Method for Groundwater Lowering. *International Journal of Environmental Protection* 1 (4), 53–58.

¹ Geoscience Centre, Dept. Applied Geology, University of Göttingen, Goldschmidtstr. 3, 37077 Göttingen, Germany

² Hölscher Wasserbau GmbH, Petzower Str. D-14542, Werder/Havel, Germany

* Corresponding author

Abstract

Groundwater lowering is usually required at construction sites, and for open pit mining, sometimes for aquifer remediation measures. Conventional methods lower the groundwater table by galleries of pumping wells. The pumped-out water is conducted to a distance place, where it is discharged back into the ground or into a surface water body. The system is criticized due to its environmental impacts, due to the disturbance of the local groundwater budget with negative effects on the eco-systems in the direct surroundings. Moreover, there may be severe problems connected with land subsidence and groundwater or surface water pollution. In contrast to current and traditional techniques, we propose a novel method (DSI method), which can achieve dewatering without water conveyance above ground. In the method, dewatering is reached by pumping, while groundwater conservation is achieved by re-injecting pumped water back into the deep aquifer in the same borehole. The DSI method aims to avoid environmental problems with water pumped to the surface and meanwhile to reduce the costs. In the paper, the DSI concept, referred to as “borehole pump and inject” is described in detail. We report the current state of a project with two test sites for field experiments as well. Numerical models, based on Darcy’s Law as physical principle, are built up in 2D and 3D to evaluate the field experiments. The lowering of the groundwater table is implemented using ALE (Arbitrary Lagrangian-Eulerian) and moving mesh methods.. Aquifer parameters are calibrated by inversely matching the modelled result to the measured field data. Our studies show a high potential for a promising future of the DSI method. The challenges are pointed out by discussing the limitations of the new method.

Acknowledgement

The authors appreciate the support of ‘Deutsche Bundesstiftung Umwelt (DBU)’ for funding within the DSI project (AZ 28299-23).

2.1 Introduction

Groundwater, constituting around thirty percent of the fresh water reserves (USGS, 2011), plays a key role in hydrologic cycle and ecosystem balances. Naturally, it interacts closely with surface water bodies by discharging into streams, lakes, wetlands, rivers, and into the sea. As a renewable resource, it is a major desirable source for the drinking water supplies all around the globe, for agriculture irrigations, as well as for industrial uses. Therefore, adequate attention to groundwater management including water conservation, efficiency in water utilization, and contamination control are needed to guarantee the water supply and to sustain ecosystems.

Groundwater is extracted not only for drinking water supply, but also for land use demand, e.g., urban constructions and mining. Also, some changes in land use require dewatering, mostly achieved by groundwater extraction. High pumping rates and insufficient groundwater recharge are the principle reasons for environmental problems such as land subsidence and soil degradation. The changed groundwater level usually has a negative effect on the vegetation and eco-systems in general.

Moreover, if the pumped water is of low quality, special water treatment may become necessary. Environmental regulations may not allow the injection of the water into another aquifer or in a surface water body, in order to avoid unwanted contaminations. Hence, it will induce extra costs to meet environmental regulations for injection water quality.

To avoid unnecessary groundwater extraction, to prevent contaminations, and/or to lower the costs, pump and inject installations in boreholes are proposed here as a novel alternative method for groundwater lowering at a site.

2.2 Borehole Pump and Inject

The conventional approach to groundwater lowering is to install one or more pumping wells, e.g., wellpoint dewatering, by which water is pumped to the surface

(Cashman and Preene, 2003; Powers et al., 2007). In the vicinity of the pumping wells the water table decreases in dependence of the distance to the different wells and the hydraulic properties of the porous medium in the subsurface. Also ambient groundwater flow, aquifer inhomogeneity and local conditions in the direct vicinity of the boreholes influence drawdown of the water table. In the conventional approach the pumped water is re-injected into the ground at a distant location or discharged into a nearby surface water body.

Düsenauginfiltration (DSI) is an innovative method introduced by W. Wils (Wils, 2010), which is literally translated as 'nozzle-suction-infiltration'. This new technology is referred here as borehole pump and inject (Figure 2.1).

In this novel approach, a pump is installed in the upper part of the borehole for pumping groundwater. Opposite to usual installations the water is pumped downward and thus injected back into the porous medium in the lower part of the borehole. Unlike in common state-of-the-art installations, water is not withdrawn above the ground.

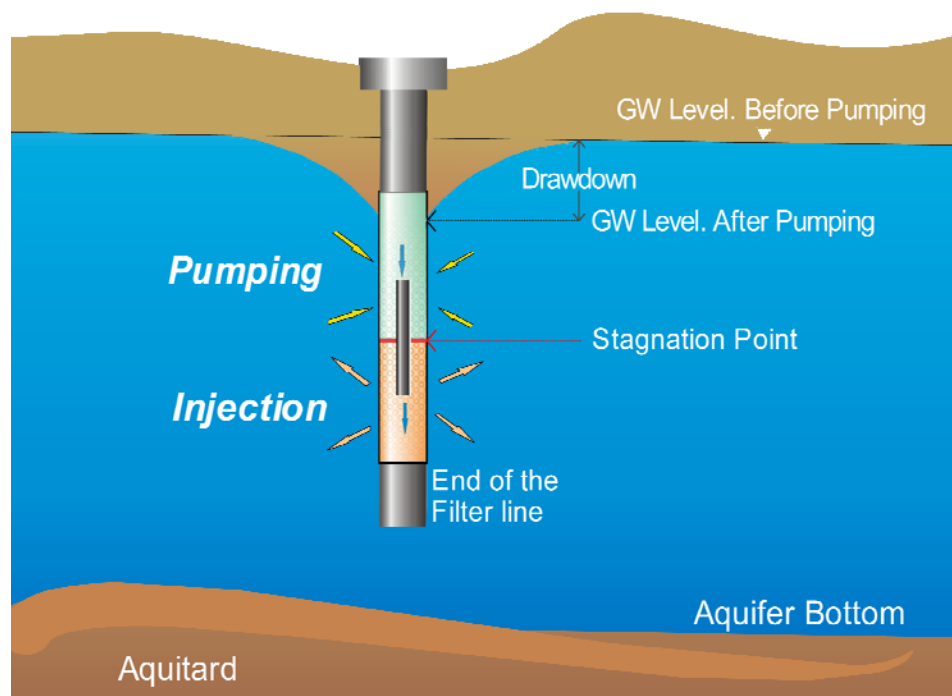


Fig. 2.1 Sketch of the borehole pump and inject concept.

Groundwater is pumped at the upper part (light green color region in Figure 2.1) of the borehole. Similar to classic pumping, pressure around the pumping region declines and consequently creates drawdown at the borehole and its surrounding. The pumped water is injected at the same rate deeper in the borehole (light orange color region in Figure 2.1). Near the injection points the pore water pressure and hydraulic head rise, forming a hydraulic barrier for the flowing groundwater. In addition some packers are usually used to separate the upper pumping and the lower infiltration part of the borehole. The installed packers prevent a shortcut between injection and pumping within the borehole.

Between pumping and injection points in the borehole, where packers are installed, stagnation point appears at the borehole wall, which separates pumping and infiltration regions. At the stagnation point the velocity of the groundwater is zero. The location of the stagnation point may also be effected by disturbed conditions in the direct vicinity of the borehole due to drilling, i.e., the skin zone.

2.3 Field Experiments

The novel borehole pump and inject technique is already applied successfully at various sites, mainly in Germany (Hölscher Wasserbau, 2011) and the Netherlands (van Tongeren, 2010), but also in other parts of the world, e.g., in China. Within a research project in Germany the DSI method is currently examined (see: acknowledgement) by using a combined approach of field experiments and numerical modeling.

As part of the above-mentioned project, two test sites are currently selected for field experiments: (i) Plötzin in Brandenburg and (ii) Korschenbroich in North Rhine-Westphalia; both sites located in Germany. While Plötzin is a pure experimental site, in Korschenbroich the technique is applied for groundwater lowering in an abandoned mining region, to prevent damages from rising groundwater.

The underground materials of the selected test sites were explored by interpreting the electrical conductivity (EC) logs. A common pumping test was performed and the aquifer parameters, i.e., aquifer permeability, were determined as results.

The unconfined aquifer at the Plötzin site contains mainly coarse sand and fine gravels. The groundwater level is around 1.5 m below ground and the aquifer depth is more than 40 m. Four groups of pumping and infiltration depths, within the range of 5 m to 12 m, are selected in the pumping well. 18 observation wells in two different depths are set up on both sides of the pumping well (or DSI well). The shallow observation wells (shallow observation in Figure 2.2) are in the depth of 6 m while the middle observation wells (middle observation in Figure 2.2) are in 8 m depth. In addition, one observation point (deep observation in Figure 2.2) was set up near the pumping well in the depth of 12 m.

Groundwater level changes are measured in all observation wells during the DSI tests and in traditional pumping tests (Kruseman and Ridder, 1994) and compared with the modeling results. First model approaches for the Plötzin site were presented in a report by Holzbecher (Holzbecher, 2009).

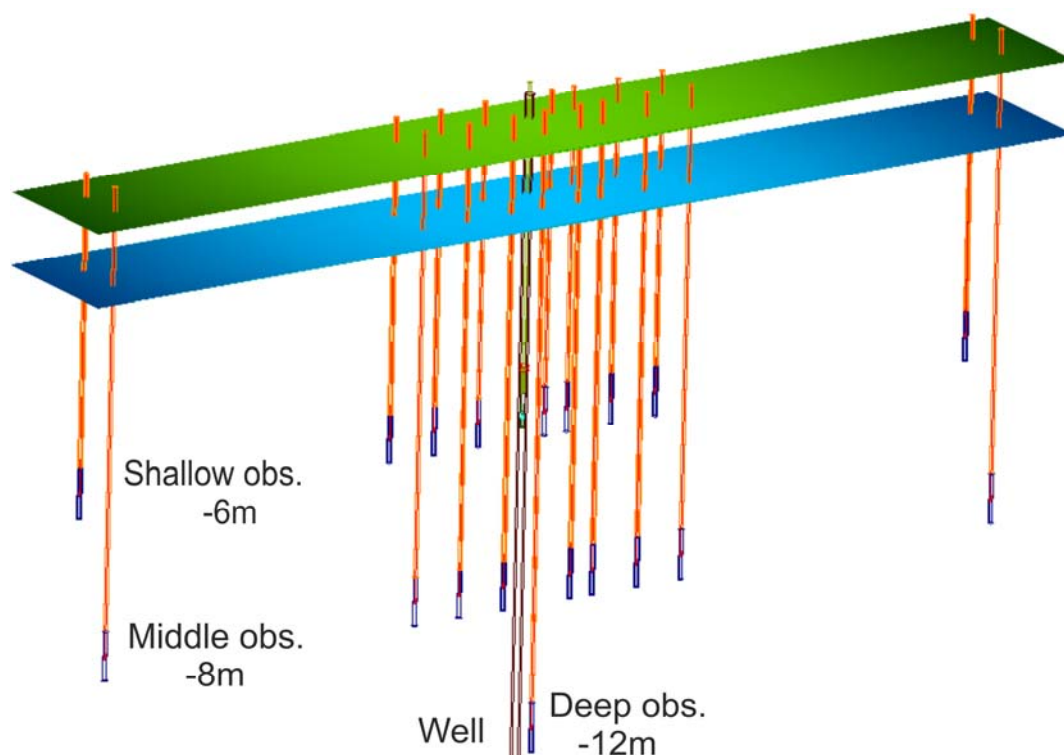


Fig. 2.2 Overview of Plötzin test site

Tests with multi pump and inject wells are scheduled also at the Korschenbroich site. The groundwater level at the test site is around 4 m below ground. The upper

layer of the aquifer, where the pumps are to be installed, contains mainly sandy materials. At the deeper part of the aquifer, where infiltration points are to be located, gravel is the dominating material. The experiments will start in autumn 2011. Results will be utilized for a numerical model.

2.4 Modeling

Computer models have been set up for a better understanding of the processes involved in the borehole pump and inject technology. They differ concerning spatial dimensions and time. The first models, presented in detail in (Holzbecher, 2009), are steady-state and transient, and in 3D. For sensitivity analysis, a simplified approach for steady-state in a 2D vertical cross-section is used. In all cases, a free boundary problem has to be solved, as the model region is identical with the saturated part of the unconfined aquifer. Radial coordinates around the well are used in the 2D simplified single well model rather than Cartesian coordinates in 3D models.

Within the project, COMSOL Multiphysics software (COMSOL Multiphysics, 2011) is used for modelling. This is a mathematical software for the solution of coupled differential equations, which is based on the finite element method. The program is equipped with a graphical user interface that allows easy modelling even for novices and technicians. Research was started using COMSOL version 3.5, but recently we switched to version 4.2.

In COMSOL Multiphysics, using different physics modes, the relevant physical processes can be coupled. Such coupling can be done in one or more physical compartments of the same or different dimensions. This allows the modeller to study processes, which in conventional approaches are usually not considered simultaneously. In this study, the groundwater flow equation is coupled with a moving boundary mode, as the geometry of the saturated part of the aquifer changes with drawdown.

2.4.1 Differential equation

In the homogeneous case, groundwater flow can be described by a potential equation for dynamic pressure p (Holzbecher, 1998; Bear and Cheng, 2010).

$$\nabla \cdot \mathbf{k} \nabla p = 0 \quad (2.1)$$

\mathbf{k} denotes the permeability tensor. The equation can be derived from empirical Darcy's Law and the principle of fluid mass conservation (Bear, 1976; Bear and Cheng, 2010). COMSOL Multiphysics solves the equation with total pressure as the dependent variable. Hydraulic head as function of space (and time in transient models) is computed as a post-processing step. In order to consider the deformation of the unconfined aquifer, i.e., the change of the saturated region in the vicinity of the wells, the Arbitrary Lagrangian-Eulerian method (ALE) (Donea et al., 2004) is applied. ALE constitutes a coordinate transformation from a fixed model region to a deformed model region; in 2D:

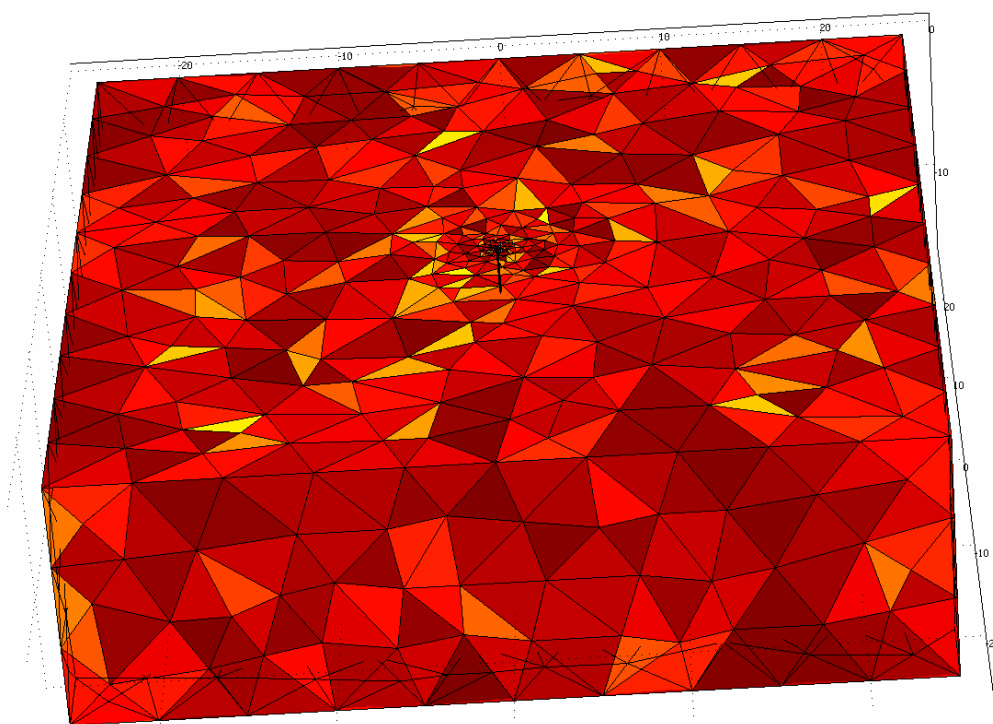


Fig. 2.3 Typical 3D finite element mesh for a single well problem.

2.4.2 Meshing and discretization

According to the finite element method COMSOL Multiphysics by default uses triangular (2D) and tetrahedron meshes (3D) with quadratic shape functions. In the vicinity of the wells the mesh is refined. In the vicinity of the pumping and infiltration points the mesh is extra refined. A typical mesh for 3D model is presented in Figure 2.3.

The shown mesh has 45,917 elements 8,496 nodes and the problem has 64,785 degrees of freedom. A 2D model of the same complexity has much lower degree of freedom.

2.4.3 Model region and boundary conditions

The model region concerns the saturated part of the aquifer, i.e., the groundwater table is upper (free) boundary of the model region, where we require atmospheric pressure as boundary condition. A sketch of the situation is depicted in Figure 2.4.

At the free boundary (part d in Figure 2.4), which is the interface to the vadose zone, we require a no-flow condition, i.e., the pressure derivative in normal direction to vanish:

$$\frac{\partial p}{\partial n} = 0 \quad (2.2)$$

or formulated in terms of velocity. Note that we here consider the situation without groundwater recharge. As a second condition we require atmospheric pressure $p = 0$ atm at this boundary, which in the model is fulfilled due to the ALE condition described above.

Lower boundary is the base of the aquifer, i.e., at the aquitard (part b in Figure 2.4), where a no-flow boundary is required. At the outer model edge ($r = r_o$, part c in Figure 2.4) we require a constant hydraulic pressure, i.e., we assume that the flow is horizontal.

The well itself is not modelled. In 3D models the wells appear as holes within the model region. In 2D models the inner radius of the model region is identical with the borehole radius r_b (part a in Figure 2.4).

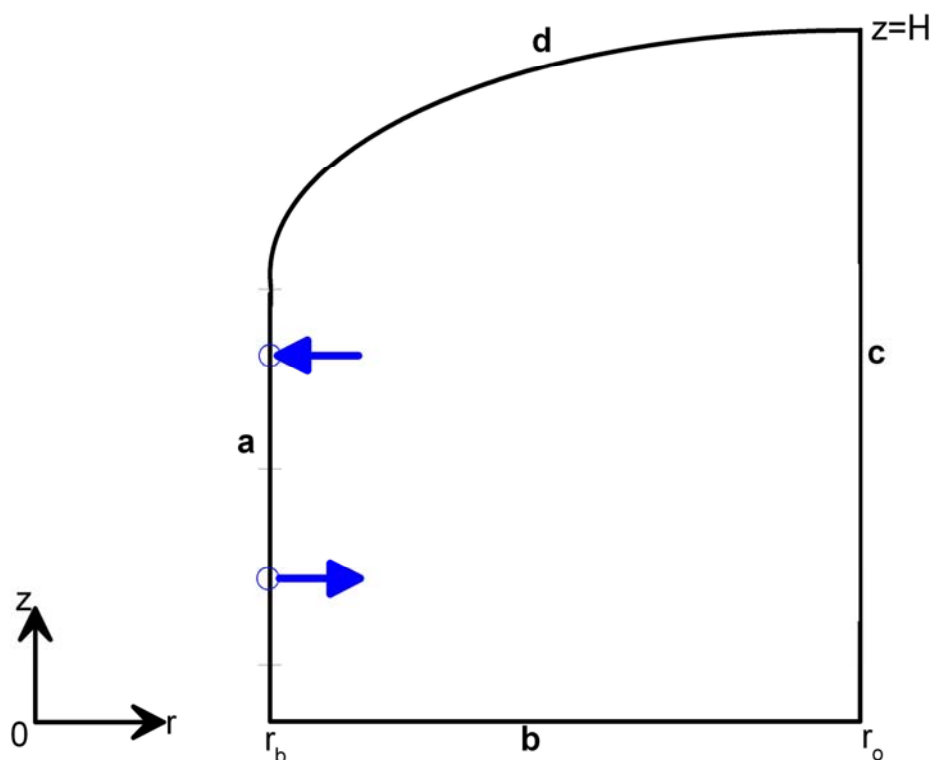


Fig. 2.4 Sketch of deformed model region and boundaries in a 2D model.

The borehole boundaries are divided into five different parts, which are indicated in Figure 2.4 (compare also with Figure 2.1). Listed from top to the bottom these are:

- above the pump location
- below pump location and stagnation point
- between stagnation point and infiltration level
- between infiltration level and end of borehole
- between bottom of the borehole and base of aquifer

In the uppermost two parts water is pumped, while in the two parts below water is injected. This is reflected by the boundary conditions.

Different boundary conditions have to be applied for every part of the divided region. In the upper part of the well, above the pumping position, the coordinate transformation, mentioned above is effective. The radial velocity is specified based on the equation:

$$v_r = \frac{\theta Q_{well}}{2\pi r_b H} \log\left(\frac{z' - z_p}{H}\right) \quad (2.3)$$

The radial velocity v_r is given by a logarithmic distribution at the upper sides of both pumping point z_p , as function of variable depth in the transformed system. The influencing parameters are the pumping rate Q_{well} , the length of the boundary part H , and the distribution factor θ . For $\theta = 0.5$ half of the water is pumped above the pumping position.

For the three parts below the pumping position we use the same approach as in Equation (2.3) with the difference that we do not have to distinguish between the fixed and the transformed coordinates. In analogy to Equation (2.3) we require:

$$v_r = \frac{\theta Q_{well}}{2\pi r_b H} \log\left(\frac{z - z_s}{H}\right) \quad (2.4)$$

In Equation (2.4) z_s denotes the pumping position for the part between pump and stagnation point, while it denotes the infiltration position for those two parts, in which infiltration appears.

With this choice of boundary conditions we obtain singularities of radial velocity at the pumping and the injecting location. However, this is not a serious problem for the numerical method, as the computed values always remain finite due to numerical imprecision. The advantage of the approach is that for appropriate values of θ the change of v_r at the stagnation point is smooth (even differentiable).

In the lowest part of boundary a (Figure 2.4), i.e., below the well screen and below the bottom of the borehole it is reasonable to require the no-flow condition.

2.4.4 Input values

Parameter values for a reference case are listed in Table 2.1. The aquifer parameters are mainly obtained from the result of the classic pumping test. Water is pumped from the pumping well, and the responses are measured at the observation wells. Aquifer parameters are calibrated and applied for pump-inject tests. In several sensitivity analyses we studied the effect of the different parameters. These are mainly taken from the Plötzin test site.

Table 2.1 Input values for reference set up.

Parameter	Value	Unit
Hydraulic conductivity	1.5×10^{-3}	m/s
Anisotropy factor	10	-
Width of skin region	0.12	m
Hydraulic conductivity inside skin	1.5×10^{-1}	m/s
Pumping rate (Pumping test)	59.6	m ³ /h
Pumping/Infiltration rate (DSI test)	22	m ³ /h
Porosity	0.2	-
Distribution factor	0.5	-

Note that we have introduced an anisotropy concerning the permeability. Moreover a skin zone is assumed to extend in the direct vicinity of the borehole, which appears due to the disturbances of the porous medium via the pumping process.

2.5 Results and Discussion

Here we describe two experiments performed at the Plötzin test site. The constellation of the experiment was already shown in Figure 2.2. The results of a classical pumping test are contrasted with measurements from a DSI-test. To understand and visualize the processes and to obtain an insight how the system works under different test conditions, computer models were set up and the results are present below. The final subchapter concerns the modelling of the tests.

2.5.1 Aquifer response on pumping test

The pumping test was conducted at 6.5 m depth with the pumping rate of 59.6 m³/h. Figure 2.5 displays the measured hydraulic head change in the observation wells respecting the distances of observation points from the pumping well. The figure respects the geometry of the test site. The absolute value of x-axis

shows the distances of observation wells from the pumping well. And the positive and negative symbols indicate the right and left side of the pumping well. The observation wells are grouped respecting the depth and their locations, which are shallow (-6m), middle (-8m), and deep (-12m).

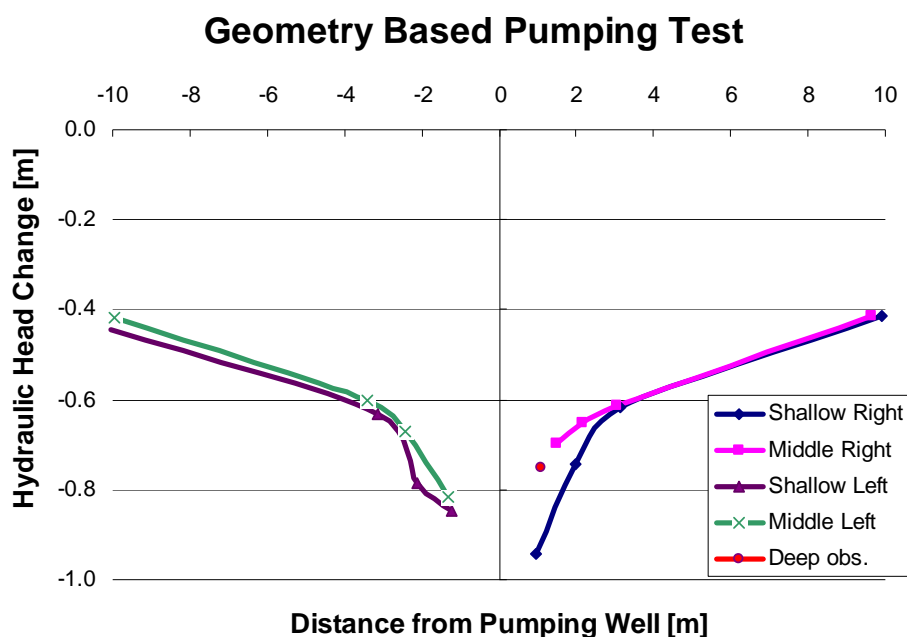


Fig. 2.5 Hydraulic head changes in dependence of distance from the well and well screen position (shallow, middle, deep), observed in a classical pumping test.

Note that the change of head is dependent on the depth, reflecting the fact that the flow towards the well is highest at the groundwater table and decreases with the depth (in an ideal well). Also the Dupuit-assumption of pure horizontal flow, which is often taken into account in groundwater studies (see for example Harr, (1991)), does not hold in the very vicinity of the well.

The result shows lower head on the right side (-0.95) of the pumping well than on the left side (-0.85). Also, higher drawdown (lower head) values are measured at the shallow observation wells rather than the deeper observation wells. The measured values reflect the horizontal and vertical inhomogeneity of the aquifer. In horizontal direction, the inhomogeneity may also occur due to the groundwater flow from the left to right direction. To simplify the model, anisotropic factor of 10 is applied only in vertical direction.

2.5.2 Aquifer Response on pump-inject (DSI) Test

We measured the aquifer responses of four groups of the DSI tests. Here we demonstrate one of the obtained results, where the pump was installed at the depth of 5.5 m and water was injected at 8.5 m depth in the case Different with the pumping test, the pumping and injection rates ($22 \text{ m}^3/\text{s}$) were reduced in the DSI test. For that reason the drawdown is smaller than in the pumping test. As result Figure 2.6 displays the drawdown measured at the same observation wells as in the pumping test above.

The change of hydraulic head depends on the observation depth. Here the depth is represented by the different well screens, i.e., shallow, middle and deep wells. Note that lowering of hydraulic head can be observed in the shallow observation wells only, corresponding with a lowering of the water table. In comparison to the pumping test the head values in the intermediate depth can be expected to remain more near the original level, while the head in the deep aquifer will rise due to the influence from injection.

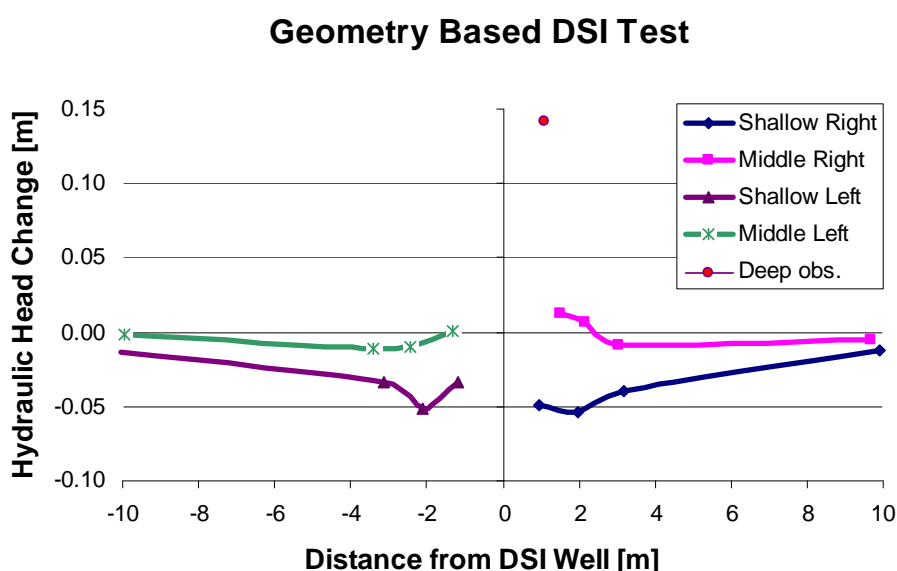


Fig. 2.6 Hydraulic head changes in dependence of distance from the well and well screen position (shallow, middle, deep), observed in a pump-inject DSI test.

As expected, lower hydraulic heads (-0.05 m) are observed near the pumping area from the shallow observation wells. Hydraulic pressure increases slightly (0.02 m)

near the injection area, as observed in the middle observation wells. Relatively high hydraulic pressure (0.15 m) is measured at the deep observation well. Very low or no responses were observed at the observation wells far away from pump-inject region.

2.5.3 Aquifer parameter evaluation

Aquifer parameters, e.g., aquifer conductivity, are estimated in a calibration procedure, which provides the best matches of numerical results with the measured data. The pumping test result is used for calibration.

Figure 2.7 depicts the differences between model and field results in a histogram. Shallow (*-1) and middle deep (*-2) observation wells are listed along the x-axis (* is the well number). The y-axis measures the absolute value of the difference of the modelled results with the measured hydraulic heads in the observation wells accordingly. The maximum difference of approximately 0.1 m is very satisfactory, in relation to the maximum drawdown in the borehole of approximately 1 m. The obtained aquifer parameters are directly applied in the DSI models.

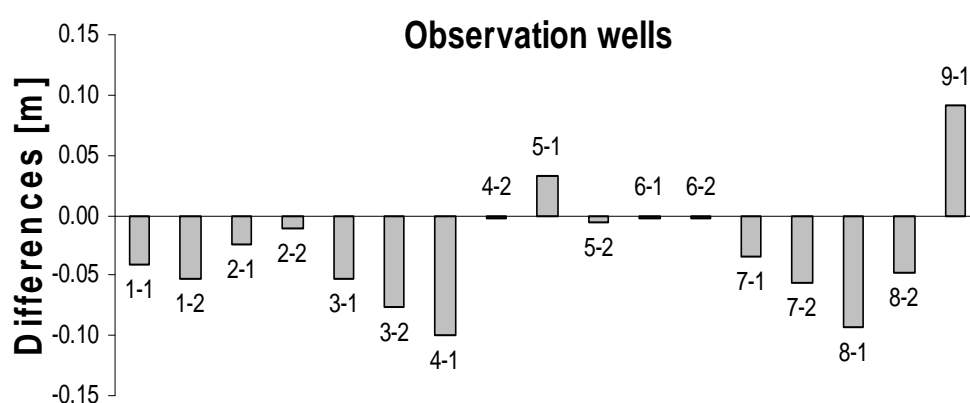


Fig. 2.7 Differences in hydraulic head of model results and pumping test observations in a histogram.

2.5.4 Modelling result of DSI test

Figure 2.8 illustrates the typical result obtained with a 2D model concerning the vertical cross section for a single well (in the figure on the left). Drawdown is created and presented by the deformed geometry.

In the display hydraulic head is lowered to more than -1 m at the upper part (blue color) of the borehole. However, the measured result showed only 0.05 m decline of hydraulic head. That is due to the deformation scale factor used in COMSOL software. A large scale factor helps to present a better view of the physical system. The actual calculated drawdown from the model result was 0.04 m near the borehole, which matches quite well with the measurements.

At the lower part (dark red color) of the borehole, the potential of hydraulic head is increased. That corresponds well with the observed result shown in Figure 2.8. The groundwater flow directions and velocities are indicated with arrows in the figure.

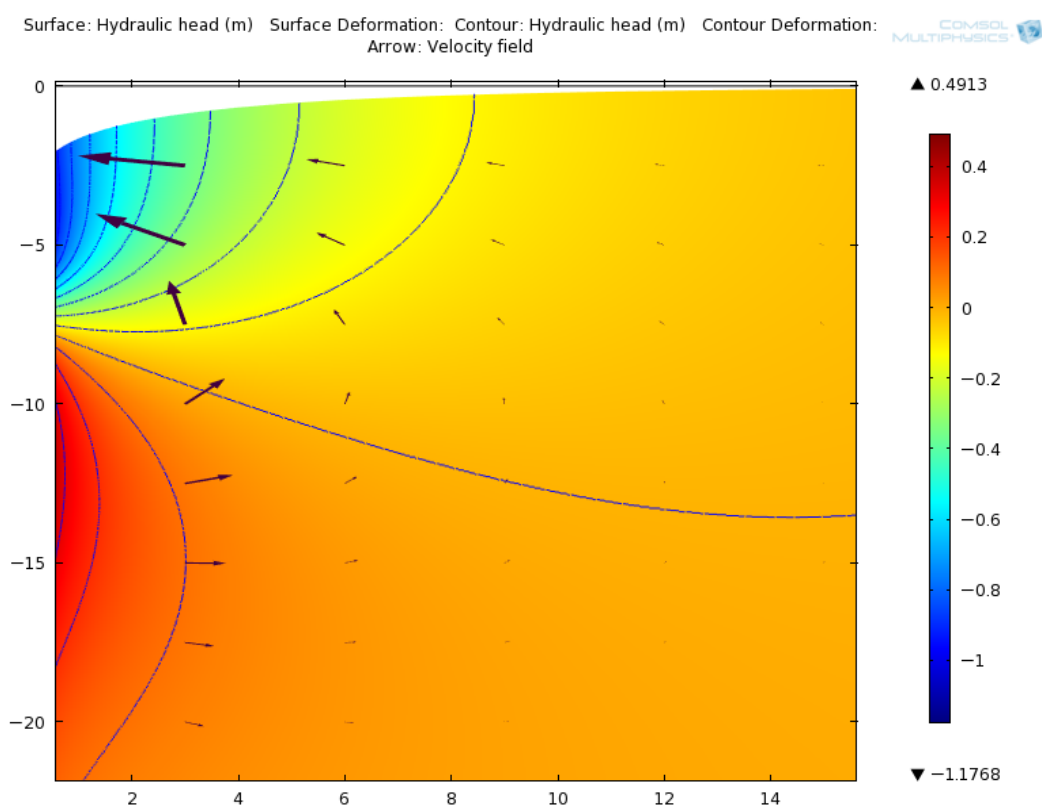


Fig. 2.8 Example of model output for vertical cross section around a single well: potential contours (filled) and velocity field in deformed geometry.

For a better view the model result is also illustrated by a 3D image (Figure 2.9). Drawdown at the top of the aquifer can clearly be observed (light blue region). Similar with the 2D result, higher hydraulic pressure is indicated with red color around the injection area.

A 3D model is required for the Korschenbroich test site with several pump-inject wells. It gives the opportunity to consider the horizontal and vertical anisotropic conditions of the aquifer, as well as the influence of regional groundwater flow.

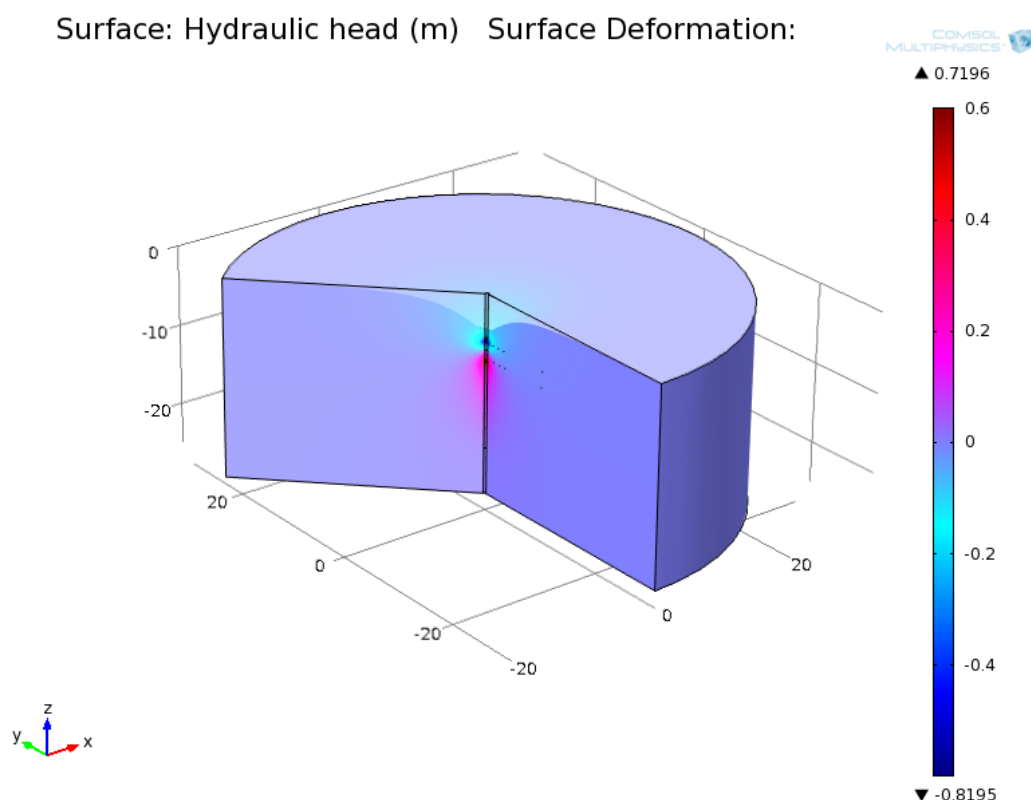


Fig. 2.9 3D visualization of model output .

2.6 Conclusions

In the paper, a novel dewatering technique (DSI) is proposed and investigated through a first field test. Computer models were set up to understand the involved physics and to estimate the relevant parameters.

The results show that dewatering can be achieved without groundwater conveyance above ground. Due to its advantages concerning environmental and

economical aspects, the presented borehole pump and inject technique can be expected to have an optimistic future as it may become a state-of-the-art method of groundwater lowering in permeable aquifers

However, the following limitations still have to be studied

- the method can be applied for permeable aquifers only
- a shortcut between pumping and infiltration region in the direct vicinity of the borehole has to be avoided
- temporal or long time changes of conditions, e.g., seasonal changes in groundwater recharge, may affect the groundwater circulation and drawdown

While these limitations surely can not be overcome in principle, it is yet not clear, under which conditions the DSI technique delivers sufficient drawdown of the groundwater table. Therefore, future work will focus on understanding site-specific conditions, which are relevant for the application of DSI method. The project will conduct further experiments at the two mentioned sites considering situations with different installations concerning pump and packers. In order to examine the influences of the different parameters a sensitivity analysis will be performed by already set-up and extended numerical models.

Furthermore, an understanding of the long-term performance of the method is still needed. The influence of ambient groundwater flow on the performance of the method is to be examined as well.

2.7 References

Bear, J., 1976. *Hydraulics of Groundwater*, Mc Graw Hill, New York.

Bear, J., Cheng, A.H.-D., 2010. *Modeling Groundwater Flow and Contaminant Transport*, Springer, Heidelberg.

Cashman, P.M., Preene, M., 2003. *Groundwater Lowering in Construction: A Practical Guide*, Second ed., CRC Press, USA.

COMSOL Multiphysics, 2011. Version 4.1, <http://www.comsol.com>, [Accessed September 12, 2011].

- Donea, J., Huerta, A., Ponthot, J.-Ph., Rodriguez-Ferran, A., 2004. Arbitrary Lagrangian-Eulerian methods, In: Stein, E., de Borst, R., Hughes, T.J.R. (Eds.), *Encyclopedia of Computational Mechanics*, Vol. 1, John Wiley & Sons, New York, pp. 413-434.
- Harr, M.E., 1991. *Groundwater and Seepage*, Dover Publ., New York.
- Hölscher Wasserbau, 2011. Hölscher dewatering DSI, <http://www.hoelscher-wasserbau.de/seiten/index.html>, [Accessed September 23, 2011].
- Holzbecher, E., 1998. *Modeling Density-Driven Flow in Porous Media*, Springer, Berlin.
- Holzbecher, E., 2009. *Modellierung Pumpexperiment Magna-Park*, Juli/August 2009. Report by order of Hölscher Wasserbau.
- Kruseman, G.P., de Ridder, N.A., 1994. *Analysis and Evaluation of Pumping Test Data*. Second ed., Publication 47, Intern. Inst. for Land Reclamation and Improvement, Wageningen, The Netherland.
- Powers, J.P., Corwin, A.B., Schmall, P.C., Kaeck, W.E., Herridge, C.J., 2007. *Construction Dewatering and Groundwater Control-New Methods and Applications*. Third ed. John Wiley and Sons, United States of America.
- van Tongeren, H., 2010. DSI, “Het duurzame alternatief”, <http://www.henkvantongeren.nl/index.php?page=dsi>, [Accessed September 13, 2011].
- Wils, W., 2010. *Druckwellen System Düsenauginfiltration*.
- USGS, 2011. *The water cycle: groundwater storage*, <http://ga.water.usgs.gov/edu/watercyclegwstorage.html>, U.S. Geological Survey, [Accessed September 17, 2011].

Chapter 3

3 A Novel Modeling Approach Using Arbitrary Lagrangian-Eulerian (ALE) Method for the Flow Simulation in Unconfined Aquifers

Yulan Jin*, Ekkehard Holzbecher, Martin Sauter

Citation:

Jin, Y., Holzbecher, E., Sauter, M., 2014. A Novel Modeling Approach Using Arbitrary Lagrangian-Eulerian (ALE) Method for the Flow Simulation in Unconfined Aquifers. *Computers & Geosciences* 62, 88–94.

Geoscience Centre, Dept. Applied Geology, University of Göttingen, Goldschmidtstr. 3, 37077 Göttingen, Germany

* Corresponding author

Abstract

The problem of groundwater flow in an unconfined aquifer, formulated as a free-surface problem, is solved numerically through a new approach by employing the arbitrary Lagrangian-Eulerian (ALE) method. The domain of interest is three dimensional or a two dimensional vertical cross section of a phreatic zone of an aquifer, where the groundwater table is the upper boundary that is allowed to move. The ALE method allows capturing the location of the free-surface by transforming the moving domain to a fixed reference domain through arbitrary forced boundary conditions. The results of the verification runs of this new approach agree well with the known analytical solutions for aquifer characterization tests. Beside the comprehensive and accurate evaluation of the groundwater flow in the tested cases, the approach is also suitable for modeling complex situations. The implementation of our method for selected cases is illustrated by means of practically relevant examples.

Acknowledgement

The authors appreciate the support of ‘Deutsche Bundesstiftung Umwelt (DBU)’ for funding within the DSI project (AZ 28299-23).

Nomenclature

α	porous medium compressibility
β	fluid compressibility
μ	fluid viscosity
ρ	fluid density
φ	porosity
Ω_x	spatial domain
Ω_x	reference domain
g	acceleration due to gravity
h	hydraulic head
\mathbf{k}	tensor for aquifer permeability
p	pressure
q	recharge/discharge
t	time
z	spatial axis in vertical direction
F	mesh deformation gradient
K	hydraulic conductivity
\mathbf{K}	tensor for hydraulic conductivity
L	length of an aquifer
Q	pumping rate
S	storage coefficient

3.1 Introduction

The characterization of subsurface flow in unconfined aquifers is a challenging task, given the difficulty of identifying the precise groundwater table (free-surface) positions (Castro-Orgaz and Giráldez, 2012). Analytical solutions can be obtained only when simplifying assumptions, such as Dupuit approximation, are introduced. It assumes 1) that the streamlines are horizontal for small inclinations of the line of seepage and 2) that the hydraulic gradient does not depend on depth and thus equals to the slope of the free surface (see also Harr, 1962; Strack, 1989). Steady-state unconfined flow and flow towards a well were described by Dupuit (1863) under these assumptions. Subsequently, analytical solutions were derived for unsteady unconfined flow (i.e., Boussinesq, 1904) and also for specific applications, such as evaluation of a pumping test (i.e., Neuman, 1972). However, all these analytical solutions assume a fixed water table condition even close to the pumping well, where a large drawdown is usually observed (Mishra and Kuhlman, 2013). The groundwater flow here is more complex and, therefore, the vertical flow can not be neglected for many relevant applications (Bevan et al., 2005; Dagan et al., 2009; Bunn et al., 2011; Mishra and Kuhlman, 2013). Moreover, the inaccuracy of Dupuit's assumptions was demonstrated by Desbarats and Bachu (1994), Tartakovsky et al. (2000) and Dagan et al. (2009).

Another exact solution for two-dimensional steady flow is given by the so-called hodograph method, which depends on finding conformal mappings of the flow region in the physical plane (i.e., Bear, 1972; Bakker, 1997). However, the method also fails to yield an analytical solution, when the geometry of the boundaries becomes complicate (Bear, 1972). Consequently, the main limitation of analytical methods is that they are only available for relatively simple problems and are not flexible to describe complex application problems in detail (Bear and Verruijt, 1987).

Numerical methods, which have been developed since the 1960s' (Fayers and Sheldon, 1962; Remson et al., 1965; Freeze and Witherspoon, 1966), have the advantage that they are applicable for more general situations when compared with analytical methods. In principle, two conceptual approaches are used: 1) the partially saturated or unsaturated-saturated flow approach, and 2) the fully

saturated or water table/free-surface flow approach. On the one hand, the first approach considers the entire flow domain and solves the Richards equation above the water table and the groundwater flow equation at the saturated parts of an aquifer. The second approach, on the other hand, considers only the saturated parts of an aquifer and solves a free-surface problem. Models following the first approach are able to provide a more holistic and rigorous analysis of flow processes. However, the solution is usually hampered due to the difficulties of obtaining site-specific data for the unsaturated zone and due to the computational complications (Knupp, 1996; Feddes et al., 2004).

In the view of these difficulties, the majority of groundwater models use the second approach, which takes the groundwater table as the upper moving boundary of the saturated zone and relocates its position iteratively during the computation. One of the most common methods is that employed in MODFLOW (McDonald and Harbaugh, 1988; Harbaugh et al., 2000). It solves either the confined or the unconfined groundwater flow equation depending on whether the grid is saturated or contains the water table. Limitations associated with this method, i.e., dry cells, numerical instability, and numerical errors, have been discussed in Harbaugh et al. (2000), Naff et al. (2003), Banta (2006), Zyvoloski and Vessilinov (2006), Keating and Zyvoloski (2009). Another idea is to solve the free-surface problem with the location of the groundwater table as an additional unknown and adjust the mesh accordingly. Following this idea, Diersch (2009) introduced a so-called BASD (Best-Adaptation-to-Stratigraphic Data) method to trace the location of the free-surface with the software FEFLOW. However, this method requires a 3D model.

The main objective of this study is to provide a comprehensive simulation method that is able to capture the groundwater table position of an unconfined aquifer without having the above mentioned restrictions. In this paper, we follow the second conceptual approach and solve the free-surface problem only for steady-state. The novel treatment of the free-surface is implemented making use of a generic mathematical algorithm, the arbitrary Lagrangian-Eulerian (ALE) method, in the flow simulation.

The paper is structured as follows. After reviewing the governing equations for groundwater flow in unconfined aquifer, the ALE method as well as its application

on solving free-surface problem is intensively discussed. This new method is tested by comparing the simulation results with the analytical solutions derived for classical cases. Furthermore, the advantages of this simulation method are presented through the relevant application cases. Finally, we summarize the paper and present the conclusions.

3.2 Governing Equations

The governing equation that describes the flow of groundwater in saturated porous media is developed from the fundamental principle of mass conservation (continuity equation) and Darcy's Law. A detailed derivation of the governing equations is provided by Bear (1972) and Bear and Verruijt (1987). The governing equation for transient flow in unconfined aquifers is given as:

$$(\alpha + \varphi\beta) \frac{\partial p}{\partial t} - q = \nabla \cdot \frac{\mathbf{k}}{\mu} \nabla (p + \rho g z) \quad (3.1)$$

where β , ρ and μ denote the fluid properties compressibility, density and viscosity, α and φ represent the porous medium compressibility and porosity, q is the recharge or discharge, \mathbf{k} indicates the tensor for aquifer permeability, t is time, g is the acceleration due to gravity and z denotes the spatial axis in vertical direction. The unknown variable of the differential equation is the pressure p .

Equation (3.1) can be also stated in terms of hydraulic head h that is defined as $h = z + p/\rho g$. For constant ρ results:

$$S \frac{\partial h}{\partial t} - q = \nabla \cdot \mathbf{K} \nabla h \quad (3.2)$$

where the tensor for hydraulic conductivity \mathbf{K} is given by $\mathbf{K} = \mathbf{k} \rho g / \mu$, and the storage coefficient or storativity S is presented by $S = \rho g (\alpha + \varphi\beta)$.

At steady-state, Equation (3.2) can be simplified to:

$$\nabla \cdot \mathbf{K} \nabla h + q = 0 \quad (3.3)$$

In the case where q is not considered, Equation (3.3) results in Laplace's equation.

3.3 The Novel Numerical Approach

3.3.1 Model domain and groundwater flow equation

In the following examples, we solve the problems for steady-state only. Two conditions need to be fulfilled at the free-surface: 1) zero pressure and 2) flow of groundwater recharge or discharge across the interface. Condition 1) is a Dirichlet condition for pressure where the atmospheric pressure is set to zero. Condition 2) is a Neumann condition for flow across the surface. In case that q can be neglected, it is of usual no-flow type. In the problem formulation, our strategy is to connect these two conditions by defining the flux condition for the flow equation and the pressure condition for the free-surface. To fulfill both conditions, the flow equation and the free-surface algorithm are coupled.

3.3.2 Tracing free-surface deformation with the ALE method

The ALE method is a hybrid description which uses a moving mesh to follow the change of a boundary simultaneously. More precisely, in this formulation, the coordinate system of the problem domain moves in a certain prescribed manner, which allows the computational mesh to follow or to deform together with the change of a free-surface. For more details about this algorithm one may refer the articles by Denea et al. (2004). The ALE method has already been used for simulating general free-surface problems (e.g., Maury, 1996; Duarte et al., 2004; Pohjoranta and Tenno, 2011). To our knowledge, however, it has not yet been implemented in the area of groundwater flow simulations.

The basic principle of the ALE method is to superimpose the arbitrary deformed domain Ω_x , or spatial domain, and the corresponding coordinates (x, y, z) on top of a reference domain Ω_x where the coordinates are (X, Y, Z) , for the three dimensional Cartesian coordinates. For a 2D axi-symmetric geometry, cylindrical coordinates (r, z) and (R, Z) can be used for the spatial and reference domain respectively. To implement the ALE method in our model, the reference domain Ω_x , where initial conditions are applied, is fixed to provide the base. Equation (3.1) is formulated in the spatial domain Ω_x with the respective coordinate system of (x, y, z) , where the

mesh deforms to fit the pressure condition at the free-surface. As a result, a mesh deformation gradient, $\mathbf{F} = \partial\mathbf{x}/\partial\mathbf{X}$, is generated in time. The simulation results are delivered back to the reference domain Ω_x through inverse transformation (\mathbf{F}^{-1}). This implies that all the differential terms calculated in the differential equations of the spatial coordinate system are formulated as a function of differentials in the reference system. The detailed description of the inverse transformation functions are provided by Donea et al. (2004) and Pohjoranta and Tenno (2011). In the result, mesh deformation is modified via considering the difference of the locations ($x-X$) in the current and the reference systems.

Numerical investigations are carried out using COMSOL Multiphysics (2012), a finite element method (FEM) based software package for the solution of coupled systems of partial differential equations (PDEs). The user may choose to use general PDEs formulations directly or to use predefined modes for application fields. In this paper, we couple Darcy's Law mode and ALE mode to solve flow equation and free-surface problem respectively. In the Darcy's Law mode, groundwater flow is simulated by solving Equation (3.1) for the spatial domain. In the ALE mode, where free deformation of the domain is allowed, mesh displacements are defined at boundaries to obtain mesh velocities. In this paper as typical constraint at the groundwater table atmospheric pressure (Dirichlet boundary) is applied for mesh displacements along the free-surface.

To obtain the mesh point location in the current coordinate system, meshes need to be updated by using one of the following smoothing methods. These are Laplace smoothing, Winslow smoothing or hyperelastic smoothing (Knupp, 1999; Zhang et al., 2012). Among the various smoothing methods, we utilize stationary Laplace smoothing throughout, due to its generality and to its ease of implementation (Knupp, 1999; Shontz, 2005; Pohjoranta and Tenno, 2011). The method is applied through Equation (3.4), where the coordinates are taken for a 2D axi-symmetric model.

$$\frac{\partial^2 R}{\partial r^2} + \frac{\partial^2 R}{\partial z^2} = 0 \quad \frac{\partial^2 Z}{\partial r^2} + \frac{\partial^2 Z}{\partial z^2} = 0 \quad (3.4)$$

The limitation of the Laplace smoothing is that it sometimes result in mesh folding or spillover. This limitation can be solved when the Winslow smoothing is used due to its resistance to grid folding (Knupp, 1999; Shontz, 2005). Hyperelastic smoothing can give even smoother result than Winslow especially in regions where mesh is stretched (Shontz, 2005). However, both Winslow and hyperelastic smoothing are nonlinear, and therefore, more expensive in terms of computations than the Laplace smoothing method.

3.4 Simulation Experiments

The verification runs for our model are conducted for two classic cases, steady groundwater flow and steady radial flow towards a well in an unconfined aquifer. We formulate these two cases expressly simple in order to be able to compare the results with analytical solutions. Hence, uniform homogenous and isotropic unconfined aquifers are assumed in our simulations.

3.4.1 Case 1: Steady-state unconfined flow

3.4.1.1 Analytical approach

Figure 3.1 illustrates steady groundwater flow induced by a natural hydraulic gradient in an unconfined aquifer underlain by an impermeable bottom, essentially 1D flow. Following Darcy's Law, the governing equation for 1D steady flow was described by Forchheimer (1901):

$$\frac{K}{2} \frac{\partial(h^2)}{\partial x^2} + q = 0 \quad (3.5)$$

where K denotes horizontal hydraulic conductivity and x represents the distance. Following Dupuit assumption, the analytical solution to Equation (3.5) is:

$$h(x) = \sqrt{-\frac{q}{K}x^2 + \left(\frac{h_L^2 - h_0^2}{L} + \frac{qL}{K}\right)x + h_0^2} \quad (3.6)$$

where L denotes the length of an aquifer, h_0 and h_L are the hydraulic heads at ($x = 0$) and ($x = L$) respectively. When q is neglected, we obtain:

$$h(x) = \sqrt{h_0^2 + \frac{h_L^2 - h_0^2}{L}x} \quad (3.7)$$

Equation (3.7) is also known as Dupuit Parabola. (detail derivation see i.e., Fetter, 1994).

3.4.1.2 Numerical approach using the ALE method

We simulated groundwater flow along 100-meter long aquifer with a hydraulic gradient, $dx/dh = 0.02$. Although Equation (3.6) and (3.7) represent 1D situation, we require a 2D (xz -plane) vertical cross section for the problem domain to present the deformation of the geometry (see Figure 3.1).

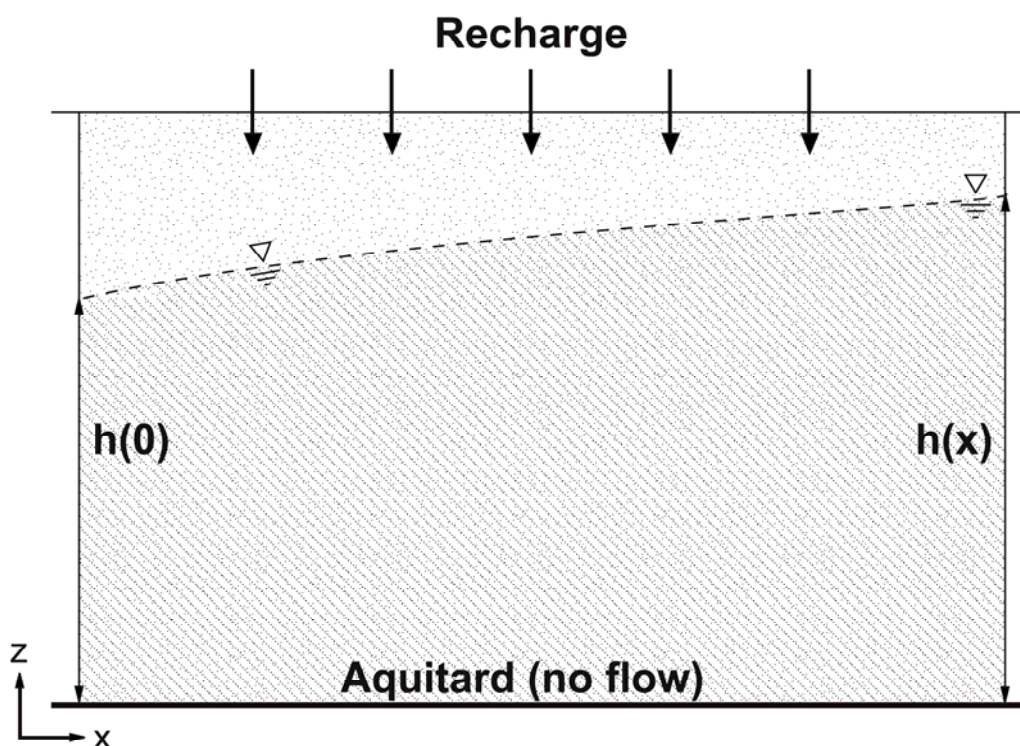


Fig. 3.1 Definition sketch of unconfined groundwater flow for 2D vertical-cross-section geometry.

In the Darcy's Law mode, a no-flow condition is used for the impervious bottom of the aquifer. The hydraulic gradient is generated by using fixed hydraulic heads, e.g., 10 m for $h(0)$ and 12 m for $h(x)$, for inner and outer boundaries, respectively. Recharge (e.g., $q = 10^{-6}$ m/s), is reflected by an inflow condition at the upper

boundary with a uniform and constant rate. When $q = 0$, no-flow condition is applied instead.

In the ALE mode, the entire modeling domain can be freely deformed. The displacements of the boundaries are specified accordingly to allow or to stop boundary movement. We impose a pressure condition at the upper boundary to fit to atmospheric pressure. The outer vertical boundaries are allowed to move only vertically. No displacement is enforced at the lower boundary.

Due to the simplistic shape of the model area, we use a mapped mesh containing 9,000 quadrilateral elements. Along the upper boundary, where deformation is expected, the mesh is especially refined to have a higher resolution. The demonstrated problem is solved for 10,973 degrees of freedom.

3.4.1.3 Comparison with analytical solutions

Figure 3.2 depicts the simulated groundwater flow and the direction, from right to left, generated by hydraulic gradient of 0.02. Since the graphical outputs of the computed two cases for $q = 10^{-6}$ m/s and $q = 0$ are nearly identical, we only present the result for the case where q is considered.

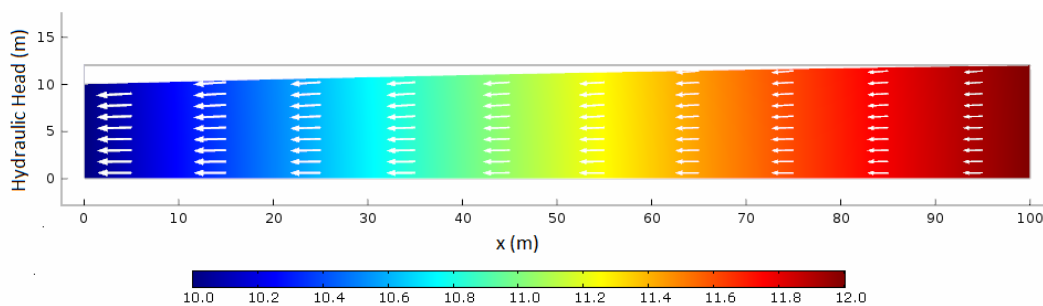


Fig. 3.2 Hydraulic head and flow velocity field along the aquifer. The scale of arrow lines in the figure also implies the flow velocity, which increases with a decrease in hydraulic head. The solid rectangle frame, which stays constant through-out simulation, represents the initial geometry. The deformed geometry is highlighted with the color coded area (red for higher and blue for lower hydraulic heads).

We compared the simulated hydraulic heads along the upper boundary with the results delivered from Equation (3.6) and (3.7) in Figure 3.3. When q is neglected,

our simulation matches excellently with the result obtained from Equation (3.7). However, a slight deviation of 4 mm compared with the analytical solution is observed for the case that q is taken into account. The deviation is not generated by meshing, while a constant difference was observed with different mesh sizes. In fact, the deviation is likely to occur because of the non-ideal condition of the upper boundary resulting from mesh deformation. In analytical analysis, a uniform recharge rate is applied at the fixed length of the aquifer ($L = 100$ m). In our simulation, on the other hand, the deformation of the upper boundary increases the boundary length to 100.02 m. This increase leads to a higher mass flux crossing the boundary and consequently higher hydraulic heads are being generated. Note no deviation occurs at either side boundaries, because the hydraulic heads are fixed by Dirichlet conditions.

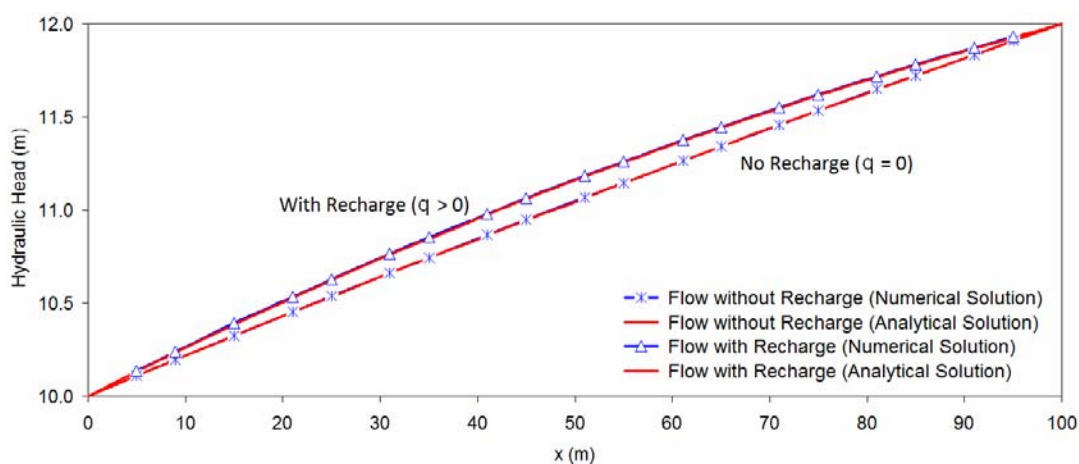


Fig. 3.3 Comparison of the simulated hydraulic heads with corresponding analytical results.

3.4.2 Case 2: Steady-state radial flow towards a well

3.4.2.1 Analytical approaches

According to Darcy's Law, the velocity of groundwater flow v_r in terms of radial hydraulic head gradient may be expressed as:

$$v_r = K \frac{\partial h}{\partial r} \quad (3.8)$$

Combining Equation (3.8) with mass conservation $Q = (2\pi rh)v$ across a cylindrical shell concentric with the well results:

$$r \frac{\partial h^2}{\partial r} = \frac{Q}{\pi K} \quad (3.9)$$

Q denotes pumping rate, r is the radial distance from the pumping well.

Integrating Equation (3.9) between two radial distance r_1 and r_2 from a well, we obtain

$$h(r_2) = \sqrt{h_1^2 + \frac{Q}{\pi K} \ln\left(\frac{r_2}{r_1}\right)} \quad (3.10)$$

3.4.2.2 Numerical model set up

We employ a similar modeling approach as above. Since radial flow towards the well is considered, an axi-symmetrical geometry (rz -plane) with polar coordinate is configured. The simulation example represents a model domain of a vertical cross section of 500 m wide and 20 m deep aquifer plane (Figure 3.4). Groundwater is extracted from the well, on the left hand side in Figure 3.4, with a constant pumping rate of 60 m³/h. The borehole itself is excluded from the model region. Typical sandy aquifer parameters, hydraulic conductivity ($K_r = K_z$) of 1×10^{-3} m/s, are applied in the example formulation.

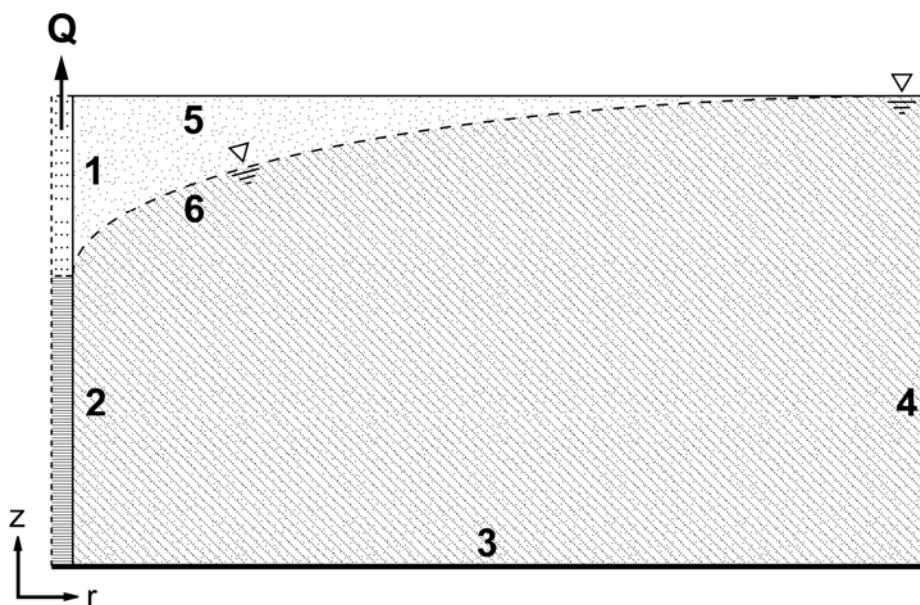


Fig. 3.4 Definition sketch for 2D vertical-cross-section geometry with labeled boundaries.

In Darcy's Law mode, a condition of no-flow is prescribed at boundaries 3 and 5. Pressure of zero across the model edges was specified at boundary 4 for pressure constrains. Mass flux (j), obtained from Equation (3.11), is given at boundary 1 and 2 for a constant pumping rate Q (positive for pumping),

$$j = -\frac{Q\rho}{2\pi r_o|D-d|} \quad (3.11)$$

Where D denotes well screen length, r_o is the well radius, d (absolute value) represents drawdown in the well. Note that $D-d$ denotes the active screen length where the pumped water flows. Initially $d = 0$ that water pumped out at boundary 1 and 2. Constant pumping results the increase of d , consequently, groundwater is pumped across boundary 2 only.

In the basic set-up the model is very similar to case 1 and, therefore, we present the differences only. In the ALE mode, zero displacement is enforced at 4, since a significant distance is assumed to avoid the influence of pumping at the boundary. Along boundary 1 and 2, only vertical displacement is allowed to avoid horizontal flow crossing the inner boundary. Since z is initially set as zero, at boundary 5, the pressure condition can be expressed through, where h is simulated in the Darcy's Law mode. The dashed line 6 is expected to be the (new) location of the free-surface.

We applied triangular shape finite element meshes in the model where it is drastically refined in the vicinity of the borehole and at the upper boundary (Figure 3.5). The presented model contains 4,344 mesh elements and the problem has 27,177 degrees of freedom. Note that the given normal inflow velocity at the inlet boundary condition is constant. However, the horizontal Darcy velocity is quantitatively calculated in the model. Hence, the Darcy velocity profile may not correspond to the given flux value, when a too coarse mesh is applied. Extremely fine meshes for the whole model domain are required to have perfect agreement, which results in a computational resource dilemma. Regardless of the slight discrepancy, the accuracy of our model is high enough to capture the problem, which is indicated through the comparison with analytical solution in the following section.

3.4.2.3 Simulation result and its comparison with analytical solution

Figure 3.5 depicts the deformed meshes over the radial distance from the pumping well. Only part of the model region, up to a distance of 16 m from the borehole, is displayed in the figure for better visualization. The upper solid line of the rectangle represents the initial position of the free-surface, while its new location is depicted with the filled meshes.

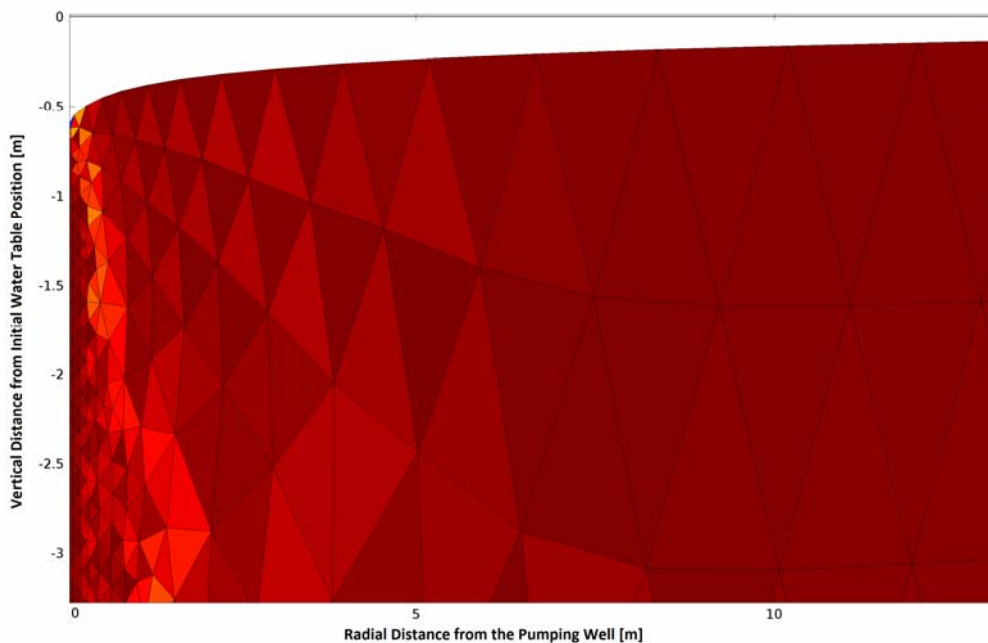


Fig. 3.5 Deformed mesh in upper inner part of model region.

The comparison of the hydraulic head distribution obtained from numerical simulation and from Equation 10 is depicted in Figure 3.6. Following Dupuit, Equation (3.10) delivers a uniform hydraulic head over depth, however, the vertical variation of hydraulic heads can be delivered by our model approach. In the figure this variation is presented at three dimensionless elevations, $z/D = 0, -0.5, -1$, which represent aquifer top (groundwater table), middle and bottom as an example.

We compare the numerical and analytical simulation through the head differences that are obtained by subtracting the hydraulic head values of the analytical result from the numerically computed values at three different depths. Hence, positive head differences indicate under estimation of hydraulic head (or drawdown) in the numerical simulation, while negative values indicate over estimation. While our

simulation of the hydraulic head distribution shows good agreement with the analytical result (solution of Equation (3.10)), the difference is more pronounced at the aquifer top and bottom than in the central parts. The largest deviation of ca. 5 cm is observed in the vicinity of the pumping well. Nevertheless, with increasing radial distance there is better agreement independent of aquifer depths. The vertical variation of hydraulic heads at the different vertical levels decreases with distance larger than 3 m from the well and disappears completely beyond a distance of 15 m.

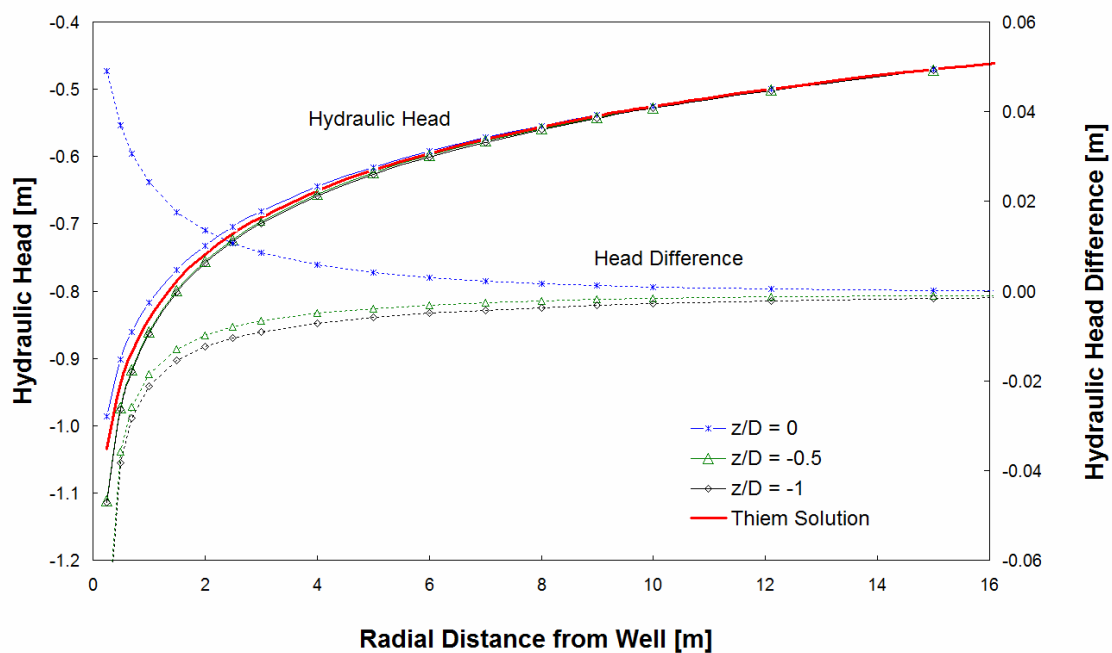


Fig. 3.6 Steady-state hydraulic head and head difference compared to the analytical solution, versus radial distance (r) from pumping well at aquifer top, middle and bottom ($z/D = 0, -0.5, -1$) when groundwater is pumped from a fully penetrating well on the left hand side.

3.5 Application Cases

3.5.1 The effect of anisotropy on drawdown

In contrast to the conventional approach, the anisotropy ratio, relating hydraulic conductivities in different spatial directions, can be defined by setting tensor values in our model. We demonstrate the role of anisotropy on drawdown by extending the example model that is discussed in Section 3.4.2. A scalar value for aquifer

conductivity is applied in the example model in Section 3.4.2, since isotropic conditions are assumed. In the following example, the anisotropy is defined by setting a diagonal tensor for hydraulic conductivities K_r and K_z in radial (horizontal) and vertical directions respectively. The anisotropy ratio is obtained via K_z/K_r . To compare it with the isotropic case, K_r is fixed at 1×10^{-3} m/s. The K_z/K_r values are considered for 0.1 to 0.5 for alluvium (Todd, 1980).

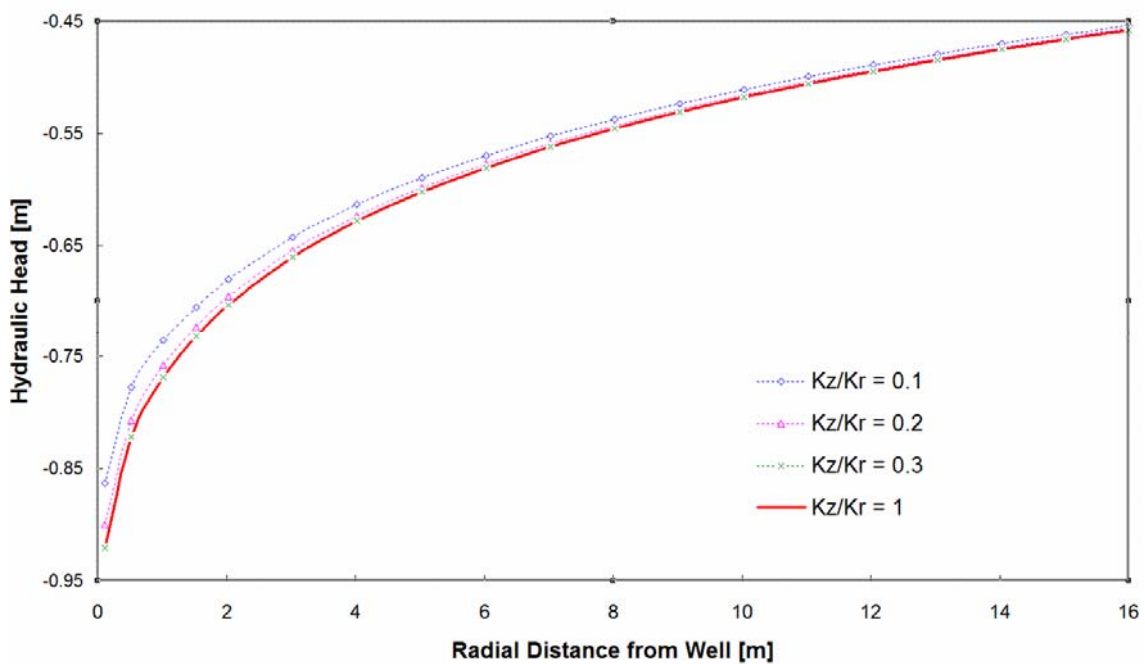


Fig. 3.7 Hydraulic head distribution with radial distance (r) from pumping well at aquifer top for different anisotropy ratios.

Figure 3.7 compares stationary hydraulic head over radial distance from the pumping well when different anisotropy ratios are applied. Lower hydraulic head is observed with increasing anisotropy ratio. The influence of anisotropy is mostly pronounced in the vicinity of the well. The influence of anisotropy on hydraulic head diminishes with increasing radial distance from the well and disappears after 20 m. The influence of anisotropy on hydraulic head distribution is insignificant for ratios higher than 0.3.

3.5.2 Pumping and injection from a single borehole

Apart from simulating above mentioned simple cases, our model is also capable of modeling more complex applications. As an example, we demonstrate an application to a recently developed dewatering technology, termed ‘nozzle-suction-infiltration’, also ‘DSI (termed as “Düsensauginfiltration” in German)’, for construction sites. The principle of the DSI method is shown in Figure 3.8. Groundwater is abstracted at the upper aquifer section. Instead of discharging the pumped water, it is re-injected at larger depth in the same borehole. Technically, packers separate the pumping and injection sections in the well. The detailed implementation of this technology is described by Holzbecher et al. (2011).

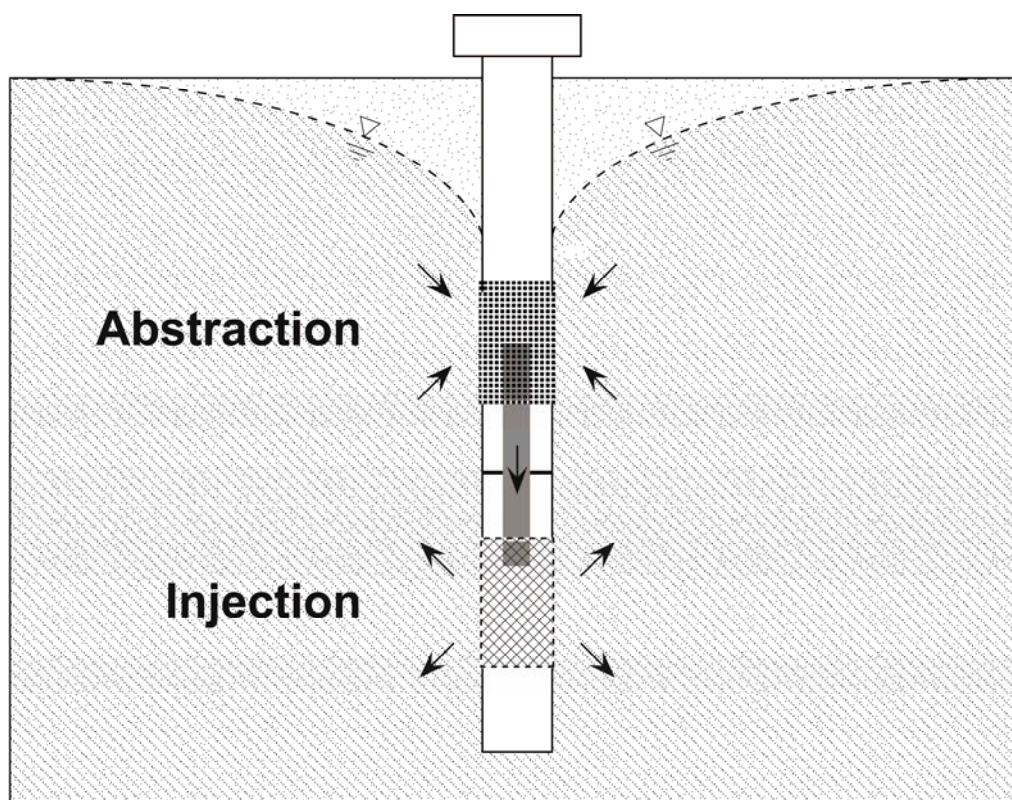


Fig. 3.8 Sketch of the single borehole pumping and injection concept.

Regardless of the successful practical applications of the DSI method, numerical simulations of the method are a challenge. The model requires a high grid resolution in the immediate vicinity of the borehole and the screen. The vertical change in velocity and head plays an important role in the system.

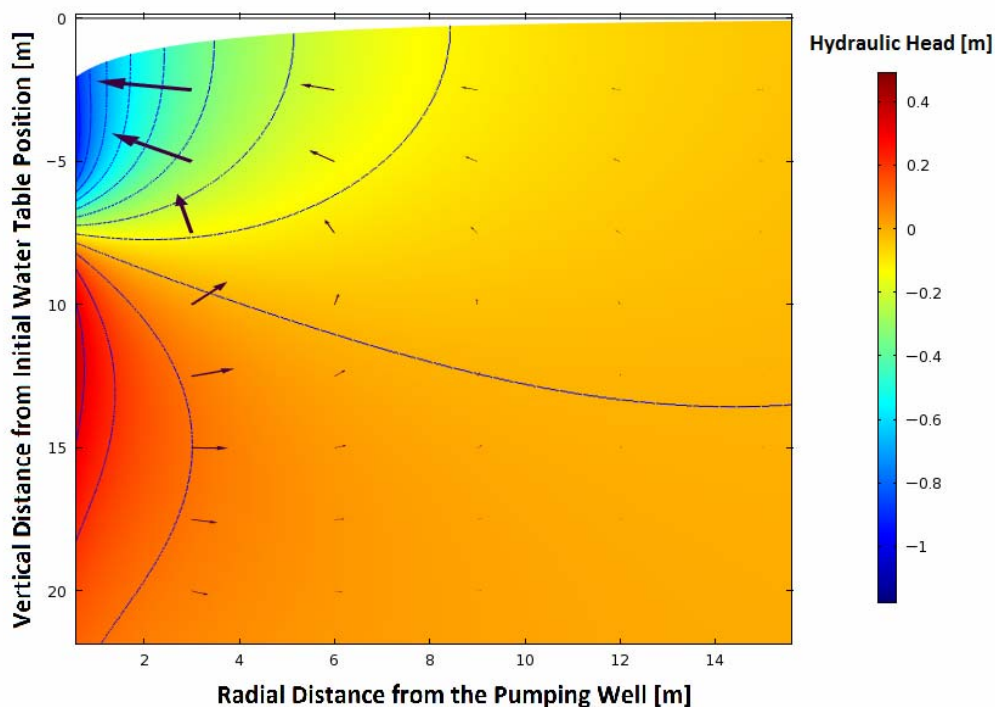


Fig. 3.9 2D vertical cross section model output. Shown are the hydraulic head (color plot), the mesh deformation and the velocity field (arrow plot) within the aquifer.

Our new modeling approach overcomes the above difficulties and is capable of simulating the fundamental flow configuration of the DSI method. Figure 3.9 depicts one sample of simulation results. To simplify the problem for a single well, a 2D vertical cross section is simulated, where groundwater is pumped and injected from the inner boundary. Low hydraulic heads are calculated for the upper section (blue in Figure 3.9) of the aquifer, while hydraulic heads are increased in the lower aquifer section (red in Figure 3.9). The lower boundary of the dewatered area is indicated by the mesh deformation.

3.6 Summary and Conclusions

We have presented the ALE method for solving the free-surface problem arising in groundwater flow simulation. Our domain of interest was the saturated zone of an aquifer, where the groundwater table (free-surface) is the upper moving boundary. Hence, the complexity of the model is significantly reduced compared to models considering the flow in partially saturated media, since our approach does not

introduce additional and uncertain parameters (Knupp, 1996; Feddes et al., 2004). This advantage is reflected by the performance of the numerical computations. We handle the free-surface by imposing an additional condition and allow the computational mesh to move with the moving boundaries. The model is flexible and capable to capture free-surface in any spatial dimension.

The accuracy of our model is demonstrated by the good agreement between the simulation results and the analytical solutions. Unlike the approaches following the Dupuit assumption, our approach is not limited concerning the vertical change in hydraulic head, as usually observed in the close vicinity of a well. Consequently, the non-zero vertical velocity components can be fully considered. Simple model set ups were presented as examples to compare with the analytical solutions. Nevertheless, our model is not limited in the presented simple cases, but also suitable for non-ideal aquifer conditions, such as anisotropic and heterogeneous parameter field.

Moreover, the flexibility of our method allows the simulation of complex situations, e.g., partially penetrating wells, simultaneous pumping and injection in a single well. The treatment of these situations does not depend on any empirical formulae, i.e., Hantush (1961), or artificial separation with impermeable layers any more.

In conclusion, solving a free-surface problem by implementing the ALE method is a practical approach, which allows simulating groundwater flow in an unconfined aquifer, even if there are complex physical conditions, in efficient and accurate way.

3.7 References

- Bakker, M., 1997. Groundwater flow with free boundaries using the hodograph method. *Advances in Water Resources* 20(4), 207-216.
- Banta, E., 2006. Modifications to MODFLOW boundary conditions and an adaptive-damping scheme for Picard iterations for a highly nonlinear regional model. In *MODFLOW and More 2006, Conference Proceedings, May 21-24 2006, Golden Colorado*, ed. Poeter, E., Hill, M., and Zheng, C., 596-600. Golden, Colorado: Colorado School of Mines.
- Bear, J., 1972. *Dynamics of Fluids in Porous Media*, Dover Publications Inc, New York.
- Bear, J., Verruijt, A., 1987. *Modeling Groundwater Flow and Pollution*, D. Reidel Publishing Company, Dordrecht, Holland.

- Bevan, M.J., Endres, A.L., Rudolph, D.L., Parkin, G., 2005. A field scale study of pumping-induced drainage and recovery in an unconfined aquifer. *Journal of Hydrology* 315(1-4), 52-70.
- Boussinesq J., 1904. Recherches théoriques sur l'écoulement des nappes d'eau infiltrées dans le sol et sur le débit des sources. *Journal de Mathématiques Pures et Appliquées* 10(5-78), 363-394.
- Bunn, M.I., Rudolph, D.L., Endres, A.L., Jones, J.P., 2011. Field observation of the response to pumping and recovery in the water table region of an unconfined aquifer. *Journal of Hydrology* 403(3-4), 307-320.
- Castro-Orgaz, O., Giráldez, J.V., 2012. Steady-state water table height estimations with an improved pseudo-two-dimensional Dupuit-Forchheimer type model. *Journal of Hydrology* 438-439, 194-202.
- COMSOL Multiphysics, 2012. Version 4.3, www.comsol.com, [Accessed September 23, 2012].
- Dagan, G., Lessoff, S.C., Fiori, A., 2009. Is transmissivity a meaningful property of natural formation? Conceptual issues and model development. *Water Resources Research* 45(3), W03425.
- Desbarats, A.J., Bachu, S., 1994. Geostatistical analysis of aquifer heterogeneity from the core scale to the basin scale: A case study. *Water Resources Research* 30(3), 673-684.
- Diersch, H.-J.G., 2009. Treatment of free surfaces in 2D and 3D groundwater modeling. In: FEFLOW White Papers, vol. 1, DHI-WASY GmbH, Berlin, Germany.
- Donea, J., Huerta, A., Ponthot, J.-Ph., Rodriguez-Ferran, A., 2004. Arbitrary Lagrangian-Eulerian methods, In: Stein, E., de Borst, R., Hughes, T.J.R. (Eds.), *Encyclopedia of Computational Mechanics*, Vol. 1, John Wiley & Sons, New York, pp. 413-434.
- Duarte, M., Gormaz, R., Natesan, S., 2004. Arbitrary Lagrangian-Eulerian method for Navier-Stokes equations with moving boundaries. *Computer Method in Applied Mechanics and Engineering* 193(45-47), 4819-4836.
- Dupuit, J., 1863. *Études théoriques et pratiques sur le mouvement des eaux dans les canaux découverts et à travers les terrains perméables: avec des considérations relatives au régime des grandes eaux, au débouché à leur donner, et à la marche des alluvions dans les rivières à fond mobile*, 2nd edn., Dunod, Paris.
- Fayers, F.J., Sheldon, J.W., 1962. The use of a high-speed digital computer in the study of the hydrodynamics of geologic basins. *Journal of Geophysical Research* 67, 2421-2431.
- Feddes, R.A., de Rooij, G.H., van Dam, J.C., 2004. *Unsaturated-zone Modeling: Progress, Challenges and Applications*, Kluwer Academic Publishers, Dordrecht, The Netherlands.
- Fetter, C.W., 1994. *Applied Hydrogeology*. Upper Saddle River: Prentice Hall.
- Forchheimer, P., 1901. Wasserbewegung durch Boden. *Zeitschrift des Vereines Deutscher Ingenieure* 45, 1782-1788.
- Freeze, R. A., Witherspoon, P. A., 1966. Theoretical analysis of regional groundwater flow: 1. Analytical and numerical solutions to the mathematical model. *Water Resources Research*, 2(4), 641-656.
- Hantush, M.S., 1961. Aquifer tests on partially penetrating wells. *Proceedings of the American Society of Civil Engineers, Journal of the Hydraulics Division* 87, HY5, 171-195.
- Harbaugh, A.W., Banta, E.R., Hill, M.C., McDonald, M.G., 2000. MODFLOW 2000, the U.S. Geological Survey modular ground-water model – User guide to modularization concepts and the ground-water flow process. USGS Open-File Report 90-392. Reston, Virginia: USGS.

- Harr, M.E., 1962. *Groundwater and Seepage*, McGraw-Hill Companies, New York.
- Holzbecher, E., Jin, Y., Ebneith, S., 2011. Borehole pump & inject: an environmentally sound new method for groundwater lowering. *International Journal of Environmental Protection* 1(4), 53-58.
- Keating, E., Zyvoloski, G., 2009. A stable and effective numerical algorithm for unconfined aquifer analysis. *Ground Water* 47(4), 569-579.
- Knupp, P., 1996. A moving mesh algorithm for 3D regional groundwater flow with water table and seepage face. *Advances in Water Resources* 19(2), 83-95.
- Knupp, P. M., 1999. Winslow smoothing on two-dimensional unstructured meshes. *Engineering with Computers* 15(3), 263-268.
- Maury, B., 1996. Characteristics ALE method for the unsteady 3D Navier-Stokes equations with a free surface. *International Journal of Computational Fluid Dynamics* 6(3), 175-188.
- McDonald, M.G., Harbaugh, A.W., 1988. A Modular Three-Dimensional Finite-Difference Groundwater Flow Model. *Techniques of Water-Resources Investigations of the United States Geological Survey*, Book 6, Chapter A1.
- Mishra, P.K., Kuhlman K.L., 2013. *Unconfined aquifer flow theory: from Dupuit to present*. *Advances in Hydrogeology*, Springer New York, pp. 185-202.
- Naff, R., Banta, E., McCord, J., 2003. Obtaining a steady state solution with elliptic and parabolic groundwater flow equation under dewatering conditions: Experiences with a basin model. In *MODFLOW and More 2003*, Golden Colorado, ed. Poeter, E., Zheng, C., Hill, M., and Doherty, J., 330-335. Golden, Colorado: Colorado School of Mines.
- Neuman, S.P., 1972. Theory of flow in unconfined aquifers considering delayed response of the water table. *Water Resources Research* 8(4), 1031-1045.
- Pohjoranta, A., Tenno, R., 2011. Implementing surfactant mass balance in 2D FEM-ALE models. *Engineering with Computers* 27(2), 165-175.
- Remson. I., Appel, C.A., Webster, R. A., 1965. Groundwater models solved by digital computer. *Journal of Hydraulic Division Proceedings of the American Society of Civil Engineers* 91(HY3), 133-147.
- Shontz, S. M., 2005, *Numerical methods for problems with moving meshes*. Ph.D. Dissertation, Cornell University, Ithaca, NY, USA, 107pp.
- Strack, O.D.L., 1989. *Groundwater Mechanics*, Prentice Hall, Englewood Cliffs.
- Tartakovsky, D.M., Guadagnini, A., Guadagnini, L., 2000. Effective hydraulic conductivity and transmissivity for heterogeneous aquifers. *Mathematical Geology* 32(6), 751-759.
- Todd, D.K., 1980. *Groundwater Hydrology*, John Wiley & Sons, New York.
- Zhang, Z. Q., Liu, G. R., Khoo, B. C., 2012. Immersed smoothed finite element method for two dimensional fluid-structure interaction problems. *International Journal for Numerical Methods in Engineering*, 90(10), 1292-1320.
- Zyvoloski, G.A., Vesselinov, V.V., 2006. An investigation of numerical grid effects in parameter estimation. *Ground Water* 44(6), 814-825.

Chapter 4

4 Dual-screened Vertical Circulation Wells for Groundwater Lowering in Unconfined Aquifers

Yulan Jin*, Ekkehard Holzbecher, Martin Sauter

Citation:

Jin, Y., Holzbecher, E., Sauter, M., 2014. Dual-screened Vertical Circulation Wells for Groundwater Lowering in Unconfined Aquifers. *Groundwater*, in press, doi: [10.1111/gwat.12331](https://doi.org/10.1111/gwat.12331).

Geoscience Centre, Dept. Applied Geology, University of Göttingen, Goldschmidtstr. 3, 37077 Göttingen, Germany

* Corresponding author

Abstract

A new type of vertical circulation well (VCW) is employed for groundwater dewatering at construction sites. This type of VCW consists of an abstraction screen in the upper part and an injection screen in the lower part of a borehole, whereby drawdown is achieved without net withdrawal of groundwater from the aquifer. The objective of this study is to evaluate the operation of such wells including the identification of relevant factors and parameters based on field data of a test site and comprehensive numerical simulations. The numerical model is able to delineate the drawdown of groundwater table, defined as free-surface, by coupling the arbitrary Lagrangian-Eulerian (ALE) algorithm with the groundwater flow equation. Model validation is achieved by comparing the field observations with the model results. Eventually, the influences of selected well operation and aquifer parameters on drawdown and on the groundwater flow field are investigated by means of parameter sensitivity analysis. The results show that the drawdown is proportional to the flow rate, inversely proportional to the aquifer conductivity, and almost independent of the aquifer anisotropy in the direct vicinity of the well. The position of the abstraction screen has a stronger effect on drawdown than the position of the injection screen. The streamline pattern depends strongly on the separation length of the screens and on the aquifer anisotropy, but not on the flow rate and the horizontal hydraulic conductivity.

Acknowledgement

The work was conducted within the DSI project (AZ 28299-23) funded by the Deutsche Bundesstiftung Umwelt (DBU). The fieldwork was supported by Hölscher Wasserbau GmbH, Germany. The authors would like to thank Otto Strack and two other anonymous reviewers for their valuable comments and suggestions to improve the quality of the paper.

4.1 Introduction

The control of the groundwater table is a common engineering problem encountered in subsurface hydrology. In practice, construction projects often imply the excavation below the water table, which consequently demands dewatering operation to provide a dry working environment. To date, a number of well-established dewatering techniques including sump pumping, wellpoints, and deep wells, are widely applied (Cashman and Preene, 2003; Powers et al., 2007). However, massive withdrawal of groundwater from aquifers is not avoidable with the existing dewatering methods. Severe environmental and geotechnical problems, that is, soil consolidation, ground surface settlement, and contaminant migration, are the known consequences (Foster et al., 1998; Preene, 2000; Powers et al., 2007; Roy and Robinson, 2009). Furthermore, if the pumped water is of low quality, extra costs are induced to meet the environmental regulations for discharging (Powers et al., 2007).

A new type of vertical circulation well (VCW) is regarded as an alternative avoiding above-specified problems (Holzbecher et al., 2011). The VCW consists of a single borehole with two screened sections allowing synchronous extraction and injection. Groundwater is extracted from the upper section and re-injected into the lower section (left in Figure 4.1). In contrast to the conventional dewatering methods (right in Figure 4.1), groundwater extraction from aquifers, further transport and discharge can be avoided.

Before the VCW was introduced for dewatering, it was often installed with the reversed screen location, where the injection screen is mostly located above the abstraction screen. It was initially introduced by Burns (1969) to determine the vertical permeability in petroleum reservoirs. During the last two decades, VCW was widely applied to determine certain aquifer properties (Kabala, 1993; Zlotnik and Zurbuchen, 1998; Halihan and Zlotnik, 2000; Zlotnik et al., 2001; Zlotnik and Zurbuchen, 2003), and to conduct aquifer remediation operations (Herrling and Stamm, 1991; US EPA, 1995 and 1998; Chen and Knox, 1997; Knox et al., 1997; Lakhwala et al., 1998; Chen et al., 2010).

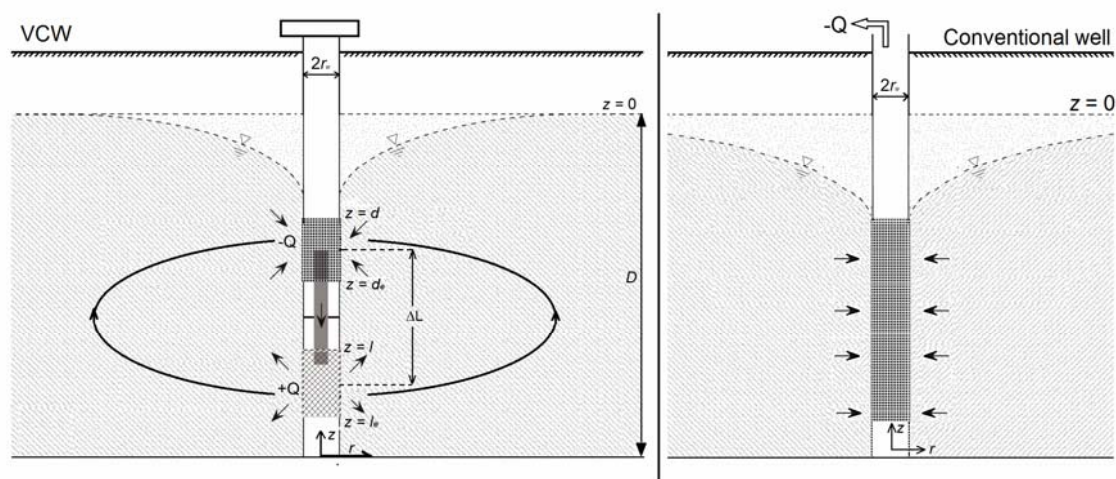


Fig. 4.1 Comparison of the dewatering concept between a VCW and a conventional well. Left: schematic illustration of groundwater flow and drawdown of a VCW. Right: schematic illustration of groundwater flow, discharge, and drawdown of a conventional dewatering well.

The various practical applications of the VCW led to intensive research to evaluate groundwater flow patterns around the well. Analytical solutions were described in Kabala (1993) and Zlotnik and Ledder (1996) by extending the solutions of Hantush (1961) and Neuman (1974). Nevertheless, analytical solutions are limited to simple geometries and idealized cases, that is, equally and symmetrically distributed screens (Halihan and Zlotnik, 2000).

Numerical methods are applicable for more general situations. Early attempts were conducted using Galerkin finite element, partial tracing and boundary element methods (Herrling and Stamm, 1992; MacDonald and Kitanidis, 1993). Subsequently, more complex cases, such as layered and/or fractured aquifers, multi circulation wells, were considered (Xiang and Kabala, 1997; Halihan and Zlotnik, 2000; Goltz et al., 2008). However, most of the models either assume a confined aquifer or simplify the free-surface as an impermeable boundary in an unconfined aquifer, because it is computationally more complicated to consider the free-surface (MacDonald and Kitanidis, 1993). Hence, flow rates are usually required to be set low enough in order to avoid the massive dewatering in unconfined aquifers accompanied by drastic lowering of the water table (Zlotnik and Zurbuchen, 1998). Since it is intended to apply the VCW for dewatering at construction sites, high flow

rates and relatively large drawdowns are expected. Consequently, the movement of the free-surface cannot be neglected any more.

The main objective of this study is to analyze and evaluate the groundwater flow patterns near a VCW by means of comprehensive numerical simulations that are validated with field observations. Moreover, the influence of well operation modes and aquifer characteristics on drawdown is specifically investigated for a better implementation of the VCW for dewatering.

4.2 Site Description and Measurements

The test site for the field experiments is located in a glacial fluvial sedimentary area around 50 km southwest of Berlin, Germany. The aquifer is unconfined having a thickness of 30-40 m (LGBR, 2014). The average hydraulic conductivity is in the order of 10^{-4} - 10^{-3} m/s (Holzbecher et al., 2011; LGBR, 2014). The hydraulic gradient is negligible. The groundwater level was measured about 1.5 m below the ground surface (bgs) when the tests were performed. The field tests were conducted in the upper 20 m of the unconsolidated sequence, which consists mainly of fine to medium sands and gravel sediments. At the depth below 20 m, the presence of very fine sand and silt increases dramatically and consequently the hydraulic conductivity is reduced significantly.

A VCW and 12 observation wells were installed with automatically recording data loggers. The depth intervals for the abstraction and injection screens of the VCW were set at 3.5–14.5 m and 17-19 m bgs, respectively. In comparison with the upper part of the aquifer a slightly higher hydraulic conductivity is expected in the depth of 17-20 m bgs, where the injection screen was installed. The observation wells were located at 1 m, 2 m, 3 m, and 10 m distance from the VCW. The hydraulic heads were measured with piezometers at three different depths (6 m, 8 m, and 12 m bgs; see Figure S1).

4.3 The Mathematical Model

The mathematical model consists of three components: (1) unconfined groundwater flow, (2) free-surface tracing, and (3) streamline simulation.

4.3.1 Unconfined groundwater flow

Groundwater flow in a saturated porous medium is simulated under the following assumptions: (1) flow in unsaturated zone is not considered; (2) the influence of ambient groundwater flow is negligible relative to the flow field induced by the VCW. The governing equation is given by (Bear, 1972),

$$S \frac{\partial h}{\partial t} = \nabla \cdot \mathbf{K} \nabla h \quad (4.1)$$

where \mathbf{K} indicates the tensor for hydraulic conductivity; S is the storage parameter presented by $S = \rho g(\alpha + \phi\beta)$ with α as porous medium compressibility, ϕ is porosity and β is fluid compressibility, t is time, h denotes the piezometric head formulated as $h = z + p / \rho g$ with p as pressure, ρ is the fluid density g is the acceleration due to gravity and z is the vertical coordinate in the flow domain. At steady-state, Equation (4.1) simplifies to

$$\nabla \cdot \mathbf{K} \nabla h = 0 \quad (4.2)$$

In our simulations, Equation (4.1) and/or Equation (4.2) are solved by taking the pressure p as the state variable. The domain of interest is the saturated part of the aquifer, where the groundwater table is considered as the upper boundary. The exact position of the upper boundary is a priori unknown and defined as a free boundary. The corresponding boundary conditions for steady-state simulation are formulated as

$$\frac{\partial h}{\partial r} = \begin{cases} 0 & \text{for } 0 > z > d \\ \frac{-Q}{2\pi r_w K |d_e - d|} & \text{for } d > z > d_e \\ 0 & \text{for } d_e > z > l \\ \frac{Q}{2\pi r_w K |l_e - l|} & \text{for } l > z > l_e \\ 0 & \text{for } l_e > z > D \end{cases} \quad \text{at } r = r_w, z \quad (4.3)$$

$$p = 0 \quad \text{at } r = r', z \quad (4.4)$$

$$\frac{\partial h}{\partial z} = 0 \quad \text{at } r, z = D \text{ and } r, z = 0 \quad (4.5)$$

where Q is the imposed flow rate, d and d_e are the vertical coordinates for the top and bottom of the abstraction screen, l and l_e are the vertical coordinates for the top and bottom of the injection screen, D is the negative value of the depth of the well and/or the initial thickness of the aquifer, r' is the radial extension of model region, and r is the radial coordinate of the problem domain.

Equation (4.3) is applied at the inner boundary along the well assuming a uniform distributed flow along the two screened intervals. Although not addressed here, notice that a time dependent boundary condition was applied for the transient simulation (i.e., field tests calibration). Equation (4.4) states the pressure constraint that is applied at the outer boundary. Equation (4.5) is a no-flow condition that is prescribed at aquifer bottom. No-flow boundary is also prescribed along the upper groundwater table in the flow simulation and coupled with ALE algorithm described below.

4.3.2 The arbitrary Lagrangian-Eulerian method

The arbitrary Lagrangian-Eulerian (ALE) algorithm is a hybrid description associated with moving imaginary meshes, which follows the movement of the free-surface. The principle of the ALE algorithm is superposition of the deformed spatial domain Ω_x obtained from the mathematical simulation on a reference domain Ω_x (Donea et al., 2004; Pohjoranta and Tenno, 2011). Jin et al. (2014) demonstrated the feasibility of the ALE method to trace the free-surface in groundwater flow simulations in

unconfined aquifers. The initial conditions are applied in Ω_x to provide the base. Equation (4.1) and/or (4.2) is formulated in Ω_x with corresponding coordinates, where the mesh deforms to fit the boundary conditions applied at the free-surface. The mesh deformation gradient $\mathbf{F} = \alpha\mathbf{x}/\alpha\mathbf{X}$ is obtained and the results are delivered back to Ω_x through inverse transformation \mathbf{F}^{-1} , which is a function of differential in the reference system (Donea et al., 2004; Jin et al., 2014)

Two conditions are fulfilled at the free-surface: (1) a flux condition across the interface, and (2) a zero pressure condition. The first condition is given as no-flow boundary (Equation (4.5)) in the flow simulation assuming no recharge or discharge across the upper interface. The second condition, a typical pressure constraint at the groundwater table, is applied for mesh displacement along the free-surface in ALE mode and consequently leads to $h(r, z) = z$. In the simulation, both of the conditions are satisfied simultaneously.

4.3.3 Streamline simulation

The steady-state streamline field is described by Stokes's streamfunction $\psi(r, z)$, (Bear, 1972; Holzbecher, 1998),

$$v_r = -\frac{1}{r} \frac{\partial \psi}{\partial z}, \quad v_\theta = 0, \quad v_z = \frac{1}{r} \frac{\partial \psi}{\partial r} \quad (4.6)$$

fulfilling the following Laplace equation:

$$\nabla^2 \psi = 0 \quad (4.7)$$

where v_r , v_θ and v_z are the scalar components representing the velocity field. Equation (4.7) is solved in the model. In- and outflow are taken into account by the respective Dirichlet boundary conditions above and below the screens. In comparison to the usual particle tracking methods, the streamfunction approach has the advantage that equal volume flux of flow between streamlines can be assumed, when the streamfunction levels are equally spaced.

4.3.4 Model calibration and validation

The numerical simulations are performed using the finite-element code implemented in the commercial software COMSOL Multiphysics 4.3b (2014). The detailed model set-up for the reference case is described in the Supporting Information.

The verification run for the model is conducted by comparing the simulation results with analytical solution obtained by Zlotnik and Ledder (1996). For comparison with an analytic solution for an idealized case, we assume a uniform and homogenous aquifer, equal screen length, and the symmetrical distribution of screens in a well. The hydraulic head distributions at the free-surface and at the depth of the abstraction screen are compared (Figure S3, S4). While the simulation results show good agreement with analytical solution at the depth of abstraction screen position, the difference is more pronounced at the free-surface.

The model was calibrated comparing the simulation results with the field measurements during the operation of a VCW. The test was performed at a constant flow rate of 30 m³/h for a period of 4 h continuously. Hydraulic head measurements were recorded for the first 10 min every minute at three different depths at the given distances. For the remaining test period, the interval length was increased to 10 min. Steady-state flow was achieved about 10 min after starting the test.

Two model layers, representing the abstraction layer (0-17 m bgs) and the injection layer (17-20 m bgs), were considered in the calibration. These layers were defined based on the results of the hydraulic characterization at the site. Calibrated hydraulic conductivities were 2.5×10^{-4} m/s and 4.9×10^{-3} m/s for the abstraction and the injection layers respectively. Figure 4.2 compares the measured with the simulated hydraulic head for selected time steps. Very good agreement between the field observations and the simulation results was achieved.

Subsequently, the model was validated with the observations from an additional flow test conducted with the same VCW. For doing so, a similar test was performed, but with a lower operation flow rate of 17 m³/h. All other conditions, that is, well screen position, piezometer location, were identical. The previously calibrated

hydraulic parameters were applied in the simulation. The same time intervals were selected as in the first test. A good agreement with an average deviation of 1.5 cm between the observed and simulated hydraulic heads was achieved (Figure S5).

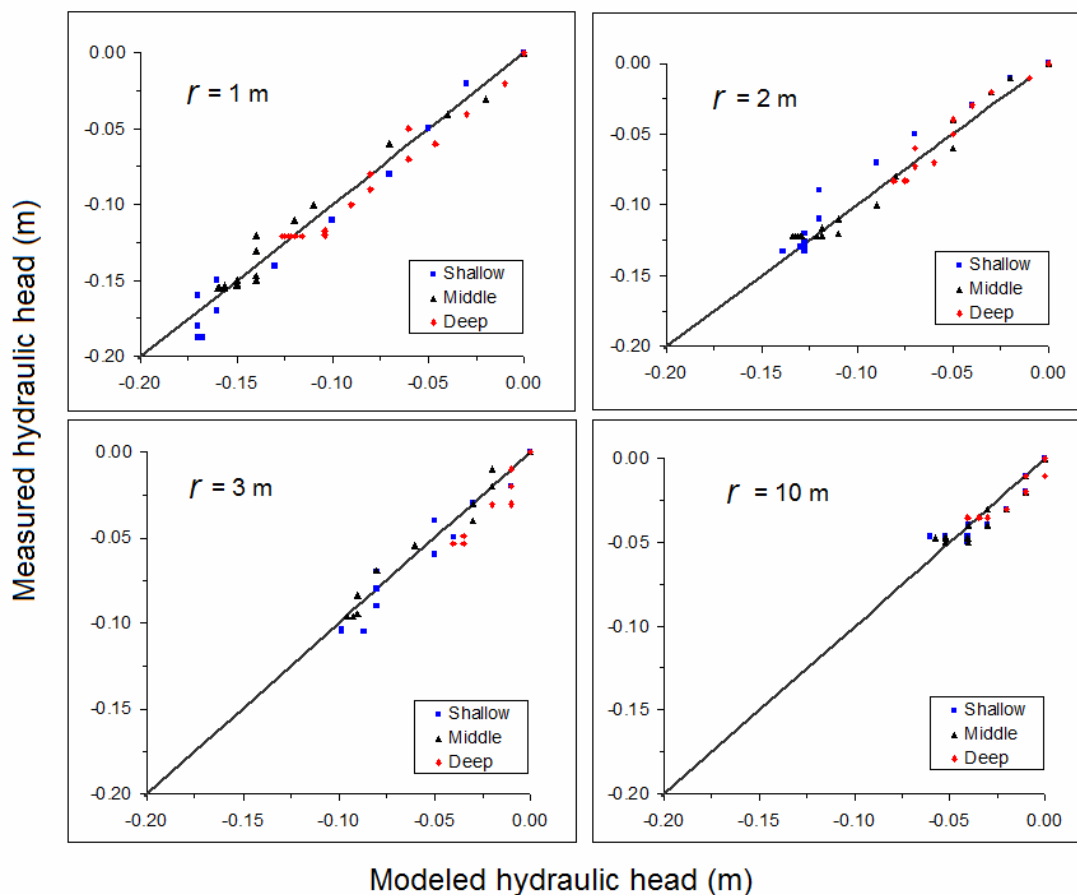


Fig. 4.2 Model calibration results obtained from comparison of numerical model results corresponding field observations for selected time steps.

4.4 Sensitivity Analysis

When a VCW is installed for dewatering, well operation and aquifer parameters are expected to play an important role in the control of drawdown. Hence, major well operation parameters, that is, flow rate, placement of the well screens, and aquifer parameters, that is, hydraulic conductivity and anisotropy, are investigated. Particularly, the influence of these parameters on drawdown is studied. In this section, we perform the parameter sensitivity studies in relation to a selected reference case.

4.4.1 Reference case

In order to investigate the dependency of the hydraulic head on geometric factors and relevant aquifer parameters, a simplified case was selected for reference, in which flow field is induced by a single VCW in an isotropic and homogenous aquifer. Zlotnik and Ledder (1996) estimated the region of influence of a circulation well in radial direction to be approximately five times higher than the separation length of the abstraction and injection screen centers. The radial extension of the reference model $r' = 50$ m is delineated at a distance beyond this estimated region of influence ($r' = 30$ m). Consequently, the influence generated by the outer boundary is avoided. Parameters used in the reference model and the simulation results are illustrated in Table S1 and Figure S2.

4.4.2 Sensitivity to well design and operation

4.4.2.1 Effect of flow rate

The effect of flow rate on drawdown was investigated by gradually increasing Q from $10 \text{ m}^3/\text{h}$ to $30 \text{ m}^3/\text{h}$. Other parameters were kept equal as in the reference case. The comparison (in Figure 4.3) shows that an increase in flow rate increases drawdown proportionally. The relationship between drawdown and the flow rate is depicted at the radial distance of 5 m as an example, where a slope of 2.4×10^{-3} and intercept of zero is obtained. A gentler slope is obtained for increasing radial distance from the VCW. Moreover, this proportionality can be also found for conventional pumping wells, but in confined media (i.e., Thiem solution). For the conventional pumping wells in unconfined aquifer, the hydraulic head or drawdown is related to the square root of the pumping rate.

Unlike drawdown, the streamlines are independent of the flow rate, if plotted for relative values (in %). Nevertheless, the absolute values of the stream function, and consequently the volumetric flux between the streamlines, changes when different flow rates are applied.

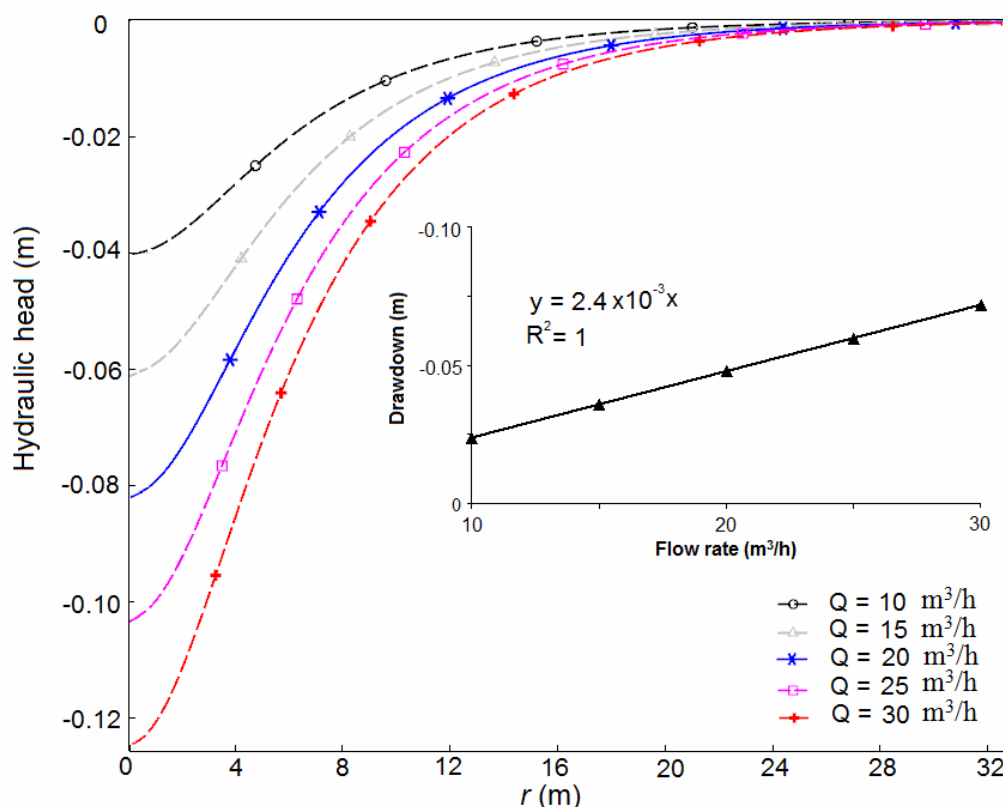


Fig. 4.3 Effect of the VCW operation flow rate, Q , on the hydraulic head at steady-state. Solid blue line indicates the reference case. The linear relationship between Q and drawdown is shown for a radial distance of $r = 5$ m.

4.4.2.2 Effect of screen positions

The influence of the position of the abstraction and injection screen intervals was studied in two separate steps. First, the abstraction screen position (d and d_e) was identical with that of reference case and the separation length ΔL was adjusted by gradually moving the injection screen interval (l and l_e) up- and/or downwards.

The simulation results show a slight decline in hydraulic head (around 4 cm) with an increase in ΔL from 4 m to 12 m. More specifically, the scatter plot in Figure 4.4 illustrates that the drawdown increases logarithmically with an increase in the separation length between the screen intervals. Moreover, the change in ΔL also shows an influence on the circulation regime around the VCW. For instance, the radial coordinate of the 80% streamline is extended from 8 m to about 13 m, when ΔL is increased from 4 m to 12 m.

Subsequently, the injection screen position (l and l_e) was identical with that of the reference case. Only the position of the abstraction screen (d and d_e) was adjusted

to achieve different ΔL . In this simulation, the maximum ΔL was 11.5 m, where the abstraction screen is placed in the interval of 1.5-3.5 m bgs. This is because a further increase in ΔL would lead to an “over-extraction”, where the simulated groundwater level is lower than the upper position of the abstraction screen.

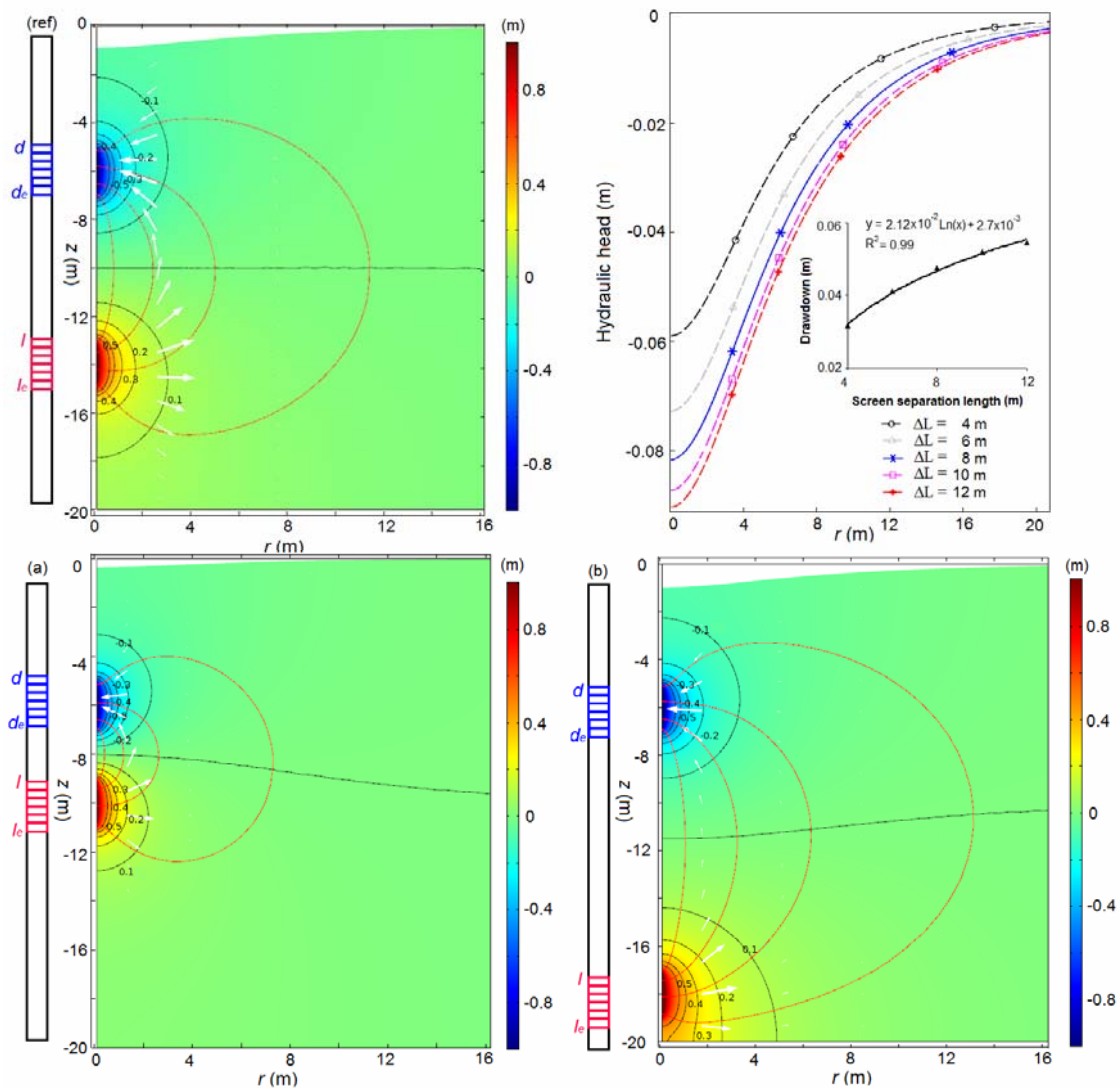


Fig. 4.4 Effect of the separation length of the screen intervals, ΔL , on steady-state groundwater flow near the VCW. The location of the abstraction interval is identical. (ref) reference case $\Delta L = 8$ m; (a) $\Delta L = 4$ m; (b) $\Delta L = 12$ m. The diagram depicts the effect of changes in ΔL on hydraulic head. The logarithmic relationship between ΔL and drawdown is shown for a radial distance of $r = 5$ m.

Hydraulic head decreases more effectively, when the abstraction screen is placed closer to the groundwater table (Figure S6). A significant decline in hydraulic head, about 23 cm, is obtained, when ΔL is increased from 4 m to 11 m. The change in

hydraulic head is around 8 times larger than the previous case where only 4 cm changes in hydraulic head was obtained by shifting the infiltration screen only. This big change in the hydraulic head is possibly caused by the combination of the following two facts, which are the separation length of the abstraction and injection screens and the distance between abstraction screen and the upper free-surface. The independent relationship between ΔL and drawdown could not be separated and identified from the combined effects.

4.4.3 Sensitivity of drawdown to change in aquifer characteristics

4.4.3.1 Effect of change in hydraulic conductivity on drawdown

A scalar value for hydraulic conductivity, $K = K_r = K_z$ in a range of 5×10^{-4} to 1×10^{-3} m/s is applied in the simulation. An inversely proportional relationship between drawdown and hydraulic conductivity was obtained (Figure S7). The proportionality constant decreases with an increase in the radial distance. Furthermore, an independent relationship between K and the streamline positions was obtained.

4.4.3.2 Effect of aquifer anisotropy

Aquifer anisotropy is represented by a diagonal tensor for the hydraulic conductivity in radial (K_r) and vertical (K_z) direction, where the anisotropy ratio, α , is defined as K_z/K_r . Lower α indicates higher anisotropy. In the simulation, K_r was kept as constant at 1×10^{-3} m/s, while K_z was decreased for different α . A larger area of influence was expected for highly anisotropic media (Zlotnik and Ledder, 1996). The model domain was therefore extended to a radial distance of 100 m in order to avoid the influence of the outer boundary on head changes.

Figure 4.5 depicts the simulated groundwater flow and hydraulic head distribution near the VCW for isotropic case and for anisotropic case with the lowest anisotropy ratio ($\alpha = 0.2$) applied in the study. The comparison of the streamlines reveals significant differences between the two cases. The extension of the groundwater circulation region with the 80% streamline as an indicator, increases by more than a

factor of 2 from 12 m for $\alpha = 1$ to 25 m for $\alpha = 0.2$. The influence of the anisotropy on the radial extension of streamlines (i.e., radial coordinate of 80% streamline position) is more significant at lower values of α (in the smaller plot in Figure 4.5). This dependency is only moderately developed for an increase in α .

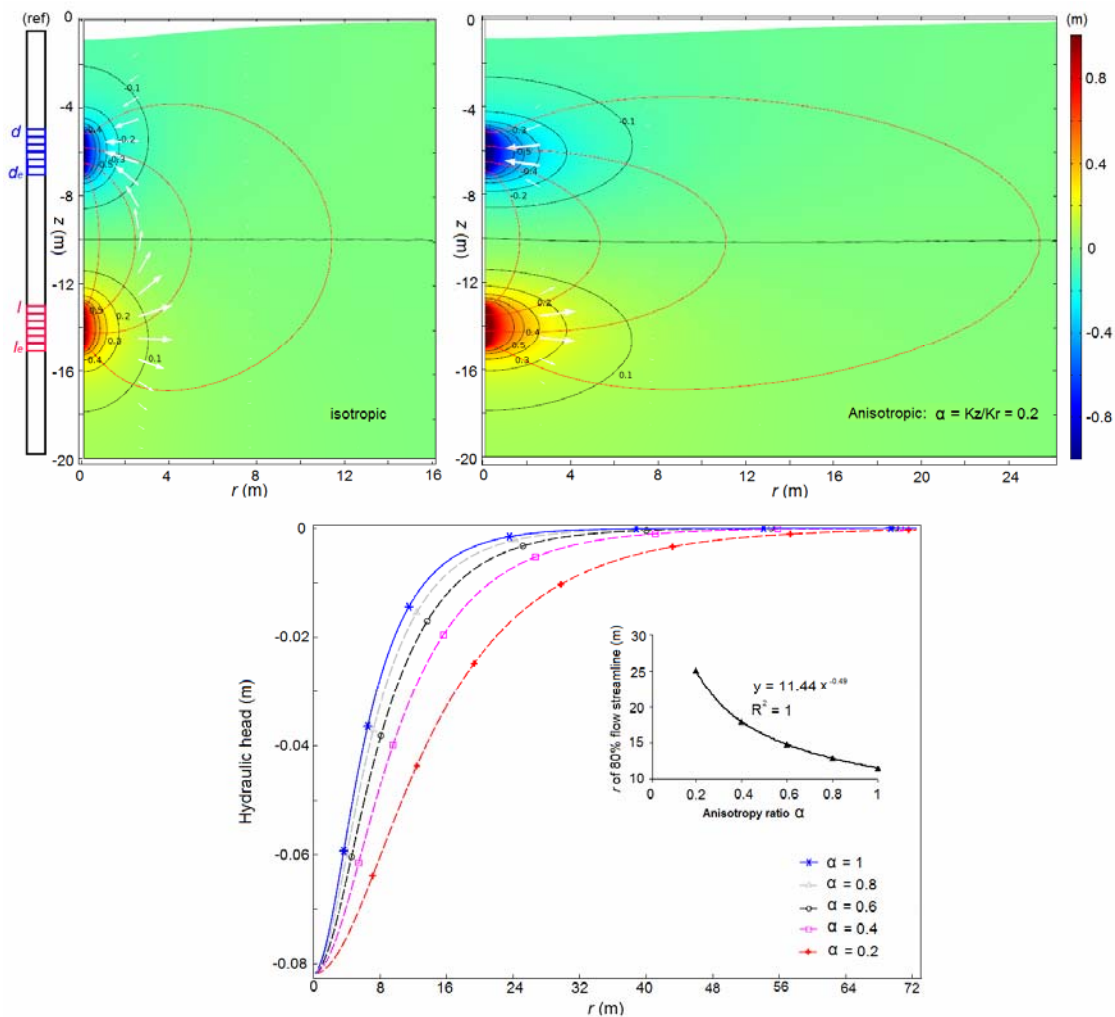


Fig. 4.5 Effect of anisotropy of the aquifer material, $\alpha = Kz/Kr$, on steady-state groundwater flow near the VCW. The reference case $\alpha = 1$ is depicted in the upper left and groundwater flow for $\alpha = 0.2$ are presented in the upper right figure. The diagram depicts the effect of α on hydraulic head distribution. The non-linear relationship between α and the radial distance of the 80% streamline is also shown.

Almost no influence of α on hydraulic head was obtained at the immediate vicinity of the VCW. This observation is in accordance with the results of Zlotnik and Ledder (1996), Zlotnik and Zurbuchen (1998) and Hvilshøj et al. (2000), who neither found a significant dependency between the hydraulic head and the degree of anisotropy.

However, considerably larger deviations in hydraulic head were obtained with increasing radial distance from the well. After reaching the largest deviation at 24 m in our simulation, it decreases with even larger radial distance and finally disappears due to the outer boundary condition, that is, $p = 0$ at $r = 100$ m in the simulation.

4.5 Conclusions

The application of the VCW for groundwater dewatering in unconfined aquifers was evaluated with comprehensive numerical simulation. The numerical model is able to trace the movement of the groundwater table and to delineate the intensive circulation regime by coupling groundwater flow equation with ALE algorithm and the streamfunction. The developed model is not limited in the borehole geometry such as the screen distributions. Further, the numerical model was verified by comparing the simulation results with the known analytical solution and validated for the test installation, for which hydraulic heads were compared with field measurements. The validation runs show that the model is flexible and capable to simulate the flow around a VCW accurately.

By means of sweeping the selected parameter values, the influences of the VCW operation modes and the sensitivity of site-specific aquifer conditions on drawdown as well as on the flow field could be characterized. The main findings are:

- Drawdown is proportional to the flow rate, and inversely proportional to the hydraulic conductivity.
- The change in water level depends to a considerably lesser extend on aquifer anisotropy in the direct vicinity of the VCW. Nevertheless, the shape of the depression cone is strongly influenced by the anisotropy factor, where the radius of groundwater circulation field increases with decreasing anisotropy ratio.
- With a fixed abstraction screen position, drawdown increases logarithmically with the increase in separation length of the screen intervals adjusted by lowering the injection screen interval. For a fixed injection screen, the change

in separation length adjusted by abstraction screen position shows a greater influence on drawdown.

- The position of the streamlines (normalized to total flow) does not depend on flow rate and horizontal conductivity, but on the screen distance and the aquifer anisotropy.

Supporting Information

Appendix S1-S3. (S1) Test site well location and measurements, (S2) description model set-up and the verification runs, (S3) results of sensitivity analysis.

4.6 References

- Bear, J., 1972. *Dynamics of Fluids in Porous Media*, Dover Publications Inc, New York.
- Burns, Jr, W.A., 1969. New single-well test for determining vertical permeability. *Journal of Petroleum Technology* 21(6), 743-752.
- Cashman, P.M., Preene, M., 2003. *Groundwater Lowering in Construction: A Practical Guide*. Second ed. CRC Press, London and New York.
- Chen, L., Knoxl, R., 1997. Using vertical circulation wells for partitioning tracer tests and remediation of DNAPLs. *Ground Water Monitoring and Remediation* 17(3), 161–168.
- Chen, J.S., Jang, C.S., Cheng, C.T., Liu C.W., 2010. Conservative solute approximation to the transport of a remedial reagent in a vertical circulation flow field. *Journal of Hydrology* 390(3), 155-168.
- COMSOL Multiphysics, 2014. Version 4.3b, <http://www.comsol.com/> [accessed May 01, 2014].
- Donea, J., Huerta, A., Ponthot, J.-Ph., Rodriguez-Ferran, A., 2004. Arbitrary Lagrangian-Eulerian methods, In: Stein E., de Borst, R., Hugges, T.J.R. (Eds.), *Encyclopedia of Computational Mechanics*, Vol 1, John Wiley & Sons, New York, pp.413-434.
- Foster, S.S., Lawrence, A., Morris, B., 1998. *Groundwater in Urban Development: Assessing Management Needs and Formulating Policy Strategies*. World Bank Publications, Washington D.C., USA.
- Goltz, M.N., Huang, J., Close, M.E., Flintoft, M.J., Pang, L., 2008. Use of tandem circulation wells to measure hydraulic conductivity without groundwater extraction. *Journal of Contaminant Hydrology* 100(3), 127-136.
- Halihan, T., Zlotnik, V.A., 2000. Asymmetric dipole-flow test in a fractured carbonate aquifer. *Ground Water* 40(5), 491–499.
- Hantush, M.S., 1961. Aquifer tests on partially penetrating wells. In *Proceedings of the American Society of Civil Engineers, Journal of the Hydraulics Division* 87(5), 171-195.

- Herrling, B., Stamm, J., 1991. In situ groundwater remediation of strippable contaminants by vacuum vaporizer wells (UVB) operation of the well and report about cleaned industrial sites. In Third Forum on Innovative Hazardous Waste Treatment Technologies: Domestic and International. June 11-13, 1991. Dallas, TX.
- Herrling, B., Stamm, J., 1992. Numerical results of calculated 3 D vertical circulation flows around wells with two screen sections for in situ or on-site aquifer remediation. In: Russell, T.F., Ewing, R.E., Brebbia, C.A., Gray, W.G., Pinder, G.F. (Eds.), *Computational Methods in Water Resources IX(1)*, Numerical methods in Water Resources, 483–492. New York, Elsevier Science.
- Holzbecher, E., 1998. *Modeling Density-Driven Flow in Porous Media: Principles, Numerics, Software*, Springer, Heidelberg, Germany.
- Holzbecher, E., Jin, Y., Ebneith, S., 2011. Borehole pump & inject: an environmentally sound new method for groundwater lowering. *International Journal of Environmental Protection* 1(4), 53-58.
- Hvilshøj, S., Jensen, K.H., Madsen, B., 2000. Single-well dipole flow tests: parameter estimation and field testing. *Ground Water* 38(1), 53-62.
- Jin, Y., Holzbecher, E., Sauter, M., 2014. A novel modeling approach using arbitrary Lagrangian-Eulerian (ALE) method for the flow simulation in unconfined aquifer. *Computers & Geosciences* 62, 88-94.
- Kabala, Z.J., 1993. The dipole-flow test: a new single-borehole tests for aquifer characterization. *Water Resource Research* 29(1), 99–107.
- Knox, R.C., Sabatini, D.A., Harwell, J.H., Brown, R.E., West, C.C., Blaham, F., Griffin, C., 1997. Surfactant remediation field demonstration using a vertical circulation well. *Ground Water* 35(6), 948–953.
- Lakhwala, F.S., Mueller, J.G., Desrosiers, R.J., 1998. Demonstration of a microbiologically enhanced vertical ground water circulation well technology at a superfund site. *Ground Water Monitoring and Remediation* 18(2), 97–106.
- LGBR, 2014. Hydrogeologiesche Karten Brandenburg, Landesamt fuer Bergbau, Geologie und Rohstoffe, <http://www.lbgr.brandenburg.de>, [Accessed May 22, 2014].
- MacDonald, T.R., Kitanidis, P.K., 1993. Modeling the free surface of an unconfined aquifer near a recirculation well. *Ground Water* 31(5), 774-780.
- Neuman, S.P., 1974. Effect of partial penetration on flow in unconfined aquifers considering delayed gravity response. *Water Resources Research* 10(2), 303-312.
- Pohjoranta, A., Tenno, R., 2011. Implementing surfactant mass balance in 2D FEM-ALE models. *Engineering with Computers* 27(2), 165-175.
- Powers, J.P., Corwin, A.B., Schmall, P.C., Kaeck, W.E., Herridge, C.J., 2007. *Construction Dewatering and Groundwater Control-New Methods and Applications*. Third ed. John Wiley and Sons, Hoboken, New Jersey, USA.
- Preene, M., 2000. Assessment of settlements caused by groundwater control. In *Proceedings of the ICE-Geotechnical Engineering* 143(4), 177-190.
- Roy, D., Robinson, K.E., 2009. Surface settlements at a soft soil site due to bedrock dewatering. *Engineering Geology* 107(3-4), 109-117.

- US EPA, 1995. Site Technology Capsule: Unterdruck-Verdampfer-Brunnen Technology (UVB) Vacuum Vaporizing Well. Technical Report EPA-540/R-95-500.
- US EPA, 1998. Field Applications of In-situ Remediation Technologies: Ground-Water circulation wells. Technical Report EPA-542-R-98-009.
- Xiang, J., Kabala, Z.J., 1997. Performance of the steady-state dipole flow test in layered aquifers. *Hydrological processes* 11(12), 1595-1605.
- Zlotnik, V., Ledder, G., 1996. Theory of dipole flow in uniform anisotropic aquifers. *Water Resources Research* 32(4), 1119-1128.
- Zlotnik, V.A., Zurbuchen, B.R., 1998. Dipole probe: design and field applications of a single-borehole device for measurements of vertical variations of hydraulic conductivity. *Ground Water* 36(6), 884-893.
- Zlotnik, V.A., Zurbuchen, B.R., Ptak, T., 2001. The steady-state dipole-flow test for characterization of hydraulic conductivity statistics in a highly permeable aquifer: Horkheimer Insel site, Germany. *Ground Water* 39(4), 504-516.
- Zlotnik, V.A., Zurbuchen, B.R., 2003. Field study of hydraulic conductivity in a heterogeneous aquifer: Comparison of single - borehole measurements using different instruments. *Water Resources Research* 39(4), 1101.

Chapter 5

5 Performance of vertical circulation wells for dewatering in layered unconfined aquifers

Yulan Jin* et al. (detailed author list needs to be determined)

Citation:

Jin, Y. et al., 2014. Performance of vertical circulation wells for dewatering in layered unconfined aquifers. In preparation for submission to a peer-reviewed journal.

Geoscience Centre, Dept. Applied Geology, University of Göttingen, Goldschmidtstr. 3, 37077 Göttingen, Germany

* Corresponding author

Abstract

Dual-screened vertical circulation wells (VCWs) can be used as dewatering wells to lower the groundwater table at a site. A vertical circulation dewatering well consists of an abstraction screen in the upper part and an injection screen in the lower part of a borehole. This type of dewatering well is increasingly used in unconfined layered aquifers, where the injection screen interval is often installed at a relatively more permeable layer. Groundwater flow near a VCW, especially in heterogeneous aquifers, is complex, and the induced drawdown cone is usually difficult to predict. The main objective of this work was to characterize the aquifer layers in more detail and to investigate the influence of the aquifer layer properties on the groundwater flow patterns near a VCW-well. To accomplish this, various field experiments were performed in order to achieve high resolution aquifer characteristics at a test site. Moreover, the problem is formulated as a free-surface problem, which is solved numerically through a new approach by employing the arbitrary Lagrangian-Eulerian (ALE) method for considering the water table deformation in unconfined aquifers. All of the performed field tests were calibrated with numerical models. Good agreement between measured data and model results was obtained. The influence of aquifer layer properties on the groundwater flow field and on the drawdown was illustrated considering the well characterized aquifer of the test site as a reference. An inversely proportional relationship between drawdown and hydraulic conductivity of the abstraction layer was found. However, the difference in hydraulic conductivity of the injection layer only shows a moderate influence on the drawdown.

Acknowledgements

The authors would like to thank the Deutsche Bundesstiftung Umwelt (DBU) for financially supporting this research within the DSI project (AZ 28299-23). The fieldwork was supported by Hölscher Wasserbau GmbH and the Helmholtz Centre for Environmental Research (UFZ).

5.1 Introduction

A dual-screened vertical circulation well (VCW) is a single borehole consisting of a pair of screened intervals, one operating in abstraction mode, and the other one in the injection mode. A packer is installed to isolate the upper and lower screen intervals. Hence, vertical groundwater circulation is induced with this well setup (Zlotnik and Zurbuchen, 1998). Two types of flow modes, “up-flow” mode and “down-flow” mode, can be technically realized with submersible pumps in VCWs (Johnson and Simon, 2007). An important feature of VCWs is that groundwater recirculates in situ and, therefore, it is not pumped above the ground surface. Due to this feature, VCWs have been widely used for the in-situ remediation of groundwater during the last two decades (Herrling and Stamm, 1991; US EPA, 1995, 1998; Knox et al., 1997; Chen et al., 2010). In addition, hydrogeologists utilize the recirculation principle specifically for determining aquifer properties (Herrling and Stamm, 1992; Kabala, 1993; MacDonald and Kitanidis, 1993; Zlotnik and Zurbuchen, 1998, 2003). For instance, Herrling and Stamm (1992) suggested estimating the large-scale aquifer anisotropy from analysis of VCWs. Kabala (1993) proposed the use of the recirculation principle for aquifer tests evaluation to determine the horizontal and vertical aquifer conductivity and specific storage coefficient.

Recently, the “up-flow” type of VCWs is increasingly used in groundwater dewatering for its unique strength of obtaining local drawdown without any net water discharge from an aquifer, for example by means of so called DSI-wells described in Holzbecher et al. (2011). In this type of VCWs the abstraction screen section is installed above the injection screen section for synchronous extraction and injection of groundwater (see schematic illustration in Figure 5.1). Consequently, a water table drawdown is achieved in the upper part of the aquifer. By employing VCWs, adverse effects of conventional pumping wells accompanied with the massive extraction of groundwater from aquifers may be reduced. Environmental and geotechnical problems, i.e., soil consolidation, ground surface settlement, and possible migration of contaminants, are the known consequences, when conventional dewatering methods are applied (Forster et al., 1998 Powers et al., 2007; Roy and Robinson, 2009). In addition, if the pumped water is of low

quality, using VCWs may circumvent extra costs induced by environmental regulations for discharge to meet the admissible level (Powers et al., 2007; Holzbecher et al., 2011). In this study, we give the focus on this “up-flow” type of VCWs used for groundwater dewatering.

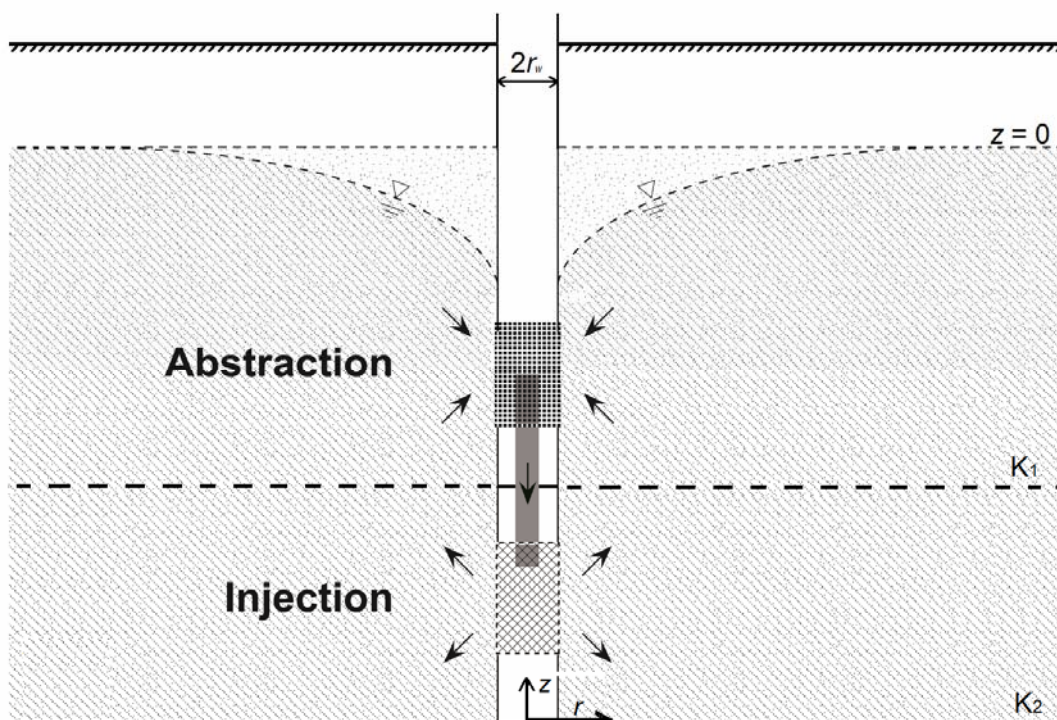


Fig. 5.1 Schematic illustration of groundwater flow patterns and drawdown near a VCW in a layered unconfined aquifer.

By installing a VCW for dewatering, the placement of its injection screen interval has to be specially considered. The aquifer layers are required to be sufficiently transmissive to guarantee an effective groundwater injection, and to avoid clogging caused by the excessive buildup of fine particles near the injection screen interval (Pyne, 1995; Bouwer, 2002; Powers et al., 2007). Therefore, the injection screen intervals of the well are often installed in relatively coarse textured (sand and gravels) unconsolidated aquifers (Holzbecher et al., 2011).

In principle, hydrogeological properties vary naturally due to the complex geologic processes through which aquifers evolve (Koltermann and Gorelick, 1996). Aquifer systems often consist of layered sediments where small changes in material properties, i.e., grain size, clay content, can generate the permeability changes of

several orders of magnitudes (Koltermann and Gorelick, 1995; Revil and Cathles, 1999). To implement VCWs for an efficient dewatering, the vertically heterogeneous aquifer characteristics can be practically exploited. This is especially true when the abstraction and injection layers are separated by a significantly less permeable layer. However, VCWs are also often installed in aquifers, where the changes in permeability are much smaller in vertical direction (Holzbecher et al., 2011; Jin et al., 2015). In this context, several questions emerge: Which role play the aquifer properties of abstraction and injection layers, respectively? How do the aquifer layer properties influence the achieved drawdown?

The main objective of this work was to characterize the aquifer layers with high resolution in order to investigate the influence of the aquifer layer properties on the groundwater flow patterns near the VCW as they are directly related to the efficiency of drawdown in unconfined aquifers. For that reason, intensive field experiments combined with numerical simulations were performed to clarify the open questions.

5.2 Site Description

The experimental field site is located in glacial fluvial sediment area at Plötzin, southwest of Berlin in Germany (Figure 5.2a). The aquifer is relatively homogenous and unconfined with a thickness of around 30–40 m and the water level fluctuates between 1.2 to 2 m below ground surface (bgs). When the field test was performed, the measured groundwater level was 1.5 m bgs. The upper 20 m of the unconsolidated sequence is characterized by alternating layers of fine sands and medium to coarse sand with some gravel sediments. Below 20 m, the presence of very fine sand and silt increases dramatically (LGBR, 2014; Jin et al., 2015). Site hydrogeology was characterized with a series of hydraulic tests, where the average value of hydraulic conductivity K was determined with 1.2×10^{-3} m/s (Holzbecher, et al., 2011).

An “up-flow” type of VCW and 27 observation wells with automatic data loggers were installed at the test site. Figures 5.2b and 5.2c illustrate the plan view and

vertical cross section of the test site, respectively. The VCW was constructed of a DN200-PVC filter pipe. The groundwater abstraction and injection screen intervals were 3.5–14.5 m bgs and 17–19 m bgs, respectively. The injection screen of the VCW is placed in a relatively large grain size layer, where efficient water infiltration was determined a priori. In total, 27 piezometers made of DN50-PVC pipe with 1 m screen starting 5.5 m, 8.5 m, and 11.5 m bgs were installed. These three depths refer to shallow-, middle-, and deep observations, respectively. These vertical observation well networks were installed at both sides of the VCW in the distance of 1 m, 2 m, 3 m and 10 m. In addition, a set of observation wells was installed in the direct vicinity of the VCW in a distance of around 0.5 m.

At the test site, core samples were taken at the three selected depths shown in Figure 5.2c. Furthermore, direct-push slug tests were performed at the same depth intervals. Detailed description of the field testing methods is illustrated below in Section 5.3.

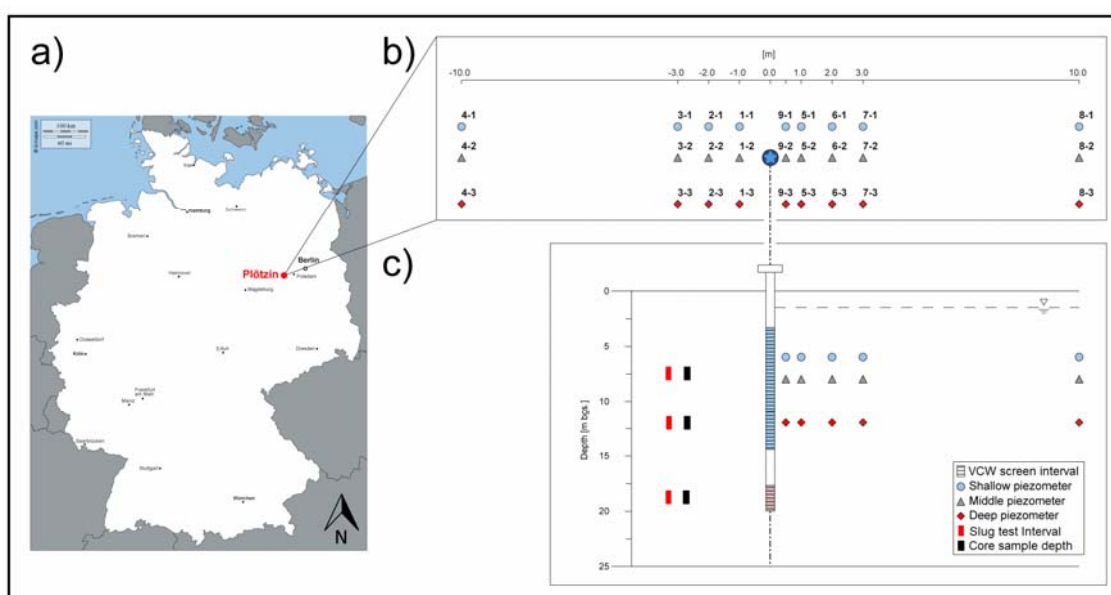


Fig. 5.2 (a) Location of Plötzing study site. (b and c) Map of the test site showing the position of the VCW and piezometers. (b) Plan view. (c) Cross-section: core sampling depths and the direct-push slug test intervals (left), depths of abstraction and injection screens and piezometers (right).

5.3 Methodology

5.3.1 Field methods for aquifer layer characterization

5.3.1.1 Empirical identification of the injection layers

At the beginning, the aquifer layers for groundwater injection were identified during the drilling process. Rotary drilling with water as the drilling fluid for circulation was applied. The suitable layers for groundwater injection are obtained at a certain depth, where a significant loss of drilling fluid was observed. Using this approach, two potentially suitable layers were found, one at 6–9 m bgs and one at 18–20 m bgs. In the following study, these two layers are defined as injection layers. However, this approach is limited in characterizing the properties of the obtained injection layers.

5.3.1.2 Aquifer characterization with direct-push technology

The direct-push technology comprises a category of equipment that allows a rapid sampling and data collection from unconsolidated soils and sediments. In shallow unconsolidated aquifers, high resolution hydrostratigraphic and K profiles can be obtained by using these direct-push methods, such as the *electric conductivity (EC) logging* (Schulmeister et al., 2003; Sellwood et al., 2005), the *hydraulic profiling tool (HPT)* (McCall et al., 2009), *direct-push slug testing (DPST)* (Butler et al., 2002), the *direct-push permeameter (DPP)* (Butler et al., 2007), and the *direct-push injection logging (DPIL)* (Dietrich et al., 2008; Lessoff et al., 2010).

Among the direct-push methods, the EC logging was applied in conjunction with the HPT at the test site. The vertical profile was taken to a depth of 25 m. EC measures the flow of electrical current through soil from which the soil stratification or layer boundaries can be inferred (Schulmeister et al., 2003; Sellwood et al., 2005). HPT measures the pressure required to inject a certain flow of water into the aquifer, which is used to estimate the relative formation of hydraulic conductivity (McCall et al., 2009). The obtained EC and HPT profiles from the test site are shown in Figure 5.3.

The principle of DPIL is in fact very similar with the HPT. DPIL profile was determined at the test site between 3–25 m bgs in every 25 cm. At each depth level, the pressure was measured for two adjusted flow rates of the injected water, ca. 200 and 500 L/h, respectively, to evaluate the dependence between the measured pressure and the flow rate.

Although EC, HPT and DPIL profiles are robust in indicating the vertical distribution of K , the direct K can be obtained from DPST only. Therefore, DPST was conducted at three different depth intervals indicated in Figure 5.2c. Two of the selected depth intervals, 7–8 m and 18–19 m bgs, are, in fact, the empirically identified injection layers. In contrast, we assumed that the third slug test interval, 11.5–12.5 m bgs, characterizes the layer between the injection layers.

5.3.1.3 Hydraulic conductivity determination from grain size analysis

Three core samples were taken from the same depth intervals than for the performed DPST, which are 7–8 m, 11.5–12.5 m and 18–19 m bgs, respectively (Figure 5.2c). The core samples have a diameter of 0.2 m and consist mainly of fine and medium sands. Larger grain sizes were observed for the injection layers. Each of the core samples was divided into 10 pieces with a length of 10 cm. Eventually, the grain size analysis (dry sieving) was performed on all resulting 30 core samples. The hydraulic conductivity K was estimated after Hazen (1893), as it is a commonly used approach to determine K from the grain size distribution. The good applicability of this method was shown by Vienken and Dietrich (2011).

5.3.1.4 Pumping test

Following the installation of the VCW and the piezometers, a step wise pumping test was performed. The VCW was fully screened from 3.5 m to 20 m bgs. The pumping rate during the test was increased gradually from 20 m³/h to 30 m³/h and eventually to 40 m³/h. The pumping rate was verified every 15 min by recording the volume change on a calibrated flow meter that was connected in line with the pump discharge. The test was performed for a period of 2 h at each pumping rate

resulting in total of 6 h test period. During the test, the hydraulic head response in all the observation wells was measured with data loggers at 1 min interval. The observations at the left hand side of the pumping well were identical with the right hand side, when comparing the same distance. A measurement failure was detected at the piezometer (7-2) and, hence, the observations at this point were not considered in the test evaluation.

5.3.1.5 Injection test

Similar to the pumping test, a step wise injection test was performed in the same borehole. The 2 m long injection screen was set at a depth of 18 m, which belongs to one of the pre-determined injection layer as described above. The injection test was performed for three different injection rates, 15 m³/h, 25 m³/h, and 40 m³/h, respectively, over a period of 4 h for each injection rate. Moreover, the change in hydraulic head was measured with a resolution of 1 min in all of the observation wells.

5.3.1.6 Vertical circulation flow test

Additionally, a circulation flow test was performed. The abstraction screen section was screened from 3.5 m to 10.5 m bgs, while the injection screen section was installed at 18–20 m bgs (Figure 5.2c). Between the two screens, a packer was installed to avoid the backflow of water. The test started with a flow rate of 17 m³/h over a period of 2 h. Then, the flow rate was increased to 30 m³/h and finally to 40 m³/h. The test was performed for a 2 h period for each of the respective operation rates. Hydraulic head response of the circulation well was again recorded at a time interval of 1 min. The performed tests rapidly reached a steady-state after around 10 min for each given flow rate. Measurements failed at two observation wells (4-3 and 7-2) and consequently excluded from the test evaluation.

5.3.2 Numerical simulation method

Numerical modeling has the potential to support the field observed data and provide insight view to refine the understanding of the conceptual model. The groundwater flow near a VCW, especially in the immediate vicinity of the well, is complex and the vertical change in velocity and head has to be considered. Furthermore, the “up-flow” type of VCWs results in a water table drawdown in unconfined aquifers, which leads to a movement of the groundwater surface (free-surface problem). Considering these difficulties, we followed the simulation approach demonstrated by Jin et al. (2014), where the a priori unknown free-surface position is traced by using the arbitrary Lagrangian-Eulerian (ALE) method. Here, the groundwater flow equation (Bear, 1972) and the ALE algorithm (Donea et al., 2004; Pohjoranta and Tenno, 2011) are simulated simultaneously.

5.3.3 Numerical model set-up

The conducted pumping, injection as well as the circulation flow tests were modeled using the finite element code COMSOL Multiphysics 4.3b. In general, axisymmetric models are suitable for multi-layered aquifer systems as they can be used to analyze complex flow fields and advanced aquifer tests (i.e., Louwyck et al., 2012). Moreover, the identical measurements on both sides at the same distance from the well support the assumption of radially homogenous aquifer conditions for simulation. Consequently, the overall problem domain can be reduced from 3D to 2D. Further assumptions are: 1) only saturated parts of the aquifer are considered in model domain; 2) the influence of ambient groundwater flow is negligible relative to the flow field induced by the VCW; and 3) sink and source terms are omitted.

The problem is simulated in a 2D axisymmetric domain (50×25 m deep), where the VCW with the radius of $r_w = 0.1$ m is situated at $r = 0$. Triangular finite element meshes are used for the discretization with a mesh refinement in the vicinity of the well, and in particular along the well screens. Moreover, the mesh is also refined along the upper boundary, where the major deformation of the free-surface is expected.

The problem domain is vertically divided in six layers respecting the obtained site specific hydraulic profiles (see Figure 5.3). Here, the pre-determined two main layers for groundwater injection (layer 2 and 5), defined as “high conductive layer”, are specially considered. The lower injection layer is surrounded by less conductive layers, which are the fourth layer and the bottom layer. These two aquifer layers are considered as “less conductive layer”. In addition, the rest of the aquifer layers are defined as “moderate conductive layer”. Horizontal (radial) hydraulic conductivities, K_{r1} , K_{r2} , and K_{r3} , are calibrated for all layers. Moreover, vertical hydraulic conductivities, K_{v1} , K_{v2} and K_{v3} , are also considered for the respective layers by assuming an anisotropy factor of 5 (Todd, 1980). The calibrated results are compared with hydraulic conductivities obtained from the three other methods in Table 5.1.

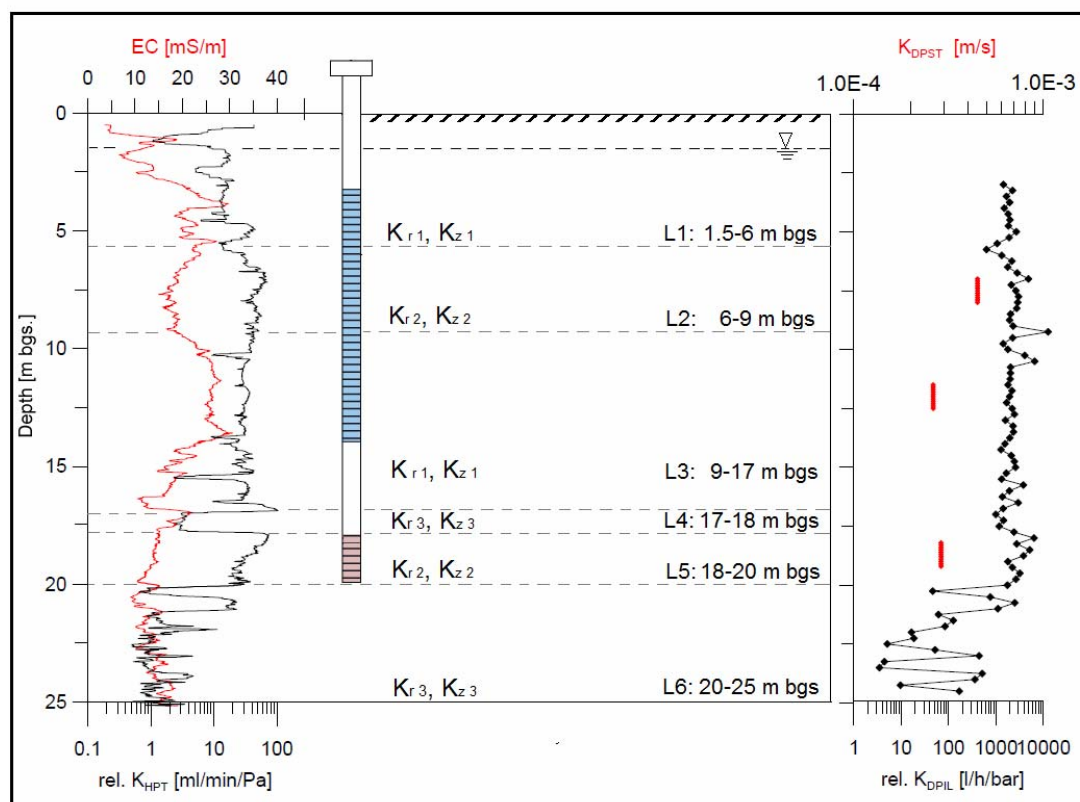


Fig. 5.3 Results of direct-push methods and the respective aquifer layers defined in numerical model. EC and HPT profile is shown on the left side. Cross-section view of the model layers (L1-L6), thickness, and calibrated parameters are defined in the middle. VCW screen setting at the test site is illustrated, where the abstraction screen interval is depicted in blue and the injection screen interval is shown in light brown. DPIL and DPST results are shown on the right side. The model layer set-ups for calibrating the pumping test and injection tests are identical. Detailed screen settings are described above.

Mass flux condition (Neumann type boundary) was applied at inner boundary along the abstraction and/or injection screen (test dependent), respectively. Pressure constrain is used at outer boundary assuming that hydraulic head is not influenced by the flow field induced by the well. Furthermore, a no-flow condition is prescribed at the lower boundary. At the upper boundary, the flux and pressure conditions are satisfied simultaneously as described in Jin et al. (2014).

5.4 Results and Discussion

5.4.1 The characteristics of the aquifer layers

Several methods for the laboratory and field investigation of aquifer characterization at the test site were applied including laboratory analyses of core samples, direct-push methods, pumping and injection tests, as well as the circulation flow tests (see Section 5.3.1). The K distributions of the corresponding aquifer layers are summarized in Table. 1.

Table 5.1 Comparison of the obtained hydraulic conductivities with different methods.

Test	slug test	Grain size analysis	Pumping test	Injection test	Circulation flow test
Layer	K_{DPST} [m/s]	K_{Hazen} [m/s]	K_p [m/s]	K_i [m/s]	K_{VCW} [m/s]
1	-	-	5.44×10^{-4}	3.66×10^{-4}	4.25×10^{-4}
2	4.50×10^{-4}	7.01×10^{-4}	6.75×10^{-4}	1.03×10^{-3}	3.87×10^{-3}
3	2.62×10^{-4}	4.51×10^{-4}	5.44×10^{-4}	3.66×10^{-4}	4.25×10^{-4}
4	-	-	1.00×10^{-5}	1.00×10^{-5}	1.00×10^{-5}
5	2.89×10^{-4}	7.08×10^{-4}	6.75×10^{-4}	1.03×10^{-3}	3.87×10^{-3}
6	-	-	1.00×10^{-5}	1.00×10^{-5}	1.00×10^{-5}

Initially, direct-push EC-logging was used in conjunction with HPT to classify the aquifer layers. In general, the lower EC values reflect more coarse sediments, whereas higher relative HPT values reflect the higher permeability (Figure 5.3). Moreover, the values of the EC-log are generally low (ca. 20–30 mS/m), which suggest the presence of sands, gravels and a possible absence of electrically conductive material such as silts and clays (Schulmeister et al., 2003). The focus was given on the two manually identified injection layers (“high conductive” layer), where the DPSTs were performed (layer 2 and 5 in Figure 5.3). In addition, the moderate conductive layer, which is intersected by the two “high conductive” layers, was selected for comparison. The conducted DPST was analyzed after Butler and Garnett (2000). The results show that the hydraulic conductivities of the injection layers are approximately two times higher than for the third layer.

Secondly, core samples were collected at the same intervals, where the DPSTs were performed. Each of the core samples was analyzed in equally divided 10 cm intervals and the arithmetic mean K values evaluated after Hazen (1893) are illustrated in Table 5.1. The comparison of the grain size analysis with the DPST results revealed a good agreement. Furthermore, the results are also consistent with the above illustrated vertical profiles. Nevertheless, the estimated K values from the grain size analysis can represent neither horizontal nor vertical K values, as the sieving process destroys the natural sediment structure (Vienken and Dietrich, 2011).

At last, the performed pumping tests, injection tests as well as the circulation flow tests were calibrated with the numerical simulation described above. Horizontal K is calibrated primarily for the respective aquifer layers and the results are compared in Table 5.1. Again, we give the focus mainly on the layers, where slug tests were performed. Hence, identical properties were given to the “low conductive layers” in the calibration. In general, the calibration results for different flow tests show good agreements in K . On the one hand, the obtained K , especially of the “moderate conductive layer”, is in accordance with the results of slug tests and grain size analysis. On the other hand, higher K were obtained in the “high-conductive” injection layers in the circulation flow test compared to other tests. The contrast of K of the aquifer layers was most pronounced in the circulation test and lowest in the pumping test.

Although not discussed here in detail, further parameters such as aquifer anisotropy, storage coefficient, and porosity were determined in the simulation as well. For all simulations, these parameters were kept constant.

5.4.2 Modeling results

Figure 5.4 illustrates the simulation results of the groundwater flow near the well for the performed pumping, injection, and the circulation tests, respectively. A 2D vertical cross section is depicted for visualizing the generated flow at the inner boundary (well). A lower hydraulic head is calculated near the abstraction screen (blue color zone), while higher hydraulic head potential is induced near the injection screen (red color zone). The change of the water table position is apparent along the deformed upper boundary, where the initial position is given by the upper solid line of the rectangular model domain. For better visualization, only a part of the model region is displayed. Moreover, vertical exaggerations of 20 and 2 are used for the mesh deformation along the upper boundary for the injection test (middle in Figure 5.4), and the circulation flow test (right in Figure 5.4). The simulation results are compared for the time step 2 h after imposing the flow rate of 40 m³/h to the respective test.

The measured hydraulic heads for selected time steps are compared with the simulation results of the conducted pumping, injection and the circulation tests in Figure 5.5, Figure 5.6, and Figure 5.7, respectively. In general, very good matching between field observations and simulation results was achieved. Among them, the best agreements were obtained from the pumping tests. In the pumping test, the borehole is almost fully screened, and therefore, relatively uniform and horizontal flow towards well is expected. Responses obtained from pumping in a fully screened well provide estimates of parameters, which are spatially integrated and limited in determining the affect of known or unknown heterogeneities (Bulter Jr, 2005). Consequently, the differences in K between the aquifer layers were least pronounced in the pumping test. The largest differences between measured hydraulic heads and the obtained model results were observed in the direct vicinity of the tested borehole in the injection and the vertical circulation tests. Hydraulic

heads are significantly higher, especially in piezometer No. 9-3, with increasing injection rates.

The cone of depression induced by the pumping well (in the pumping test) is significantly larger than for the VCW (in circulation test), when comparing an identical flow rate. For example at 40 m³/h, the obtained drawdown from the pumping well reaches ca. 70 cm at a distance of 1 m from the well, while it is around 25 cm for the VCW (see Figure 5.5 and 5.7, Piezometer No.1- or Piezometer No.5-). Moreover, the horizontal influence of the drawdown cone reaches far beyond 10 m from the well, which also represents the furthest observation points at the test site. However, the change in hydraulic head is not significant anymore at this distance from the well in the VCW-tests.

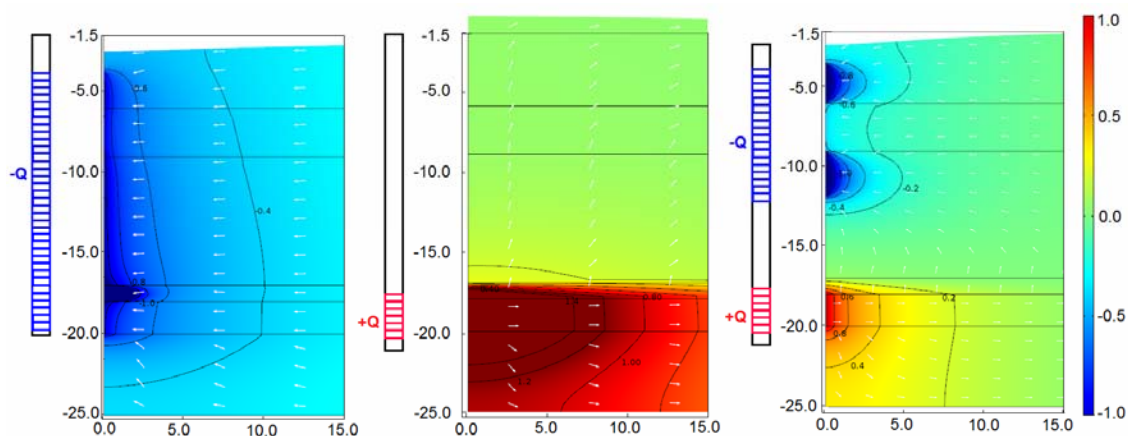


Fig. 5.4 Modeled 2D vertical cross-section of the groundwater flow field near the well. Left: pumping test; middle: injection test; right: circulation test with a VCW. Hydraulic head distributions (color plot), positions of groundwater table (deformed mesh line), equipotential contours (black solid lines with label), and the groundwater flow field (arrow plot) are also presented.

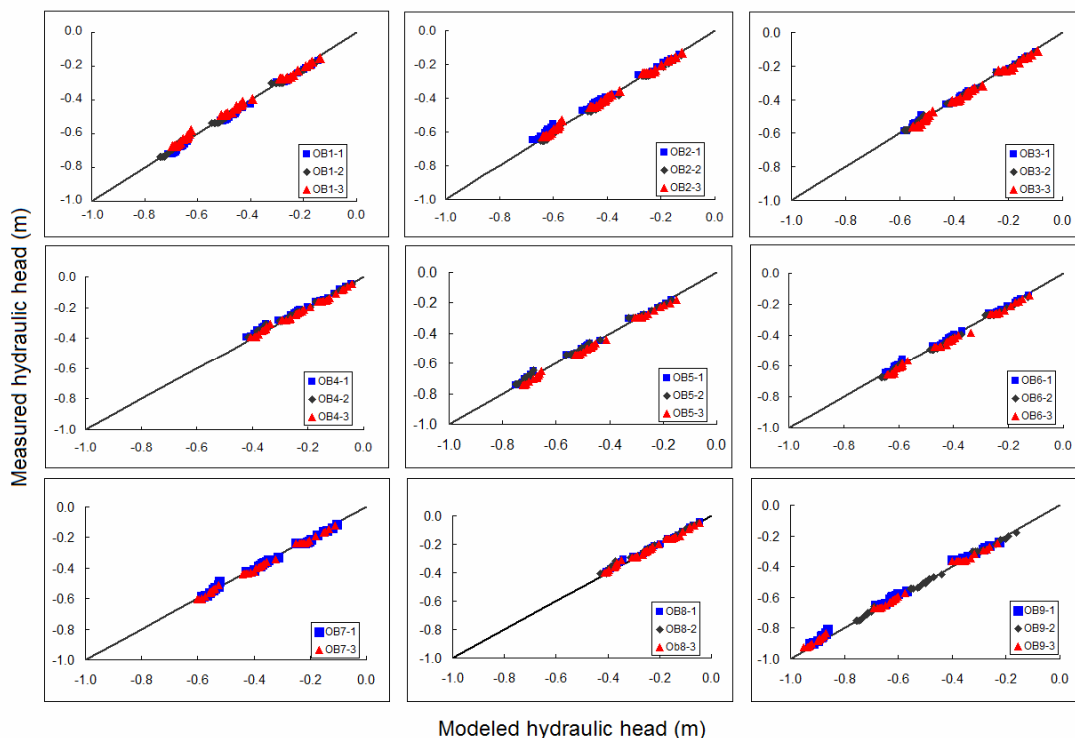


Fig. 5.5 Model calibration results for the conducted pumping tests obtained from the comparison of numerical model results with corresponding field observations for selected time steps. Locations and depths of the piezometers are shown in Figure 5.2 (b and c).

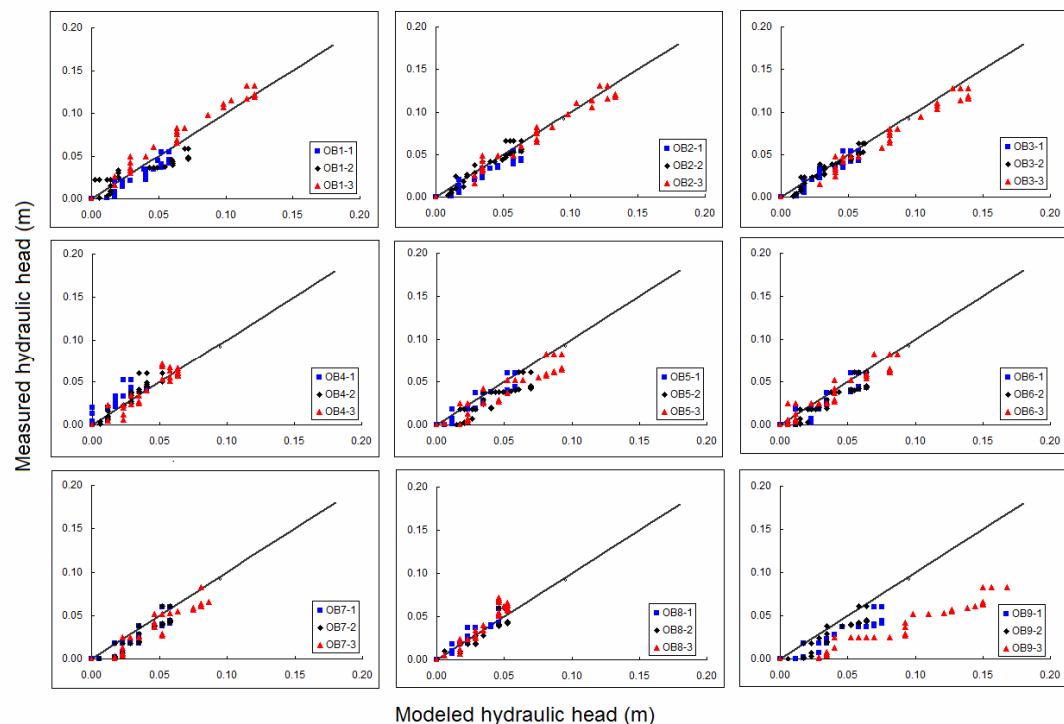


Fig. 5.6 Model calibration results for the conducted injection tests obtained from the comparison of numerical model results with corresponding field observations for selected time steps. Locations and depths of the piezometers are shown in Figure 5.2 (b and c).

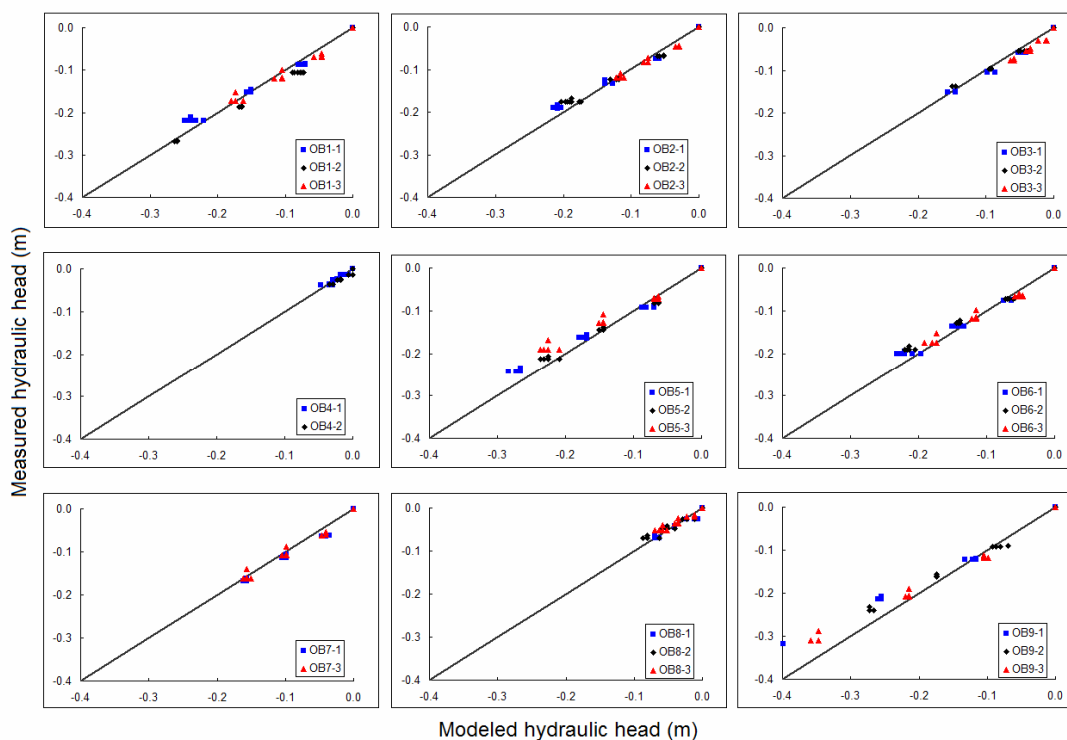


Fig. 5.7 Model calibration results for the conducted circulation flow tests obtained from the comparison of numerical model results with corresponding field observations for selected time steps. Locations and depths of the piezometers are shown in Figure 5.2 (b and c).

5.4.3 Sensitivity to the hydraulic conductivity of aquifer layers

The influences of the aquifer layer properties on circulation flow patterns as well as on the drawdown were investigated by considering the demonstrated aquifer at the test site as a reference. To simplify the problem, the defined layers were separated into two main aquifer layers, which are the pumping and the injection section, respectively. That means the top three layers in Figure 5.3 are considered as one abstraction section, where the geometric mean value for the calibrated $K_{abstraction} = 5.79 \times 10^{-4}$ m/s was considered as the averaged property for the whole pumping section (Srivastava and Guzman-Guzman, 1995).

Consequently, the test site aquifer is re-classified in three layers: (1) the abstraction layer characterized by $K_{abstraction}$ (layer 1–3 in Figure 5.3), (2) the injection layer with $K_{injection}$ (layer 5 in Figure 5.3) and (3) a less permeable layer identical with previous case with K_{low} (layer 4 and 6 in Figure 5.3). This set-up is considered as the reference case in the following sensitivity analysis. The respective K values for the different

layers are $K_{abstraction} = 5.79 \times 10^{-4}$ m/s, $K_{injection} = 3.87 \times 10^{-3}$ m/s and $K_{low} = 1.00 \times 10^{-5}$ m/s respectively.

Again, we give the focus on the properties of the abstraction and injection sections. A constant flow rate of 30 m³/h is imposed to the circulation flow system and the numerical simulations are conducted for the steady-state.

First, the influence of K of the abstraction section (layer) on groundwater flow especially on the drawdown is investigated by increasing and decreasing $K_{abstraction}$ value with a factor of 10, respectively. Other parameters are identical with the reference situation. The simulation results show a significant decline in hydraulic head, ca. 3.5 m, with a decrease in $K_{abstraction}$ to a factor of 10 shown in Figure 5.8. We also found an inverse proportional relationship between the drawdown and the K of the abstraction layer. This observation is in accordance with the results of Zlotnik and Ledder (1996) and Jin et al. (2015), who considered homogenous aquifers in their studies.

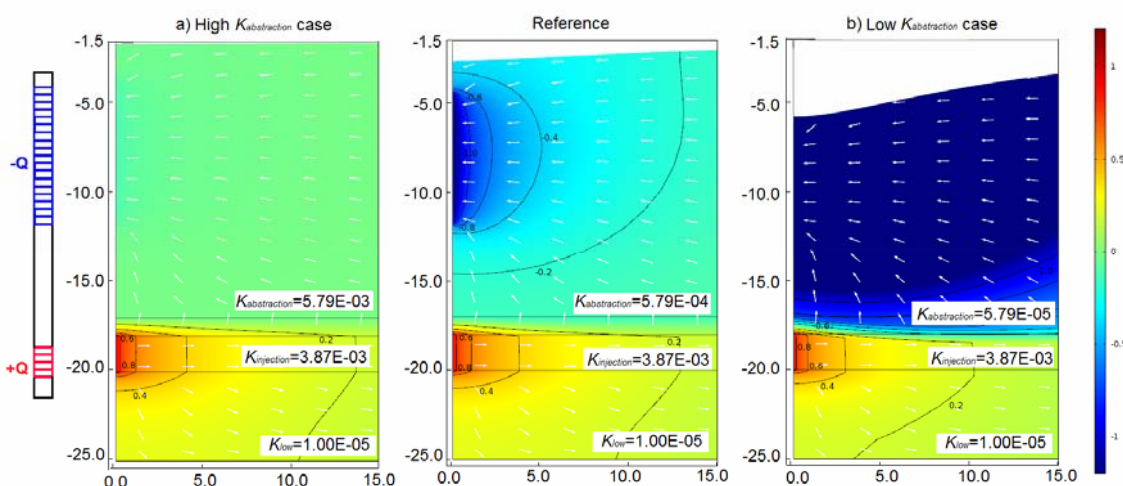


Fig. 5.8 Effect of the hydraulic conductivity of the abstraction layer on steady-state groundwater flow near the VCW. Left: higher hydraulic conductivity case with $K_{abstraction} = 5.79 \times 10^{-3}$; middle: the reference case $K_{abstraction} = 5.79 \times 10^{-4}$; right: lower hydraulic conductivity case with $K_{abstraction} = 5.79 \times 10^{-5}$. Detailed description of the test case can be found in the caption of Figure 5.4.

Subsequently, the influences of the K of the injection section (layer) groundwater flow and the drawdown were investigated by increasing and decreasing $K_{injection}$ value to a factor of 10 respectively, while keeping other parameters constant.

Although the groundwater flow pattern, especially in the injection layer is changed dramatically, the influence of $K_{injection}$ on the flow near the abstraction section and on the hydraulic head is not significant. The drawdown cone is slightly larger with increasing values of $K_{injection}$ indicated by the equipotential lines shown in Figure 5.9. Notice that the lower limit for $K_{injection}$ in the simulation reached a value of 3.87×10^{-4} m/s, which is slightly lower than the given $K_{abstraction}$. Even though this low $K_{injection}$ case is demonstrated here for evaluating the influence of injection layer properties on flow patterns, this case is not relevant for practical applications.

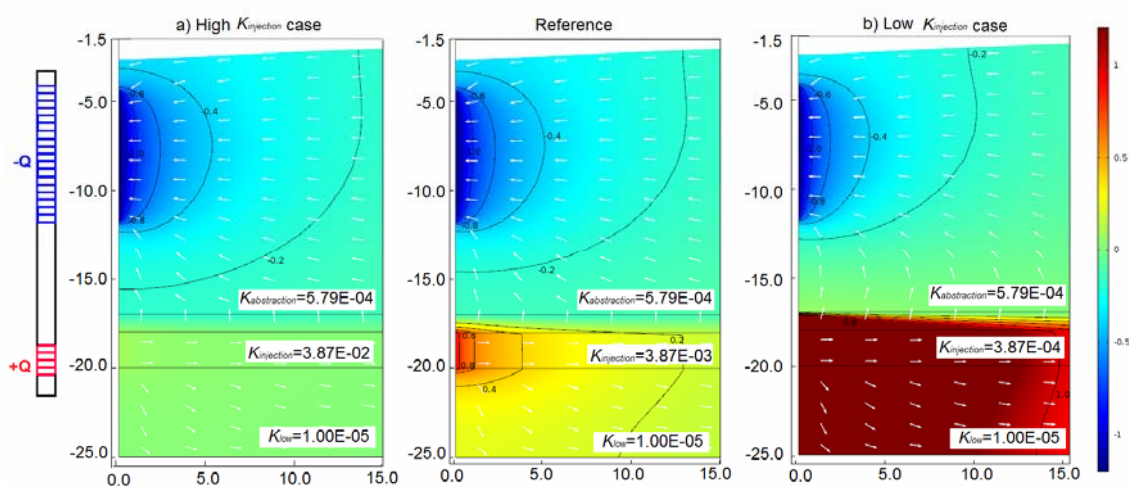


Fig. 5.9 Effect of the hydraulic conductivity of the injection layer on steady-state groundwater flow near the VCW. Left: higher hydraulic conductivity case with $K_{injection} = 3.87 \times 10^{-2}$; middle: the reference case $K_{injection} = 3.87 \times 10^{-3}$; right: lower hydraulic conductivity case with $K_{injection} = 3.87 \times 10^{-4}$. Detailed description of case can be found in the caption of Figure 5.4.

5.5 Conclusions

The interrelated hydraulic properties of aquifer layers make the prediction of drawdown induced by a VCW in an unconfined aquifer very complex. To investigate the influence of the aquifer layer properties on groundwater flow, the aquifer layers were characterized in detail with various methods including several direct-push methods, pumping-, injection-, and circulation flow tests in the field as well as grain-size analysis in lab. Furthermore, a comprehensive numerical model was set-up and calibrated to simulate the performed tests for different flow scenarios at the test site.

Regardless from the little pronounced aquifer layering of the test site, the employed field methods provide an appropriate data base, which is pertinent for an increased understanding of the hydraulic structure of the aquifer layers. Good agreements for K were observed by the evaluation of the results from various tests.

By means of sweeping the K values in selected layers, its influence on the groundwater flow field and especially on the drawdown could be assessed. In contrast to the injection layer, significantly larger effects of the K of the abstraction layer on the hydraulic head were observed. Moreover, an inversely proportional relationship between drawdown and K of the abstraction layer was specifically obtained.

The gained insight from this study provides an important contribution and gives practical implications for the future including design and operation of VCW for groundwater lowering in unconfined aquifers.

5.6 References

- Bear, J., 1972. Dynamics of Fluids in Porous Media, Dover Publications Inc, New York.
- Bouwer, H., 2002. Artificial recharge of groundwater: hydrogeology and engineering. *Hydrogeology Journal* 10(1), 121-142.
- Butler Jr, J.J., 2005. Hydrogeological methods for estimation of hydraulic conductivity. In: *Hydrogeophysics*, Springer Netherlands, 23-58.
- Butler, J.J., Healey, J.M., McCall, G., Garnett, E.J., Loheide, S.P., 2002. Hydraulic tests with direct-push equipment. *Groundwater* 40(1), 25-36.
- Butler, J.J., Garnett, E.J., 2000. Simple procedures for analysis of slug tests in formations of high hydraulic conductivity using spreadsheet and scientific graphics software. *Open-File Report* 2000, 40.
- Butler, J.J., Dietrich, P., Wittig, V., Christy, T. 2007. Characterizing hydraulic conductivity with the direct-push permeameter. *Groundwater* 45(4), 409-419.
- Chen, J.S., Jang, C.S., Cheng, C.T., Liu, C.W., 2010. Conservative solute approximation to the transport of a remedial reagent in a vertical circulation flow field. *Journal of Hydrology* 390(3), 155-168.
- COMSOL Multiphysics, 2014. Version 4.3b, <http://www.comsol.com>. [Accessed July 01, 2014].
- Dietrich, P., Butler, J.J., Faiß, K., 2008. A rapid method for hydraulic profiling in unconsolidated formations. *Groundwater* 46(2), 323-328.

- Donea, J., Huerta, A., Ponthot, J.-Ph., Rodriguez-Ferran, A., 2004. Arbitrary Lagrangian-Eulerian methods, In: Stein, E., de Borst, R., Hughes, T.J.R. (Eds.), *Encyclopedia of Computational Mechanics*, Vol. 1, John Wiley & Sons, New York, pp. 413-434.
- Foster, S.S., Lawrence, A., Morris, B., 1998. *Groundwater in Urban Development: Assessing Management Needs and Formulating Policy Strategies*. World Bank Publications.
- Hazen, A., 1893. Some physical properties of sand and gravels, with special reference to their use in filtration. *Twenty Fourth Annual Report, State Board of Health of Massachusetts*, 541-556.
- Herrling, B., Stamm, J., 1991. In situ groundwater remediation of strippable contaminants by vacuum vaporizer wells (UVB) operation of the well and report about cleaned industrial sites. *Third Forum on Innovative Hazardous Waste Treatment Technologies: Domestic and International*, Dallas, Texas, June 11-13.
- Herrling, B., Stamm, J., 1992. Numerical results of calculated 3 D vertical circulation flows around wells with two screen sections for in situ or on-site aquifer remediation. In *Computational Methods in Water Resources IX*, no. 1, Numerical methods in Water Resources, ed. T.F. Russell, R.E. Ewing, C.A. Brebbia, W.G. Gray, and G.F. Pinder, 483-492. New York, Elsevier Science.
- Holzbecher, E., Jin, Y., Ebneth, S., 2011. Borehole pump & inject: an environmentally sound new method for groundwater lowering. *International Journal of Environmental Protection* 1(4), 53-58.
- Jin, Y., Holzbecher, E., Sauter, M., 2014. A novel modeling approach using arbitrary Lagrangian-Eulerian (ALE) method for the flow simulation in unconfined aquifer. *Computers & Geosciences* (62), 88-94.
- Jin, Y., Holzbecher, E., Sauter, M., 2015. Dual-screened vertical circulation wells for groundwater lowering in unconfined aquifers. *Groundwater*, in press (doi: 10.1111/gwat.12331).
- Johnson, R.L., Simon, M.A., 2007. Evaluation of groundwater flow patterns around a dual-screened groundwater circulation well. *Journal of Contaminant Hydrology* 93(1), 188-202.
- Kabala, Z.J., 1993. The dipole-flow test: a new single-borehole tests for aquifer characterization. *Water Resource Research* 29(1), 99-107.
- Knox, R.C., Sabatini, D.A., Harwell, J.H., Brown, R.E., West, C.C., Blaha, F., Griffin, C., 1997. Surfactant remediation field demonstration using a vertical circulation well. *Ground Water* 35(6), 948-953.
- Koltermann, C.E., Gorelick, S.M., 1995. Fractional packing model for hydraulic conductivity derived from sediment mixtures. *Water Resources Research* 31(12), 3283-3297.
- Koltermann, C.E., Gorelick, S.M., 1996. Heterogeneity in sedimentary deposits: A review of structure-imitating, process-imitating, and descriptive approaches. *Water Resources Research* 32(9), 2617-2658.
- Lessoff, S.C., Schneidewind, U., Leven, C., Blum, P., Dietrich, P., Dagan, G., 2010. Spatial characterization of the hydraulic conductivity using direct-push injection logging. *Water Resources Research* 46(12).
- LGBR, 2014. Hydrogeologiesche Karten Brandenburg, Landesamt für Bergbau, Geologie und Rohstoffe, <http://www.lbgr.brandenburg.de>, [Accessed May 22, 2014].
- Louwyck A, Vandenbohede A, Bakker M, Lebbe L., 2012. Simulation of axi-symmetric flow towards wells: a finitedifference approach. *Computers and Geosciences* 44, 136-145.

- MacDonald, T.R., Kitanidis, P.K., 1993. Modeling the free surface of an unconfined aquifer near a recirculation well. *Ground Water* 31(5), 774-780.
- McCall, W., Christy, T., Christopherson, T., Issacs, H., 2009. Application of direct push methods to investigate uranium distribution in an alluvial aquifer. *Ground Water Monitoring & Remediation*, 29, 65-76.
- Pohjoranta, A., Tenno, R., 2011. Implementing surfactant mass balance in 2D FEM-ALE models. *Engineering with Computers* 27(2), 165-175.
- Powers, J.P., Corwin, A.B., Schmall, P.C., Kaeck, W.E., Herridge, C.J., 2007. *Construction Dewatering and Groundwater Control-New Methods and Applications*. Third ed. John Wiley and Sons, United States of America.
- Pyne, R.D.G., 1995. *Groundwater recharge and wells: a guide to aquifer storage recovery*. CRC press.
- Revil, A., Cathles, L.M., 1999. Permeability of shaly sands. *Water Resources Research* 35(3), 651-662.
- Roy, D., Robinson, K.E., 2009. Surface settlements at a soft soil site due to bedrock dewatering. *Engineering Geology* 107(3-4), 109-117.
- Schulmeister, M.K., Butler, J.J., Healey, J.M., Zheng, L., Wysocki, D.A., McCall, G.W., 2003. Direct-push electrical conductivity logging for high-resolution hydrostratigraphic characterization. *Ground Water Monitoring & Remediation* 23(3), 52-62.
- Sellwood, S.M., Healey, J.M., Birk, S., Butler, J.J., 2005. Direct-Push Hydrostratigraphic Profiling: Coupling Electrical Logging and Slug Tests. *Groundwater* 43(1), 19-29.
- Srivastava, R., Guzman-Guzman, A., 1995. Analysis of hydraulic conductivity averaging schemes for one-dimensional, steady-state unsaturated flow. *Groundwater*, 33(6), 946-952.
- Todd, D.K., 1980. *Groundwater Hydrology*. John Wiley & Sons. New York, 535pp.
- US EPA, 1995. *Site Technology Capsule: Unterdruck-Verdampfer-Brunnen Technology (UVB) Vacuum Vaporizing Well*. Technical Report EPA-540/R-95-500.
- US EPA, 1998. *Field Applications of In-situ Remediation Technologies: Ground-Water circulation wells*. Technical Report EPA-542-R-98-009.
- Vienken, T., Dietrich, P., 2011. Field evaluation of methods for determining hydraulic conductivity from grain size data. *Journal of Hydrology* 400 (1-2): 58-71.
- Zlotnik, V., and G. Ledder. 1996. Theory of dipole flow in uniform anisotropic aquifers. *Water Resources Research* 32 (4), 1119-1128.
- Zlonik V.A., Zurbuchen B.R., 1998. Dipole probe: design and field applications of a single-borehole device for measurements of vertical variations of hydraulic conductivity. *Ground Water* 36(6), 884-893.
- Zlotnik, V.A., Zurbuchen. B.R., 2003. Field study of hydraulic conductivity in a heterogeneous aquifer: Comparison of single-borehole measurements using different instruments. *Water Resources Research* 39(4), 1101.

Chapter 6

6 General Conclusions and Perspectives

This work introduced a new dewatering system using VCWs, which consist of two screen intervals with abstraction and injection induced in the upper and the lower interval, respectively. Groundwater level is lowered through the circulation flow induced by VCWs rather than abstraction to the surface, consequently, the water discharge is avoided. To implement the new dewatering technique, however, a sufficient understanding of the groundwater flow patterns around the well and the influence of relevant parameters are required, but still unknown. For many cases analytical methods are limited in considering complex boundaries, i.e., free-surface, and geometry, i.e., unsymmetrical distribution of pumping and injection screens, respectively, and, as a consequence, numerical simulations are needed. In this work, a novel numerical approach was developed, which was then applied for predicting groundwater flow near a VCW, and for assessing the sensitivities of influencing parameters. Furthermore, a proper knowledge of the aquifers characteristics is necessary to determine the hydrogeological conditions to successfully install VCWs. To accomplish this, various field experiments were performed in order to determine the aquifer properties at a test site with a high resolution.

6.1 Evaluation of Flow and Hydraulic Head Fields for VCWs

The developed modeling approach solves the groundwater flow in unconfined aquifers as a free-surface problem by coupling the ALE algorithm with the groundwater flow equation. The movement of the upper free-surface boundary is followed by imposing an additional condition, which allows the computational mesh

to move with the boundaries. Furthermore, unlike approaches following the Dupuit assumption, this approach is not limited in considering the vertical velocity components, which is essential for describing the flow near VCWs. The verification runs showed good agreement between the simulation results and available analytical solutions. Thus, solving a free-surface problem by implementing the ALE method is a suitable approach for simulating groundwater flow in an unconfined aquifer.

The flexibility of this modeling approach even allows the simulation of complex cases such as the above mentioned flow induced by VCWs. In addition, the regions around a VCW with intensive water circulation can be delineated with streamline modeling. The developed numerical model was calibrated and further validated by field observations of flow tests with a VCW.

The sensitivity analysis, on the one hand, revealed that the steady-state drawdown is proportional to the imposed flow rate and inversely proportional to the aquifer hydraulic conductivity, and highlights the strong influence of low hydraulic conductivities on drawdown. On the other hand, the extension of the influenced area is only controlled by the aquifer anisotropy for an identical well set-up.

Eventually, the influence of single parameters on the water table movement can be predicted. Furthermore, despite the lower dewatering efficiency in terms of absolute drawdown, the principal feasibility of this new technique as an alternative to conventional dewatering methods under certain circumstances appears promising. This applies especially for cases, where very local drawdowns are desired or environmentally adverse effects are expected by discharging the abstracted (contaminated) groundwater into surface water bodies.

6.2 Further Investigations on VCW installation at Construction Sites and Future Challenges

Despite the focus of the thesis was on evaluating the feasibility of applying VCWs for dewatering and the identification of influencing parameters through numerical simulations, much more efforts are still required to practically implement this new

well system at construction sites. Currently, VCWs have been successfully applied at sites in Germany and in the Netherlands. Most of VCWs are installed in relatively homogenous unconsolidated unconfined aquifers.

The main challenge for constructing VCW systems is the identification of suitable aquifer layers where sufficient water injection is possible. So far, these layers are empirically identified during the borehole drilling process and accompanied with drilling fluid (mostly water). During the drilling, the injection layers in an aquifer are characterized by a significant drop of the injection pressure and the loss of drilling fluid. Unfortunately, the hydrogeological key characteristics of these aquifer layers have not yet been fully investigated. In addition, the interrelated hydraulic properties of aquifer layers make the prediction of drawdown induced by a VCW very complex.

In order to enhance the understanding of the influence of the aquifer properties on the injection potential and to relate these properties with the empirical observations, a first step was done in this work by a high resolution characterization of the test site. For doing so, in-situ direct-push tests were performed and the grain sizes of the selected core samples were analyzed in lab. Slightly higher hydraulic conductivities (factor 2-3) were obtained for the injection layers at the investigated test site. However, the obtained results provide only first insight in the role of aquifer layer structures. Further investigations have to deal with the generalization and, thus, with the transferability of the findings to other aquifer systems. For this purpose, also a systematic characterization of the aquifer layers, especially on the technical factors controlling the water injectivity, is required in order to enhance the well design as well as its practical application. Furthermore, the practical limitations of this dewatering system has also to be evaluated, such as the potential risk of short cuts of the groundwater flow in the direct vicinity of the well, which may, in fact, weaken the drawdown scale dramatically.

Moreover, the numerical modeling should be extended by considering more complex cases such as multi-VCW systems, ambient groundwater flow, and heterogenous aquifer conditions, etc.

Appendix

Appendix S1: Site description and measurements

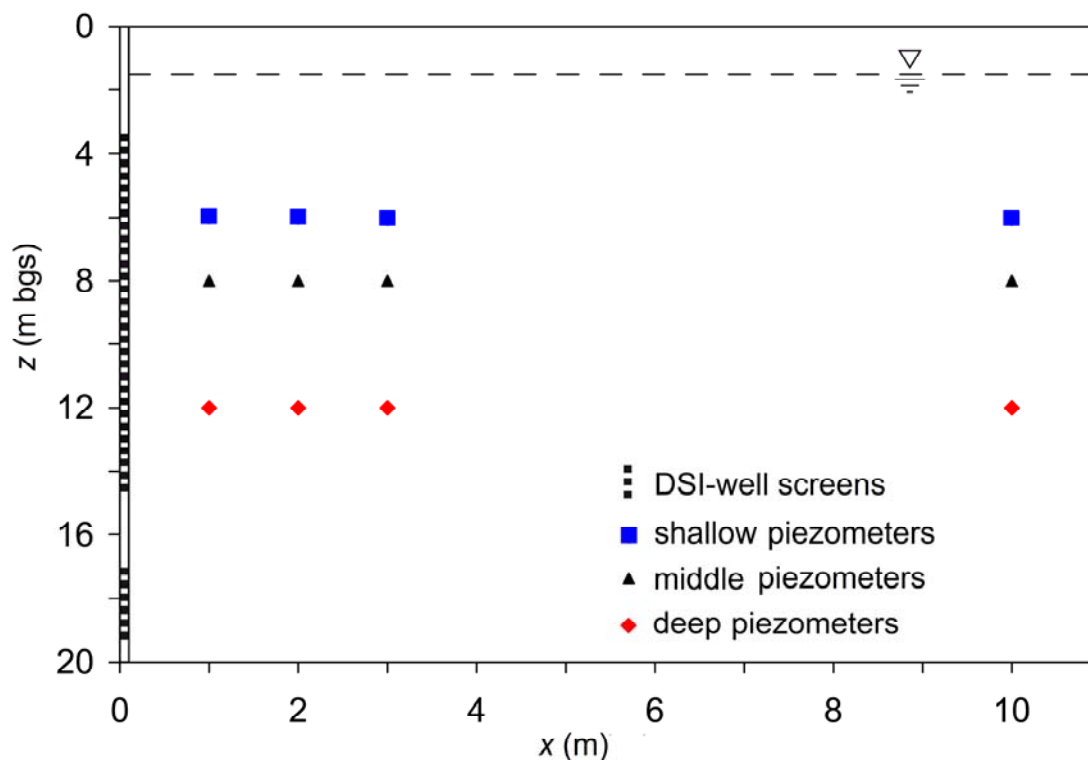


Fig. S1 : Schematic site plan view of the vertical cross section of the test field showing the locations of piezometers and DSI-well screens.

Appendix S2: The Mathematical Model

S2.1 Reference case model

The reference model considers a vertical cross section of a 50 m wide and 20 m deep aquifer. The problem is simulated in an axisymmetric domain representing a vertical cross section of an aquifer. The well itself is excluded from the model region, because we only focus on the flow in porous media. Triangular meshes are used for the discretization with a mesh refinement in the vicinity of the well and along the free-surface. The problem of the reference case is solved for 25,828 degrees of freedom using standard quadratic elements on an unstructured triangular mesh. Parameters used in numerical simulation are summarized in Table S1.

Table S1: Parameters used for groundwater flow field simulation around a VCW for reference case.

Parameter	Input value
Well radius r_w (m)	0.1
Aquifer thickness D (m)	20
Radius of influence r' (m)	50
Abstraction screen interval d, d_e (m. bgs)	5, 7
Injection screen interval l, l_e (m. bgs)	13, 15
Separation length of screen intervals ΔL (m)	8
Flow rate Q (m^3/h)	20
Horizontal/vertical hydraulic conductivities K_r, K_z (m/s)	1×10^{-3}
Anisotropy ratio $\alpha = K_z/K_r$ (-)	1

Figure 4.1 illustrates the flow configuration and the distribution of the hydraulic head induced by the VCW at steady-state. A 2D vertical cross section is depicted for visualizing the flow circulation generated at the inner boundary (VCW). The change of the water table position is apparent along the upper boundary of the colored region with the initial position given by the upper solid line of the rectangular model domain. For better visualization only part of the model region is displayed. A lower hydraulic head is calculated near the abstraction screen (blue color zone), while higher hydraulic head potential is induced near the injection screen (red color zone). Hydraulic head equipotential lines are shown by black contours in the figure. The solid curves (red) represent streamlines confining the 20%, 40%, 60% and 80% of the total flow circulated around the VCW. In addition, the velocity field is indicated in an arrow plot. The simulation results show the increase in hydraulic head at the upper boundary with increasing radial distance from the well. Notice that drawdown corresponds to the negative value of the simulated hydraulic head as the initial hydraulic head is assumed as zero.

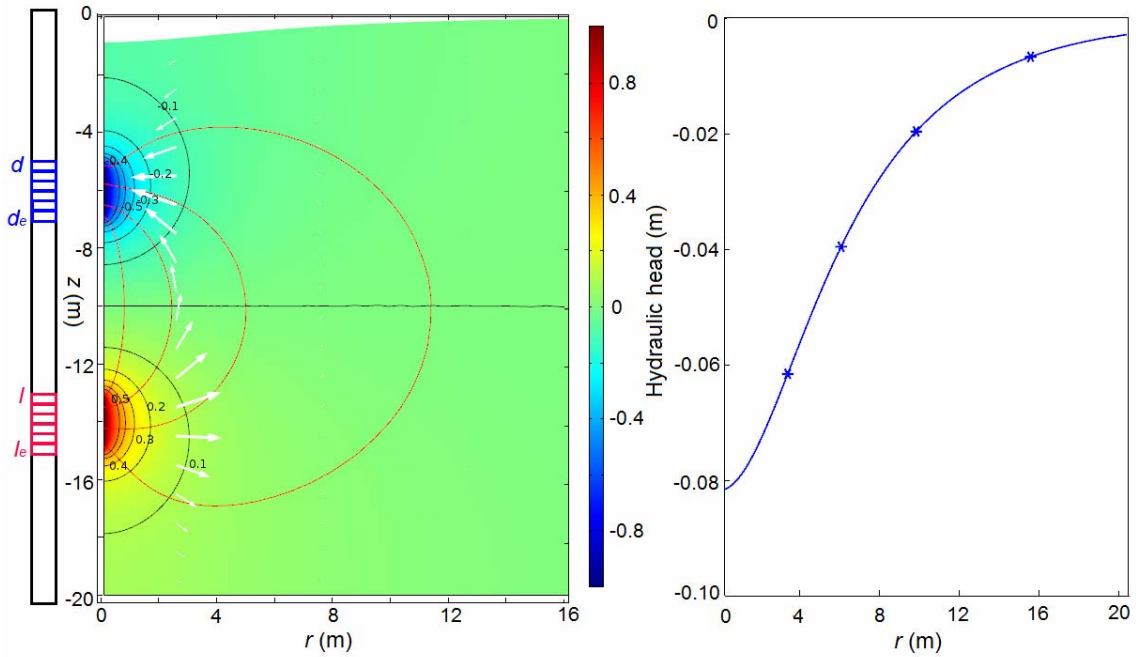


Fig. S2: Modeled 2D vertical cross-section groundwater flow field near a VCW. Left: hydraulic head distribution (color plot), and position of groundwater table (deformed mesh line), equipotential contours (black solid lines with label), velocity field (arrow plot), 20%, 40%, 60%, 80% flow streamlines (red solid lines); right: hydraulic head (or groundwater level position) change with increasing radial distance from the well.

S2.2 Model verification, calibration and validation

S2.2.1 Analytical solution

The verification runs for our model are conducted by comparing the simulation results with the analytical solutions. Zlotnik and Ledder (1996) presented analytical solutions for the drawdown and flow field induced by a vertical circulation well in uniform anisotropic aquifers. The steady-state drawdown distribution in the aquifer is estimated as:

$$s(r, z) = -\frac{q}{2} \left[\sinh^{-1} \left(\frac{z_{+-}}{\rho} \right) - \sinh^{-1} \left(\frac{z_{--}}{\rho} \right) + \sinh^{-1} \left(\frac{z_{+-}}{\rho} \right) - \sinh^{-1} \left(\frac{z_{++}}{\rho} \right) \right] \quad (S1)$$

where

$$q = \frac{Q}{4\pi K_r \Delta}, \quad \Delta = \frac{d - d_e}{2} = \frac{l - l_e}{2}, \quad z_{\pm\pm} = z \pm \Delta L/2 \pm \Delta,$$

$$a = (K_r/K_z)^{1/2}, \rho = r/a, \quad \sinh^{-1}(x) = \ln\left(\left(1+x^2\right)^{1/2} + x\right) \quad (S2)$$

S2.2.2 Comparison of simulation results with analytical solution

The comparison of the hydraulic head distribution obtained from simulation of the reference model and from Equation (S1) is depicted in Figure S3 and S4 at two difference depth, where $z = 0$ represents the free-surface and $z = -5$ at the depth of the abstraction screen.

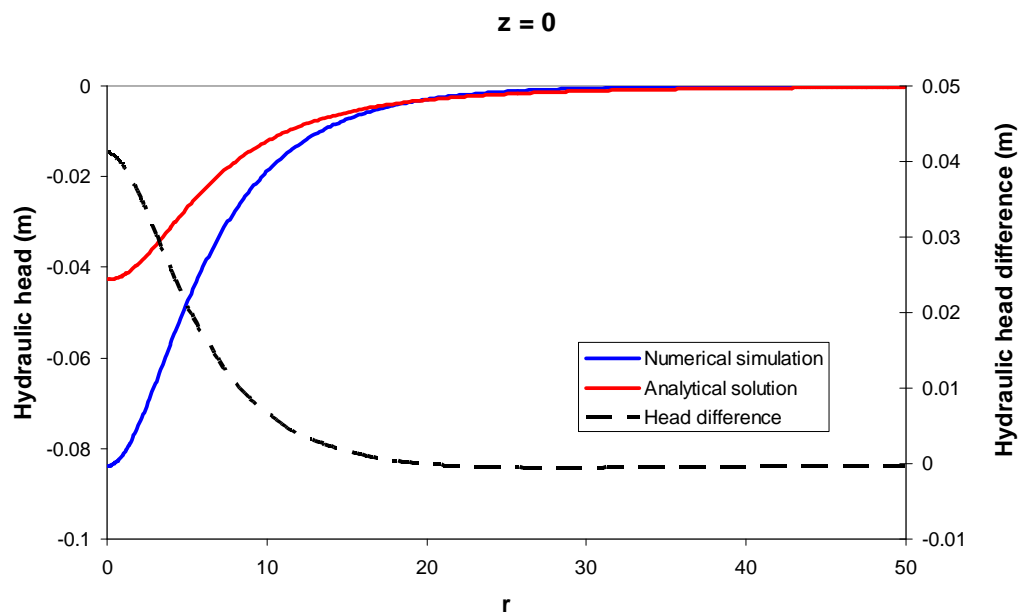


Fig. S3: Steady-state hydraulic head at free surface ($z = 0$) and head difference compared to the analytical solution, versus radial distance r from the VCW on the left hand side.

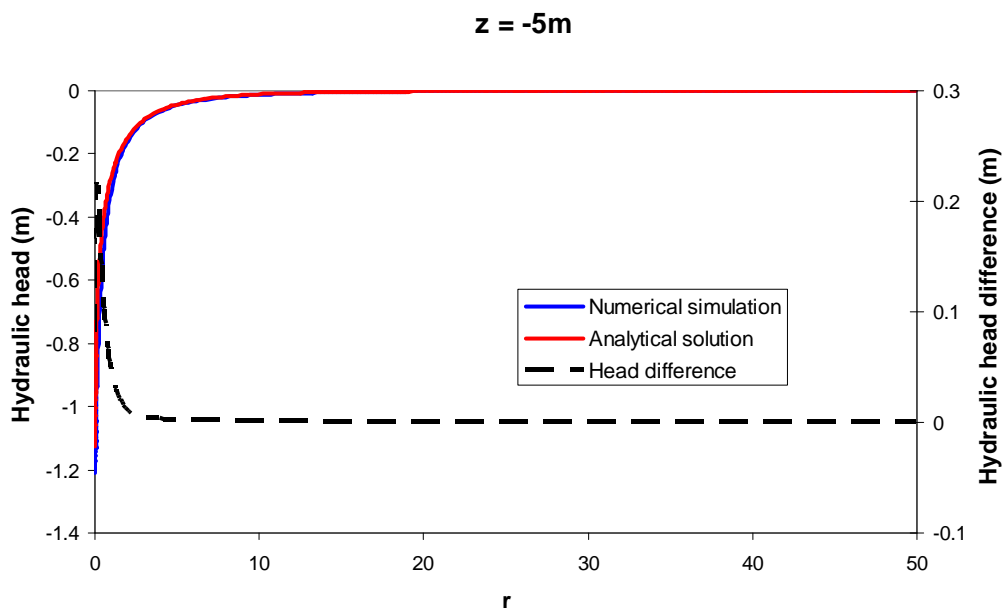


Fig. S4: Steady-state hydraulic head at the depth of abstraction screen centre ($z = -5\text{m}$) and head difference compared to the analytical solution, versus radial distance r from the VCW on the left hand side.

S2.2.3 Model validation

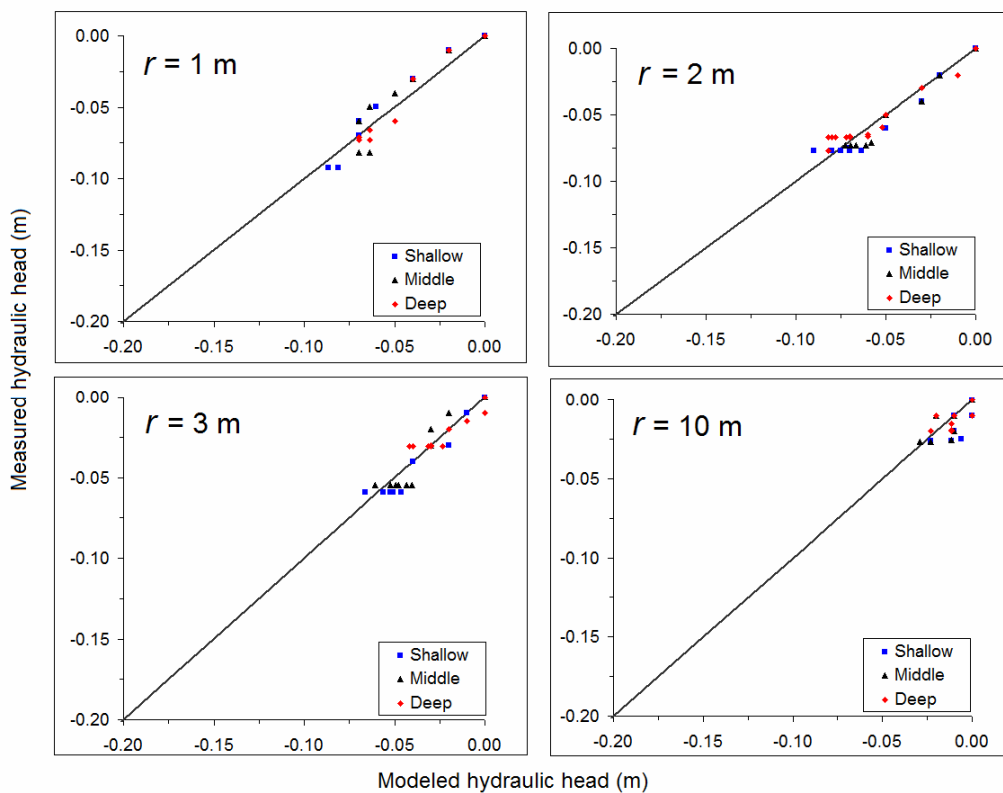


Fig. S5: Comparison between the numerical model results and the field observations for the validation experiment. Locations and depths of the piezometers are shown in Figure S1.

Appendix S3: Sensitivity Analysis

S3.1 Effect of screen positions

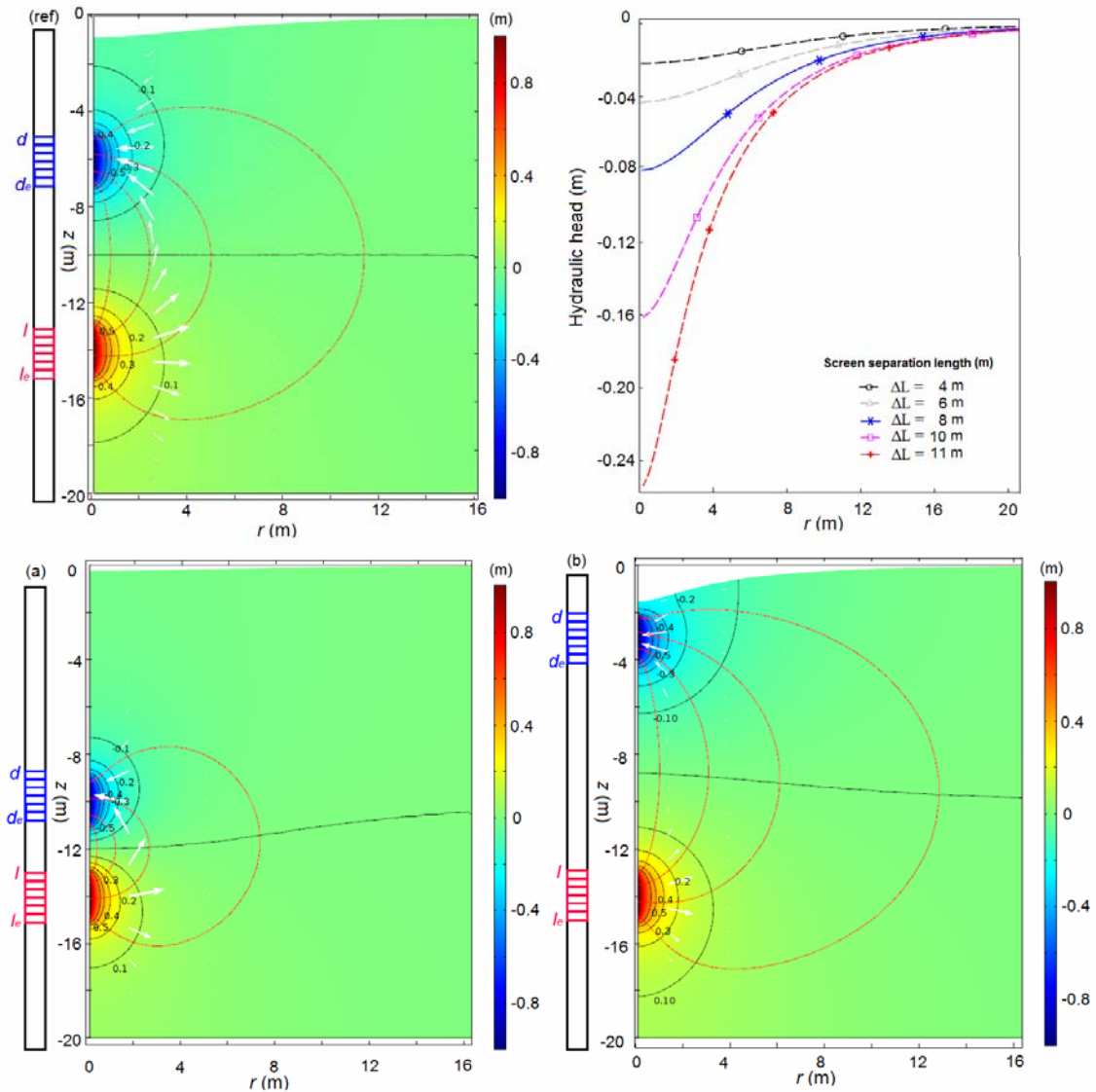


Fig. S6: Effect of the separation length between abstraction and injection screen, ΔL , on steady-state groundwater flow near the VCW. The location of the injection interval is identical. (ref) reference case $\Delta L = 8$ m; (a) $\Delta L = 4$ m; (b) $\Delta L = 11$ m. The detailed figure descriptions for each case can be found in the caption of Figure S3. The scatter plot depicts the effect of ΔL on the hydraulic head.

S3.2 Effect of hydraulic conductivity on drawdown

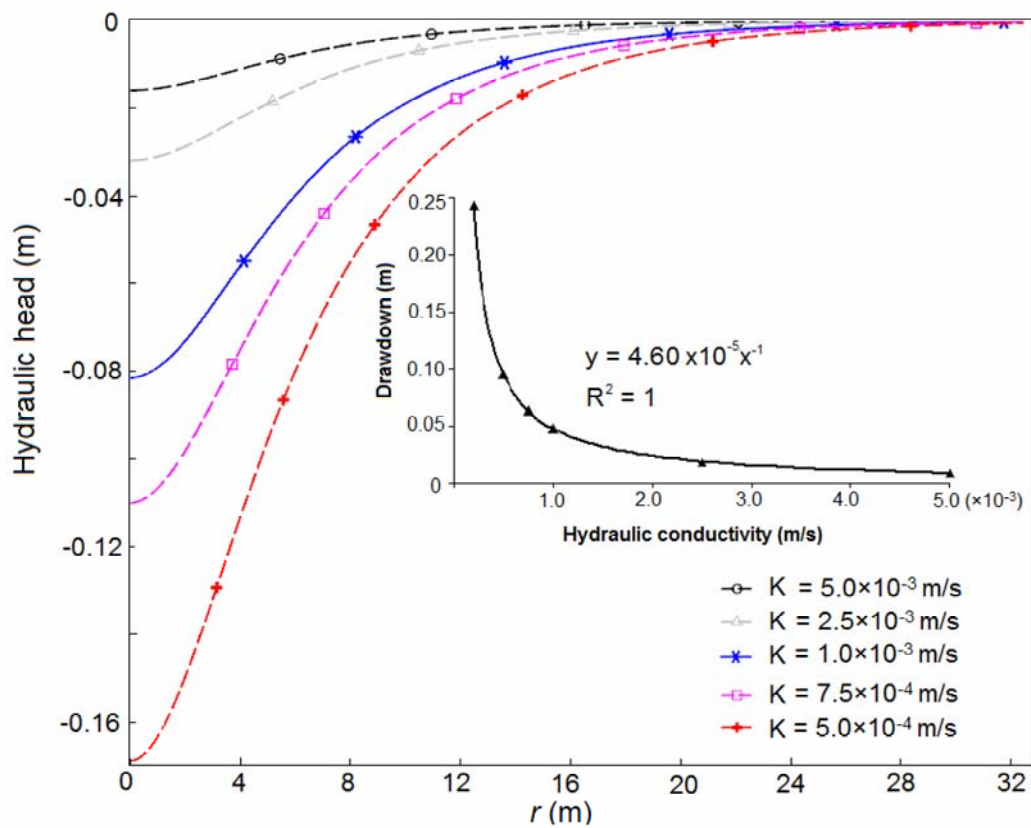


Fig. S7: Effect of the change in hydraulic conductivity, K , on the hydraulic head. Homogenous and isotropic aquifer materials ($K = K_r = K_z$) are assumed. The inverse proportional relationship between K and drawdown is shown for a radial distance of $r = 5$ m.

Publication List

List of all journal articles, conference abstracts, and miscellaneous publications authored or co-authored by me and related to the presented work (latest update: March 2015).

Journals

Holzbecher, E., **Jin, Y.**, Ebneith, S., 2011. Borehole pump & inject: an environmentally sound new method for groundwater lowering. *International Journal of Environmental Protection* 1 (4), 53–58.

Jin, Y., Holzbecher, E., Sauter, M., 2014. A novel modeling approach using arbitrary Lagrangian-Eulerian (ALE) method for the flow simulation in unconfined aquifers. *Computers & Geosciences* 62, 88–94.

Jin, Y., Holzbecher, E., Sauter, M., 2015. Dual-screened vertical circulation wells for groundwater lowering in unconfined aquifer. *Groundwater*, in press (doi: 10.1111/gwat.12331).

In preparation for submission to journal

Jin, Y., et al. (manuscript in preparation for submission, detailed author list not agreed upon yet). Performance of vertical circulation wells for dewatering in layered unconfined aquifer.

Conference contributions

Holzbecher, E., **Jin, Y.**, Ebneith, S., 2011. An environmentally sound new method for groundwater lowering. In: *Proceedings of the International Workshop on Civil Engineering and Urban Planning (WCEUP) in Hangzhou, China*.

Jin, Y., Holzbecher, E., Sauter, M., 2011. Innovative method for groundwater sustainability – the düsensauginfiltration method. In: *Proceedings of the LUMES Conference in Lund, Sweden*.

Holzbecher, E., Oberdorfer, P., Maier, F., **Jin, Y.**, Sauter, M., 2011. Simulation of deep geothermal heat production. In: *Proceedings of the European COMSOL Conference in Stuttgart, Germany*.

Jin, Y., Holzbecher, E., Oberdorfer, P., 2011. Simulation of a novel groundwater lowering technique using arbitrary Lagrangian-Eulerian method. In: *Proceedings of the European COMSOL Conference in Stuttgart, Germany*.

List of publications

- Jin, Y.**, Holzbecher, E., Ebneith, S., 2012. Promoting sustainable development in groundwater industry through innovative dewatering technology. In: *Proceedings of the IFDAA Conference in Göttingen, Germany*.
- Jin, Y.**, Holzbecher, E., Ebneith, S., 2012. Simulation of pumping induced groundwater flow in unconfined aquifer using arbitrary Lagrangian-Eulerian method. In: *Proceedings of the European COMSOL Conference in Milan, Italy*.
- Rahman, M.A., Oberdorfer, P., **Jin, Y.**, Pevin, M., Holzbecher, E., 2012. Impact assessment of hydrologic and operational factors on the efficiency of managed aquifer recharge scheme. In: *Proceedings of the European COMSOL Conference in Milan, Italy*.
- Jin, Y.**, Holzbecher, E., Sauter, M., Ebneith, S., 2012. Groundwater sustainability through a novel dewatering technology. In: *Proceedings of the AGU Fall Meeting in San Francisco, USA*.
- Jin, Y.**, Holzbecher, E., Ebneith, S., 2013. Investigating the impacts of hydrogeological parameters on DSI efficiency through Numerical Simulation. In: *Proceedings of the European COMSOL Conference in Rotterdam, Netherlands*.
- Jin, Y.**, Holzbecher, E., Ebneith, S., Tatomir, A.B., 2014. Simulation of groundwater flow patterns around a vertical circulation well. In: *Proceedings of the European COMSOL Conference Cambridge, UK*.

Other miscellaneous publications

- Hand, J., Sauter, M., **Jin, Y.**, Holzbecher, E., 2012. Pump it in and inject it out. *COMSOL News*.
- Hand, J., Sauter, M., **Jin, Y.**, Holzbecher, E., 2012. Pumping and injecting from a single Borehole. *Pumps & Process Magazine*.

Yulan Schaffer-Jin

PERSONAL DATA

Date of birth 23th September 1982
Place of birth Jilin, China
Nationality Chinese

EDUCATION

12/2010 – 10/2014 **Georg-August-Universität Göttingen (Germany)**
Geoscience Centre, Department Applied Geology
Ph.D. student

10/2008 – 11/2010 **Georg-August-Universität Göttingen (Germany)**
Hydrogeology and Environmental Geoscience (M.Sc.)

08/2006 – 08/2008 **Lund University (Sweden)**
International Master's Programme in Environmental Studies and Sustainability Science

09/2001 – 07/2005 **Jilin Agricultural University Changchun (PR China)**
Environmental Science (B.Sc.)

WORK EXPERIENCE

Since 12/2010 **Georg-August-Universität Göttingen**
Geoscience Centre, Department Applied Geology
Research associate

05/2010 – 11/2010 **Georg-August-Universität Göttingen**
Faculty of Forest Sciences and Forest Ecology
Scientific assistant

04/2009 – 10/2009 **Georg-August-Universität Göttingen**
Geoscience Centre, Department Applied Geology
Scientific assistant

07/2005 – 08/2006 **Beijing Aishida Investment Consultant Ltd (PR China)**
International Marketing Consultant
